CHARACTERIZATION OF SPATIAL NAPL DISTRIBUTION, MASS TRANSFER AND THE EFFECT OF COSOLVENT AND SURFACTANT RESIDUALS ON ESTIMATING NAPL SATURATION USING TRACER TECHNIQUES

By

JAEHYUN CHO

A DISSERTATION PRESENTED TO THE GRADUATE SCHOOL
OF THE UNIVERSITY OF FLORIDA IN PARTIAL FULFILLMENT
OF THE REQUIREMENTS FOR THE DEGREE OF
DOCTOR OF PHILOSOPHY

UNIVERSITY OF FLORIDA

2001

ACKNOWLEDGMENTS

During my four-and-a-half years of doctoral research at the University of Florida, I received assistance from many people. I greatly appreciate their help and guidance and I hold them in my heart. I would not be in the position to be writing this dissertation if it were not for their assistance and support throughout the years.

Primary thanks go to my advisory committee chair, Dr. Michael Annable, who guided me to this point with his encouragement, assistance, and support. I also gratefully thank my other committee members: Dr. Suresh Rao, Dr. William Wise, Dr. Kirk Hatfield, and Dean Rhue, for their teaching and substantial advice.

I would like to thank my previous fellows, Michael Brooks, Suzannah Kuhn, Michael Vanvalkenberg; and my present lab partners, Rick Robert, Christina Martines, and Diane Bonbehagen for their helpful support and advice in the lab or in the office. I also thank Irene Poyer, Dr. James Jawitz, and Dr. Heonki Kim for their valuable suggestions. I thank Dr. Booth for the many hours of exchanging knowledge and assistance in the lab.

I especially thank my wife, Yoonjung, who was understanding and gave me encouragement during my studies. I also thank my son, Michael. Obvious thanks go to my parents and parents-in-law for their support from far away.

TABLE OF CONTENTS

page

ACKNOWLEDGMENTS.....ii

LIST OF TABLES.....vi

LIST OF FIGURES.....vii

ABSTRACT.....x

CHAPTERS

1 INTRODUCTION.....1

2 CHARACTERIZATION OF SPARTIAL NAPL DISTRIBUTION BY COMBINED USE OF PARTITINING AND INTERFACIAL TRACER: USING GRAIN SIZE AND NAPL DISSOLUTION

Introduction..... 8
Theoretical Background..... 10
Adsorption Coefficients..... 10
Intefacial Area Estimate..... 11
NAPL Saturation Estimate.....13
NAPL Morphology Index..... 13
Materials and Methods..... 14
Materials..... 14
Interfacial Tension Measurement..... 15
Miscible Displacement Tests..... 15
Analytical Methods..... 18
Results and Disscussion..... 18
Estimation of Interfacial Adsorption and Partitioning Coefficients..... 18
NAPL-Water Interfacial Area and NAPL Saturation as a Function of Pore Size..... 20
NAPL-Water Interfacial Area and NAPL Saturation as a Function of NAPL Dissolution..... 27
NAPL Morphology Index..... 30
Conclusions..... 33

3 INFLUENCE OF SPECIFIC INTERFACIAL AREA ON MASS TRANSFER: NONEQUILIBRIUM PROCESS

Introduction..... 34

Theoretical Backgroud 36
Materials and Methods 37
Experimental Methods 38
Results and Disscussion 38
Parameter Estimation 38
Mass Transfer Coefficients 40
Influence of NAPL Reduction by Dissolution on Mass Transfer 46
Model Development 48
Nonequilibrium Mass Transfer 54
Conclusions 55

4 ESTIMATING NAPL SATURATION USING PARTITIONING TRACERS: INFLUENCE OF RESIDUAL COSOLVENTS

Introduction 57
Theoretical Background 59
Materials and Methods 60
Materials 60
Partition Isotherm Experiments 60
Solubility Experiments 61
Miscible Displacement Experiments 61
Data Analysis 63
Results and Disscussion 64
Effect of Cosolvent on Solubility 64
Effect of Cosolvent on Tracer Partitioning Isotherms 68
Effect of Cosolvent on Tracer Retardation 70
Impact of NAPL Saturation in the Systems 75
Conclusions 77

5 INFLUENCE OF RESIDUAL SURFACTANT ON PARTITIONING TRACERS

Introduction 79
Surfactant Adsorption from Aqueous Solution onto Solid Matrix 80
Surfactant Adsorption from Aqueous Solution onto Hydrophobic Organic Chemicals 82
Partitioning of Hydrophobic Organic Chemical into Residual Surfactants 83
Materials and Methods 84
Materials 84
Batch Isotherm Tests 85
Miscible Displacement Tests 86
Results and Disscussion 89
Effect of Surfactants on Batch Isotherms 89
Effect of Residual Surfactants on Tracer Transport 94
Effect of Adsorbed Surfactants on the Solids Matrix 97

Demonstration through a Flushing Test 100
Conclusions 103

6 Conclusions 105

APPENDICES

A INTERFACIAL TENSION: SDBS SOLUTION-PCE WITH OIL-RED DYE 109

B DERIVATION FOR MASS TRANSFER COEFFICIENT AT THE STEADY STATE CONDITION 110

C EQUILIBRIUM ISOTHERMS OF PARTITIONING TRACERS IN THE PRESENCE OF COSOLVENTS WITH VARYING CONCENTRATIONS 114

D EQUILIBRIUM ISOTHERMS OF PARTITIONING TRACERS IN THE PRESENCE OF SURFACTANTS WITH VARYING CONCENTRATIONS 121

REFERENCES 128

BIOGRAPHICAL SKETCH 136

LIST OF TABLES

Tables page

1-1. Summary of tracer techniques.....7

2-1. Experimental parameters and results for interfacial and partitioning tracer tests coducted with various medium sizes.....22

2-2. Experimental parameters and results of column tests conducted after ethanol flushing.....22

3-1. Mass transfer results and parameter values measured from column experiments with various grain sizes.....39

3-2. Mass transfer results with respect to reduction of NAPL saturation/interfacial area.....44

3-3. Mass transfer correlations.....48

4-1. Comparison of estimated a_c and b_c values from tracer solubility and partition experiments for four tracers.....70

4-2. Parameter values observed from miscible displacement experiments at low volume fractions of ethanol.....71

4-3. Comparison of parameter values observed from low and high NAPL (PCE) saturation column tests using 2,4-dimethyl-3-pentanol as a partitioning tracer.....76

5-1. Physical and chemical properties of surfactants used in the study.....86

5-2. Partitioning coefficients (K_{ns}) of alcohol tracers measured on various surfactant contents (% by weight).....90

5-3. Parameter values observed from column miscible experiments with PCE/DowFax 8390.....94

5-4. Results observed from pre- and post-flushing tracer tests and PCE mass balance from the flooding test with DowFax 8390 5%/AMA 80 3%/ NaCl 3%/ $CaCl_2$ 3%.....103

LIST OF FIGURES

Figures page

2-1. Experimental set-up.....16

2-2. Interfacial tensions measured at NAPL-SDBS solution interfaces.....19

2-3. Breakthrough curves of nonreactive tracer (bromide, symbol "×") and interfacial tracer (SDBS, symbol "o") from columns with various grain sizes as porous media. Shown are the plots on left-hand side without NAPL and on right-hand side with residual NAPL (PCE).....21

2-4. Geometric pore singlet models (Rhombohedral and Tetrahedral packing), log-log linear fit, and measured data for a_{nw}-d_{50} relationship.....24

2-5. NAPL-water interfacial area (a_{nw}) and trapped NAPL saturation (S_n) for different porous media sizes.....24

2-6. Breakthrough curves of nonreactive tracer (bromide, symbol "×") and interfacial tracer (SDBS, symbol "o") from column tests after ethanol flushing with various pore volumes (0, 4, 8, and 12 Pore volume).....26

2-7. NAPL-water interfacial area (a_{nw}) as a function of remained NAPL saturation (S_n) after ethanol flushing.....28

2-8. NAPL-water interfacial area (a_{nw}) as a function of NAPL dissolution.....28

2-9. Relationship of NAPL morphology index (H_N) and porous medium size. Shown are the symbols (data: ♦; fit data: solid line).....31

2-10. The H_N estimated using H_N-a_{nw}-S_n (Saripalli, 1997) and H_N-d_{50}-S_n relationships: Shown are also the predicted H_N with respect to varying NAPL saturation using the H_N-d_{50}-S_n relationship 31

3-1. An example BTCs of non-relative tracer (Br^-) fitted to an analytical solution to estimate logitudinal dispersion coefficient and dispersivity values.....40

3-2. Normalized PCE effluent concentration (C/C_s) versus pore water velocity.....41

3-3. Normalized PCE effluent concentration (C/C_s) versus specific interfacial area.....41

3-4 Bulk mass transfer rate coefficients (K_l) versus Reynolds number (Re) for various grain sizes.....42

3-5. Bulk mass transfer rate coefficients (K_l) versus specific interfacial area for various velocities.....42

3-6. Intrinsic mass transfer coefficients versus specific interfacial area for various velocities.....45

3-7. Bulk mass transfer rate coefficients (K_l) as a function of NAPL dissolution. $f_D = (S_n^* - S_n)/ S_n^* = 1- (S_n/ S_n^*)$ is volumetric fraction of dissolved NAPL; S_n^* is the initial NAPL saturation; S_n is the NAPL saturation remained after reduction of NAPL by dissolution.....45

3-8. Intrinsic mass transfer coefficients (k_l) as a function of NAPL dissolution 47

3-9. Averaged intrinsic mass transfer coefficients for various velocities.....47

3-10. Comparison of modified Sherwood numbers (Sh') from this study with previous investigation (d_{50} = 0.073 cm, a_{nw} = 44 cm^2/cm^3, S_n = 0.14, ϕ = 0.39, UI = 1.2) 51

3-11. Bulk mass transfer rate coefficients measured versus those predicted from the developed model ($Re/ a_{nw}/d_{50}$ model) for all data pooled together.....51

3-12. Intrinsic mass transfer coefficients measured with those predicted from the model (Re/Sc) for all data pooled together.....53

3-13. Damkohler number ($Da = k_i/v$) with respect to Reynolds number for various grain sizes.....53

3-14. Damkohler number ($Da = k_i/v$) with respect to specific interfacial area for various grain sizes.....54

4-1. Relationship between tracer solubility (S_c) and cosolvent content (%, volume) for (A) ethanol, (B) tert-butanol, and (C) isopropanol.....65

4-2. Solubility of 2,4DMP with respect to Tert-butanol content (%, volume).....66

4-3. Relationship between tracer partition coefficient (K_{nc}) and cosolvent content (%, volume) for (A) ethanol, (B) tert-butanol, and (C) isopropanol.....67

4-4. Comparison of the K_{nc} values from batch tests to the K_{col} estimated from column

tests for 4-methyl-2-pentanol, n-hexanol, 2-methyl-3-hexanol, and 2,4-dimethyl-3-pentanol in the ethanol/water system; ♦ Column test; ■ Batch test.....72

4-5. Breakthrough curves of residual ethanol cosolvent and partitioning tracers (n-hexanol and 2,4-dimethyl-3-pentanol) to display a degree of mixing, explaining the effect of residual ethanol on the NAPL saturation estimation. Initial residual ethanol content in the column is 10% (volume).....74

5-1. S-shaped adsorption isotherm for an ionic surfactant on an oppositely charged substrate.....81

5-2. Schematic diagram of the experimental set-up.....87

5-3. Relatioship between tracer partition coefficients (K_{ns}) and surfactant [(A) AMA-80, (B) DowFax 8390, and (C) Brij97] contents (%, weight).....91

5-4. Comparison of the K_{ns} values measured by batch tests to the K_{col} estimated by column tests for (A) n-hexanol and (B) 2,4-dimethyl-3-pentanol in the PCE/ DowFax 8390 system.....96

5-5. Results from column experiments with A) no surfactant, B) AMA 80, C) Brij 97, and D) DowFax 8390 adsorbed surfactants and no NAPL. Shown are BTCs for nonpartitioning tracer (methanol, plus symbols) and partitioning tracer (n-hexanol, circles).....98

5-6. BTCs of preflushing tracer test with only residual NAPL ($S_{PCE} = 0.16$), and post-flushing tracer test with residual NAPL ($S_{PCE} = 0.0125$) and surfactant (DowFax 8390).....101

5-7. BTC of removed PCE during the surfactant mixture flooding.....102

Abstract of Dissertation Presented to the Graduate School
of the university of Florida in Partial Fulfillment of the
Requirements for the Degree of Doctor of Philosophy

CHARACTERIZATION OF SPATIAL NAPL DISTRIBUTION, MASS TRASFER AND THE EFFECT OF COSOLVENT AND SURFACTANT RESIDUALS ON ESTIMATING NAPL SATURATION USING TRACER TECHNIQUES

By

Jaehyun Cho

December, 2001

Chair: Michael D. Annable
Major Department: Environmental Engineering Sciences

The non-aqueous phase liquid (NAPL) specific interfacial area and morphology as a function of pore size and NAPL dissolution were studied using the interfacial and partitioning tracer techniques. The NAPL-water interfacial areas increased in a log-linear fashion with decreasing grain sizes used as porous media, but did not show a clear trend with residual NAPL saturation formed in the various grain sizes. At a given grain size, however, the interfacial areas showed a proportional linear relation to a decrease in NAPL saturation by dissolution. The NAPL morphology indices, which represent the spatial NAPL distribution, increased exponentially with decreasing grain size.

Mass transfer across interfaces between NAPL and the aqueous phase was investigated. The investigations consisted of the influence of specific interfacial area, NAPL saturation, grain size, and aqueous phase velocity on mass transfer. Bulk mass transfer rate coefficients increased with increasing the specific interfacial area as well as

NAPL saturation and pore velocity, and with decreasing grain sizes. Whereas, intrinsic mass transfer coefficients were nearly independent of specific interfacial area and NAPL saturation, but dependent on pore velocity. Reduction of NAPL saturation by dissolution caused a linear decrease in the bulk mass transfer rate coefficients. Phenomenological correlation models developed using dimensionless Sherwood number produced good prediction for bulk and intrinsic mass transfer coefficients.

A series of batch and column tests was conducted to elucidate the influence of residual cosolvents and surfactants on partitioning and transport of alcohol tracers through soil columns containing residual tetrachloroethylene (PCE). Batch equilibrium tests showed that as the volume fraction of cosolvents (≤10%, vol.) increased, partitioning coefficients for alcohol tracers linearly decreased for ethanol, linearly increased for tert-butanol, and did not exhibit an evident relationship for isopropanol. The column tests using ethanol as a residual cosolvent exhibited earlier partitioning tracer breakthrough which caused an under-estimate of NAPL saturation. The under-estimates of NAPL saturation were 1 to 10% lower than the actual saturation. Comparison between low (0.5%) and high (15%) saturation columns revealed that the effect of residual cosolvent was different depending on the amount of NAPL in the column.

The influence of residual surfactants in aqueous and adsorbed phases on tracer transport behavior was evaluated by estimating PCE saturation using partitioning tracers. The batch equilibrium tests using residual surfactants ranging from 0.05 to 0.5% by weight showed that as the concentrations of the surfactants increased, the partitioning coefficients linearly decreased for Diphenyl oxide disulfonates (DowFax 8390), increased for Polyoxyethylene (10) oleyl ether (Brij 97), and decreased slightly or exhibit no

observable trend for Sodium dihexyl sulfosuccinate (AMA 80). Results from column tests using clean sand media with residual DowFax 8390 and PCE were consistent with those of batch tests. In the presence of DowFax 8390 (less than 0.5% by weight), the PCE saturations were underestimated by up to 20%. Adsorbed surfactants on a loamy sand soil with strongly positive charged oxides without PCE showed false indications of PCE saturation. Using no surfactant (background soil) gave a false PCE saturation of 0.0004 while AMA 80, Brij 97, and DowFax 8390 gave false PCE saturations of 0.0024, 0.043, and 0.229, respectively.

CHAPTER 1
INTRODUCTION

The contamination of soil and aquifers by organic contaminants is a major problem caused by leaks, spills, and disposal of waste over long periods of time. A large amount of organic substance has contaminated many sites and the threat to public health has been recognized. Many of these contaminants exist as liquids immiscible with water. The immiscible fluids serve as a long-term source contributing to groundwater contamination. Most contaminants slowly dissolve and produce plumes that spread over long distances from the source. Although the solubility of the contaminants is very slight, it can affect groundwater quality both for drinking water and water supplied to ecosystems. Characterizing these sources is a necessary primary step to cleaning up the contaminants in an efficient and effective manner.

Characterization methods used for contaminant source zones can be divided into three periods: before, during, and after remedial efforts. Before remediation, characterization processes include estimating of saturation of liquids and distributing contaminants in the target area. In the past, estimation has been typically achieved by historical information, soil core samples, and inferences based on groundwater concentration. These methods were used to estimate site characteristics through a partial search of the target area. Given the difficulty and cost of complete site characterization, the recently proposed partitioning and interfacial tracer techniques for characterization of contaminant source in the aquifer can be useful tools.

Tracer Techniques

Tracer techniques can be divided into four categories; nonreactive tracers, partitioning tracers, interfacial tracers, and biogeochemical tracers (Rao et al., 2000) (Table 1-1). The partitioning tracer technique has been used in the petroleum industry to estimate oil saturation and was initially developed by Cooke (1971) and Dean (1971). Jin et al. (1995) proposed the application for characterization of contaminant source zones in aquifers. The partitioning tracer technique, based on the travel time difference between nonpartitioning and partitioning tracers, is a method to quantify the nonaqueous phase liquids (NAPLs) trapped in a swept zone (Jin et al., 1995; Annable et al., 1995). The applicability of this technique has been evaluated through field applications in previous studies (Rao et al., 1997; Annable et al., 1998; Sillan et al., 1999; Jawitz et al., 1999). Use of a network of multi-level samplers can provide information about the spatial location of NAPL (Annable et al., 1994, 1998; Rao at al., 1997). Jawitz (1999) extended the method to estimate NAPL spatial distribution using higher moments of partitioning tracer breakthrough curves measured at a single well. Appropriate tracers and concentration range should be carefully selected to minimize the time required to conduct the tracer study (Annable et al., 1995) as well as error by nonlinear tracer partitioning (Wise, 1999).

Interfacial tracers were first developed by Saripalli et al. (for NAPL-water, 1997) and Kim et al. (air-water, 1997). The first field application to estimate NAPL-water interfacial area along with NAPL saturation took place at Hill AFB in 1996 (Annable et al., 1998). The interfacial tracer technique is a method to estimate specific interfacial area between NAPL and water in a swept zone (Saripalli et al., 1997, 1998; Kim et al., 1997, 1998; Annable et al., 1998). For the partitioning and interfacial tracer techniques, the

basic approach is the same since they are both based on travel time differences between nonreactive and reactive tracers. Unlike partitioning tracers, however, interfacial tracers are retarded because of tracer adsorption at interfaces between phases. The adsorption isotherm for interfacial tracers can be determined using the Gibbs model, which is based on a nonlinear correlation between tracer concentration and surface/interfacial tension. Kim et al.(1997) reported that for gaseous interfacial tracers, a linear isotherm approximation is valid at low concentration.

The combined tracer techniques (partitioning and interfacial tracers) makes it possible to characterize spatial NAPL distribution in the subsurface (Saripalli et al., 1997; Annable et al., 1998). The ratio of interfacial area to volumetric NAPL content, which is defined as a contaminant morphology index, shows how the contaminant is distributed in a porous medium (Saripalli et al., 1997). NAPL characterization can provide information important in characterizing remedial performance efficiency. The efficiency often depends on the contact area between NAPL and flushing agents. The contact area is related to the effective NAPL-water interfacial area as well as NAPL morphology. The interfacial area and morphology are characterized by capillary forces (Sarapalli et al, 1998). This shows that porous media size can act as a primary factor related to interfacial area as well as the morphology of trapped NAPL.

In Chapter 2, the dependence of specific NAPL-water interfacial area and NAPL morphology on pore size was investigated using the combined tracer techniques. Various grain sizes of sand as porous media were used to measure NAPL saturation and interfacial area. The observed results were correlated to evaluate their relationships with

respect to grain size. In addition, NAPL-water interfacial area was investigated as a function of the reduced NAPL saturation by dissolution.

NAPL characterization process during a remediation effort is related to its efficiency. The efficiency depends on contact area and time between NAPL and a flushing agent as well as the type of flushing agents. We can assume that the contact area is same as to an effective interfacial area between NAPL and aqueous phase. In a chemical remediation work based on NAPL dissolution, it is especially important to investigate the relationship of NAPL-water interfacial area and mass transfer rate to predict the remediation efficiency. To date, most studies were limited in investigation of overall mass transfer rate coefficient, which is defined as the product of a mass transfer coefficient and the specific interfacial area because of the difficulty in measuring NAPL-water interfacial area (Miller et al., 1990; Powers et al., 1992; Imhoff et al., 1997; Mayer et al., 1999). In Chapter 3, mass transfer across NAPL-water interfaces was studied using the NAPL-water specific interfacial areas measured in Chapter 2. It was related to how the specific interfacial areas and other related factors (NAPL saturation, grain size, and pore velocity) contribute to bulk and intrinsic mass transfer coefficients. In addition, prediction models using dimensionless Sherwood number were developed and verified through comparison with measured and predicted values. Nonequilibrium process in the mass transfer can be also a critical factor to predict the remediaiton efficiency. It is a rate-limited process related to physichemical properties such as flow velocity. The nonequilibrium mass transfer here was described with the observed system parameters such as NAPL-water interfacial area and pore velocity.

NAPL characterization after remediation efforts is related to performance assessment of clean up. A primary purpose of the post-remediation works is quantification of remaining and removed NAPL, which can be evaluated by the partitioning tracer technique. After remedial flushing, some amounts of flushing agents, such as cosolvent or surfactant, are likely to remain in the swept zone. The residual flushing agents can modify the chemical properties of partitioning tracers such as activity and solubility, and partitioning behaviors. The resulting effects can cause some errors on NAPL saturation estimation. In Chapter 4, the influence of residual cosolvent was investigated on NAPL volume estimation using partitioning tracers. Partitioning coefficients and solubilities of alcohol tracers were measured in the presence of cosolvents with varying concentration. The observed results were verified through miscible displacement tests. Additionally, the dependence of the cosolvent impact on the magnitude of residual NAPL saturation was evaluated on the NAPL saturation estimate.

Surfactants tend to remain adsorbed on the solid phase and dissolved in the aqueous phase after surfactant flooding efforts. Above the critical micelle concentration, surfactant molecules form micelles including a hydrophobic inner core in which the alcohol tracers can partition. Also, adsorbed surfactants can act as a good adsorbent for hydrophobic chemicals (Ko et al., 1998a), causing tracer retardation. These processes can be a problem for NAPL saturation estimation based on retardation of partitioning tracers. In Chapter 5, the influence of residual surfactants was investigated on NAPL saturation estimation using partitioning tracers. Anionic and nonionic surfactants with varying concentration were used to investigate influences on partitioning coefficients and transports of alcohol tracers. A positively charged soil was also used to investigate the

effects of adsorbed surfactants on retardation of partitioning tracers. The observed results were used to evaluate a false indication of NAPL saturation.

Table1-1. Summary of tracer techniques (adapted from Rao et al., 2000)

Attribute	Partitioning tracers	Interfacial tracers	Biogeochemical tracers
Tracers used	Low molecular weight; methyl-substituted alcohols; Radon-222	Anionic and cationic surfactants; high molecular weight alcohols	Biologically labile carbon compounds (benzoate, sugars)
Parameter estimated	NAPL residual saturation (average, and spatial patterns)	Interfacial area (average, and spatial patterns)	Transformation rate constant (average, and spatial patterns)
Applications	NAPL distribution; remediation effectiveness; impacts of remediation	NAPL "morphology"; interfacial mass transfer	Potential for abiotic and biotic reaction rates
Mechanisms	Phase partitioning	Interfacial adsorption	microbial or geochemical reaction
Isotherm model	$C_n = K_n C_w$	$\Gamma = -\frac{C}{2RT}\left(\frac{d\gamma}{dC}\right)_{T,C=C_0}$	$C_s = K_d C_w$
Retardation model	$R_{pt} = 1 + \frac{S_n K_n}{(1-S_n)} + \frac{\rho K_d}{\theta_w}$	$K_i' = -\frac{1}{2RT}\left(\frac{d\gamma}{dC}\right)_{T,C=C_0}$, $R_{ift} = 1 + \frac{\rho K_d}{\theta_w} + \frac{a_i K_i'}{\theta_w}$	$R_d = \frac{R_{non-d}}{\sqrt{1+\frac{4\omega}{P}}}$
Degradation model	N/A	N/A	Zero- or first-order

K_n is the NAPL–water partition coefficient; K_d is soil sorption coefficient, ρ is soil bulk density; θ_w is the volumetric water content; S_n is the NAPL saturation; a_i is the NAPL–water interfacial area; K_i is the interfacial adsorption coefficient; R is the retardation factor, with the subscripts pt and ift, indicating partitioning and interfacial tracers; R is gas constant, T is absolute temperature; γ is the NAPL–water interfacial tension; C and C_0 are tracer concentration in the effluent and influent solutions, respectively; ω is dimensionless rate constant; P is Peclet number; R_d is retardation factor for a degrading tracer; R_{non-d} is retardation factor for a non-degrading tracer.

CHAPTER 2
CHARACTERIZATION OF SPATIAL NAPL DISTRIBUTION BY COMBINED USE OF PARTITIONING AND INTERFACIAL TRACER : USING GRAIN SIZE AND NAPL DISSOLUTION

Introduction

Characterization of NAPL introduced into the subsurface is difficult because of complex intra- and inter-relationships between NAPL and soil properties. NAPL source zone characterization requires knowledge of physio-chemical characteristics such as the pore size distribution of a soil and the volume, shape, size, and spatial distribution of NAPL. Capillary forces, which are results of the unbalanced forces from solid-liquid adhesion and liquid-liquid cohesion, are inversely proportional to soil pore size. NAPL is trapped in the pore space as isolated ganglia due to capillary forces. Thus, the pore size of porous media can determine trapped NAPL saturation and morphology. The quantity and distribution of the trapped NAPL is closely related to the ratio of pore body to pore neck radii, which is called the aspect ratio. Homogeneous packs of uniform size media have a low aspect ratio and NAPL blobs are nearly spherically shaped, single pore bodies, whereas heterogeneous packs have a high aspect ratio and are irregularly shaped, and can be connected by multiple pores (Chatzis et al., 1983; Morrow and Heller, 1985). Thus, pore size and pore size distribution can be significant parameters for characterization of trapped NAPL in porous media.

The primary consideration in trapped NAPL characterization is likely estimation of the amount of residual NAPL and interfacial area between NAPL-water in the subsurface. Residual NAPL can be quantified using the partitioning tracer technique proposed by Jin et al. (1995). Its usefulness and effectiveness in measurements of NAPL trapped in the subsurface have been reported in laboratory and field tests by previous researchers (Jin et al., 1995; Annable et al., 1995, 1998a,b; Rao et al., 1997; James et al., 1997; Sillan et al., 1998; Jawitz et al., 1999, 2000; Zhang et al., 2001; Wu et al., 2001). Interfacial area between NAPL and water is also an important factor for characterizing NAPL of distribution. Many approaches have been used to predict specific NAPL-water interfacial area, such as geometric analysis (Gvirtzman and Roberts,1991), thermodynamic models (Leverett, 1941; Bradford and Leij, 1997), pore singlet models (Saripalli, 1997), and empirical models (Cary, 1994). These approaches were used to predict the specific interfacial area through theoretical methods. Recently, the interfacial tracer technique, using surface adsorption of surfactant, was developed to measure interfacial areas between fluids: liquid-liquid (Saripalli et al., 1997); and liquid-air (Kim et al., 1998, Rao et al., 2002). The interfacial tracer technique has been evaluated through field and laboratory tests in several previous studies (Saripalli et al., 1997, 1998; Annable et al., 1998; Kim et al., 1998, 1999; Rao et al., 2000). Because partitioning and interfacial tracers can be used in tandem, characterization of spatial NAPL distribution is feasible.

The objective of this study is to characterize spatial NAPL distribution as a function of the mean grain size and NAPL reduction by dissolution. NAPL-water interfacial area and trapped NAPL saturation were measured using tracer techniques for various media sizes as well as gradually reducing NAPL saturation. The functional

relationships between mean grain size (or NAPL dissolution) and NAPL-water interfacial area (or NAPL saturation) were investigated and then evaluated in terms of spatial NAPL distribution. Finally, the measured results were also used to develop an empirical model to evaluate NAPL morphology as a function of grain size.

Theoretical Background

Adsorption Coefficients

Surfactants have been used as interfacial tracers because of their unique tendency to accumulate at the interface between two immiscible fluids such as NAPL-water (Saripalli et al., 1997; Annable et al., 1998; Kim et al., 1998). The interfacial tracer technique is an indirect measurement: that is, the amount of adsorbed surfactant per unit interface area is calculated from interfacial tension measurements. The adsorption of surfactant at the NAPL-water interface can be described by the Gibbs adsorption equation (Rogen, 1989; Adamson, 1982):

$$\Gamma = -\frac{C}{2RT}\left(\frac{d\gamma}{dC}\right)_T \qquad (2\text{-}1)$$

where Γ (mM/cm^2) is the Gibbs surface excess of surfactant or the interfacial adsorption; γ (dynes/cm) is the interfacial or surface tension; R is the Universal gas constant (dyne-cm/Mm °K); C is the bulk concentration of surfactant (mM/cm^3); and T is absolute temperature (°K). If the surfactant adsorption from aqueous bulk solution occurs in the presence of a swamping constant amount of electrolyte (1:1 elctrolyte) containing a common nonsurfactant counterion, the Gibbs equation (Eq. 2-1) is used without the factor 2 in the denominator (Rogen, 1989; Adamson, 1982).

The Gibbs equation (Eq. 2-1) can be used to determine the interfacial adsorption coefficient, which describes equilibrium adsorption between the interface and the bulk aqueous solution. The interfacial adsorption coefficient (K_i) is expressed as (Saripalli et al., 1997; Kim et al., 1997):

$$K_i = \frac{\Gamma_o}{C_o} = -\frac{1}{2RT}\left(\frac{\partial \gamma}{\partial C}\right)_{T,C=Co} \tag{2-2}$$

where C_0 is the influent tracer concentration. Equation (2-2) requires knowledge of the interfacial tension (γ) as a function of aqueous concentration of surfactant (C) used as the interfacial tracer. The γ-C relationship can be obtained by measuring interfacial tension at various surfactant concentrations. The γ-C relationship can be approximated by nonlinear adsorption regression with the Freundlich sorption model. Then, the K_i can be determined from the slope of the γ-C plot. Measurements of NAPL-water partitioning coefficients for alcohol tracers were described in Chapter 4 and 5.

Interfacial Area Estimate

The interfacial tracer technique is based on measuring retardation of the interfacial tracer relative to a nonreactive tracer. It can be used as a method appropriate for NAPL-water phases with the following four assumptions: (1) the interfacial tracer adsorbs at the NAPL-water interface but does not partition or dissolve into the NAPL; (2) the adsorption culminates as a monolayer coverage; (3) each tracer molecule occupies a known molecular area; and (4) the tracer solution does not alter the properties of the NAPL. The interfacial tracer is retarded due to adsorption at the NAPL-water interface during its travel through a porous medium under steady water flow. The retardation factor

(R_{ift}) of interfacial tracer with respect to the non-reactive tracer is defined as (Saripalli et al., 1997):

$$R_{ift}=\frac{\mu_{ift}}{\mu_{nr}}=1+\frac{a_{NW}K_i}{\theta_w}+\frac{\rho K_s}{\theta_w} \tag{2-3}$$

where the subscripts *ift* and *nr* describe interfacial and nonreactive tracers, respectively; K_i (cm) is the interfacial adsorption coefficient; θ_w is the volumetric water content; K_s (mL/g) is the tracer adsorption coefficient onto the solid matrix; ρ is the bulk density (g/cm^3). For a step-input tracer experiment, μ can be obtained by integrating the area above the breakthrough curve measured for continuous tracer input:

$$\mu = \int_0^\infty (1-\frac{C}{C_0})dt \tag{2-4}$$

where C_0 is the influent tracer concentration; C is the effluent tracer concentration. For a pulse-input tracer experiment, μ can be obtained by the first, normalized, temporal moment adjusting for the finite pulse duration of t_0:

$$\mu=\frac{\int_0^\infty t\,C\,dt}{\int_0^\infty C\,dt}-\frac{t_0}{2} \tag{2-5}$$

The NAPL-water interfacial area can be estimated by arranging equation (2-3):

$$a_{NW}=\frac{(R_{ift}-1-\rho K_s/\theta_w)\theta_w}{K_i} \tag{2-6}$$

Note that $K_s = 0$ if the tracer adsorption onto the solid matrix is negligibly small.

NAPL Saturation Estimate

Partitioning tracers are retarded due to interaction with NAPL during travel through a porous medium under steady water flow. The retardation factor of a partitioning tracer (R_p) is a measure of the tracer mobility. The R_p is obtained by dividing the first temporal moment of a partitioning tracer by the normalized first temporal moment of a non-partitioning tracer. The R_p is given by Jin et al.(1995):

$$R_p = \frac{\mu_p}{\mu_{nr}} = 1 + \frac{S_n K_{nw}}{(1 - S_n)} + \frac{\rho K_d}{\theta_w} \tag{2-7}$$

where the subscripts p denotes partitioning tracer; K_{nw} is the partitioning coefficient between NAPL and water, which is determined by the slope of the regressed curve between partitioning tracer concentrations distributed into NAPL and water phases; K_d (mL/g) is the tracer distribution coefficient onto the solid matrix. Partitioning tracer tests have generally been performed using a pulse input experiment and the μ can be obtained by equation (2-5). When sorption of the tracer to the background soil is negligible (K_d = 0), the NAPL saturation (S_n) is can be estimated by rearranging equation (2-7):

$$S_n = \frac{(R_p - 1)}{(R_p - 1 + K_{nw})} \tag{2-8}$$

NAPL Morphology Index

As NAPL migrates through the subsurface, the trapped NAPL saturation can be influenced by capillary forces and ambient groundwater flow conditions. The retained

NAPL can exist in several forms, such as single large or small blobs, doublets or extensive ganglia, and films sorbed on the porous media. The morphology of NAPL trapped can be different depending on pore size as well as NAPL saturation. As NAPL saturation increases in a unit pore space, the blobs of trapped NAPL are larger and thicker. This results in a decrease of interfacial area per unit NAPL volume. The ratio of interfacial area to volumetric NAPL content provides information on how the NAPL is distributed within the pore space. Saripalli at al. (1997) proposed the ratio of NAPL-water interfacial area to NAPL saturation as a NAPL morphology index (H_N):

$$H_N = \frac{a_{nw}}{\phi S_n} \tag{2-9}$$

where a_{nw} is the NAPL-water interfacial area per unit volume of porous media; S_n is the NAPL saturation or volume of NAPL per unit volume of pore space; ϕ is the soil porosity. A high value in H_N indicates that NAPL is spread out, thus providing large contact area between the NAPL and aqueous phase. In contrast, small value in H_N indicates that the NAPL is locally isolated in small pools.

Materials and Methods

Materials

Sodium dodecylbenzenesulfonate (SDBS, Aldrich, 85%) and potassium bromide (KBr, Fisher, 98%) were used as interfacial and non-reactive tracers, respectively, for interfacial tracer tests. Tetrachloroethylene (PCE, Acros, 99 %), colored red with Oil-red-

O dye ($\leq 1 \times 10^{-2}$ mM, Fisher) was used as a NAPL for all column experiments. A suite of partitioning tracers was selected to examine the effects of varying retardation factors. Methanol (Fisher, 98 %) was used as a non-partitioning tracer while 3,3 dimethyl-2-butanol (3,3DMB) (Acros, 99+ %) and n-hexanol (Acros, 98 %) were used as partitioning tracers. Silica sand with various particle sizes (0.165 – 1.425 mm) was used as porous media in all column experiments. The sand was sieved, washed with water, oven-dried at 105°C for 24 hr, and baked at 550°C for 24 hr. The baked sand was washed several times with concentrated nitric acid to remove metals, washed with water and dried in oven for 24hr, before use as porous media. All experiments were conducted at room temperature ($23 \pm 1\,^{\circ}C$).

Interfacial Tension Measurement

NAPL-water interfacial tensions (γ) were measured at various SDBS concentrations ranging from 0 to 2 mM (0 - 697 mg/L) (Appendix A). Glass crystallization vessels (50 mm diam. × 35 mm depth) were cleaned for IFT measurements using the procedure of Wilson et al. (Wilson et al., 1990). The interfacial tensions (IFT) between the PCE with 0.01 mM Oil-red-O dye and SDBS solution at various concentrations were measured using a Du Nuoy ring tensiometer (Fisher Scientific Model 21 Tensiomat). The measured interfacial tensions were used to estimate the adsorption coefficient of the interfacial tracer (SDBS).

Miscible Displacement Tests

The columns used for all miscible displacement experiments were glass columns, 2.54 cm in diameter and 5 cm in length (HPLC column, Kontes company) with Teflon end pieces and fine wire mesh screen. The packing and assembling procedures of

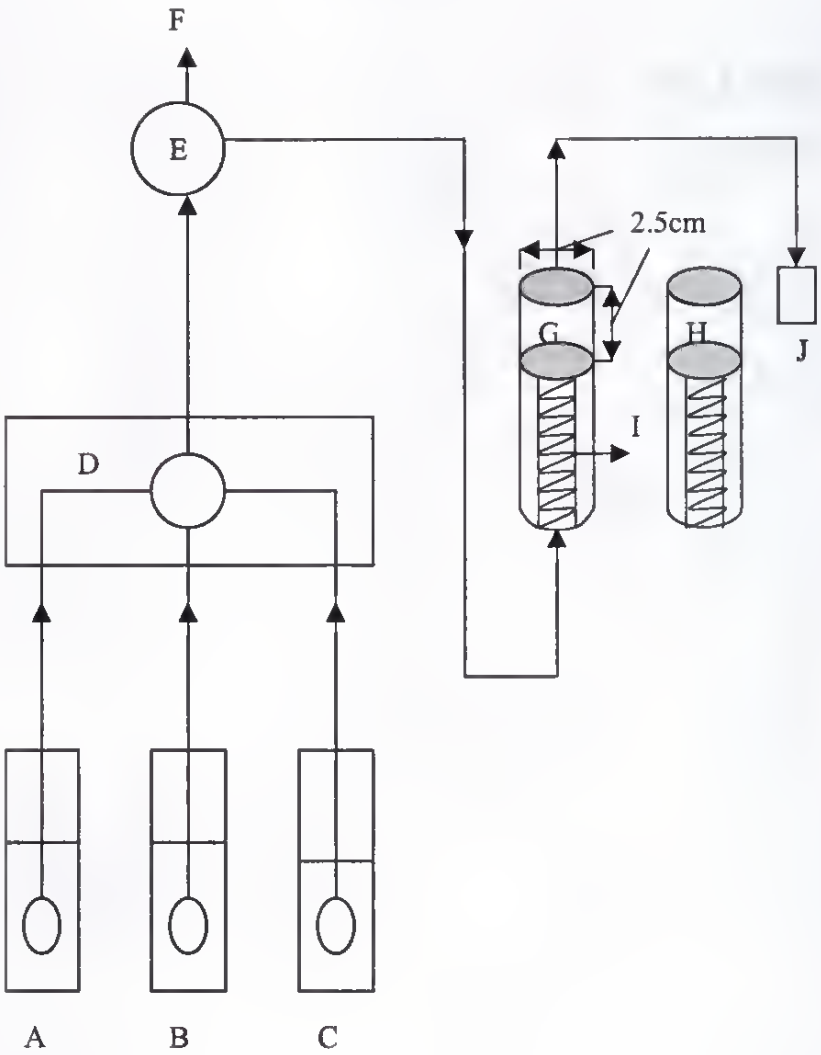

A : Bromide Solution
B : SDBS Solution
C : Water
D : HPLC Pump
E : Switching Valve
F : Waste
G : Sand /PCE Column
H : Sand Column
I : Adjustable Adapter
J : Sampling Vial

Figure 2-1. Experimental set-up

columns were accomplished under water to avoid trapped air, which can cause an error due to the air-water interface.

Two series of miscible displacement tests were performed for this study. The schematic diagram of the experimental set-up is shown in Figure 2-1. The first series of miscible displacement tests was conducted using the columns packed with various sizes of clean sand to investigate NAPL-water interfacial area, NAPL saturation, and morphology as a function of pore size. Each column was packed with each sand size (10/20, 20/30, 30/40, 40/60, and 80/100 mesh) up to 2.5 cm in length using an adjustable adapter (Figure 2-1), and cleaned by passing 20 pore volumes (PV) of degased DI water. Before injecting NAPL (PCE) for all the columns, both non-reactive tracer (Br^-) and interfacial tracer (SDBS) tests (step-input) were conducted to measure background adsorption of interfacial tracer on to sand, producing tracer retardation. The Br^- and SDBS concentration used in this study were approximately 50 mg/L. Then, PCE was introduced in the water-saturated columns using a syringe pump at gradually increased water flow rates (0.1, 0.2, 0.5, 1, 3, 5, and 7 mL/min) until no water was observed in the outlet of the columns. Some of the PCE was then displaced with water through both up- and down-flow modes to create a homogeneous distribution of trapped PCE. Residual saturation of PCE was achieved by gradually increased flow rates (0.1, 0.2, 0.5, 1, 3, 5, and 7 mL/min steps). Non-reactive tracer and interfacial tracer tests were separately run with residual NAPL to estimate NAPL-water interfacial areas applying step-inputs until the relative concentration (C/C_o) reached unity. Then, partitioning tracer tests (pulse input) were conducted to measure the residual PCE volume or saturation.

The second series of miscible displacement tests was conducted to investigate a_{nw}, H_N, and S_n as a function of NAPL dissolution. A column packed with 20/30 mesh sand from the previous series was used and prepared for each miscible displacement experiment by flushing a 4 pore volume (PV) 50 % (by volume) ethanol solution through both ends of the column. Each flushing resulted in reduction of about 20 % of the total residual PCE. No free phase PCE was observed in the effluent during flushing. This indicates that NAPL reduction was by dissolution, not mobilization. The columns were then flushed with 5 PV of water. Non-reactive, interfacial, and partitioning tracer tests were conducted next using the procedures described for the first series of experiments. A HPLC pump (Shimadzu 500) was used to inject water and tracer solutions at a steady flow rate (0.5 mL/min).

Analytical Methods

Samples from partitioning tracer tests were collected in 2 mL vials with a 100 µL insert and analyzed for alcohols by Gas Chromatography (Perkin Elmer GC, Autosystem XL) with a flame-ionization detector. Br^- (205 nm) and SDBS (225 nm), from interfacial tracer experiments, were analyzed using a high performance liquid chromatography (HPLC) systyem (Perkin Elmer series LC 200) with UV detector.

Results and Discussion

Estimation of Interfacial Adsorption and Partitioning Coefficients

The interfacial adsorption coefficient (K_i) was estimated from a relationship of NAPL-water interfacial tension and tracer bulk concentration based on Gibbs adsorption

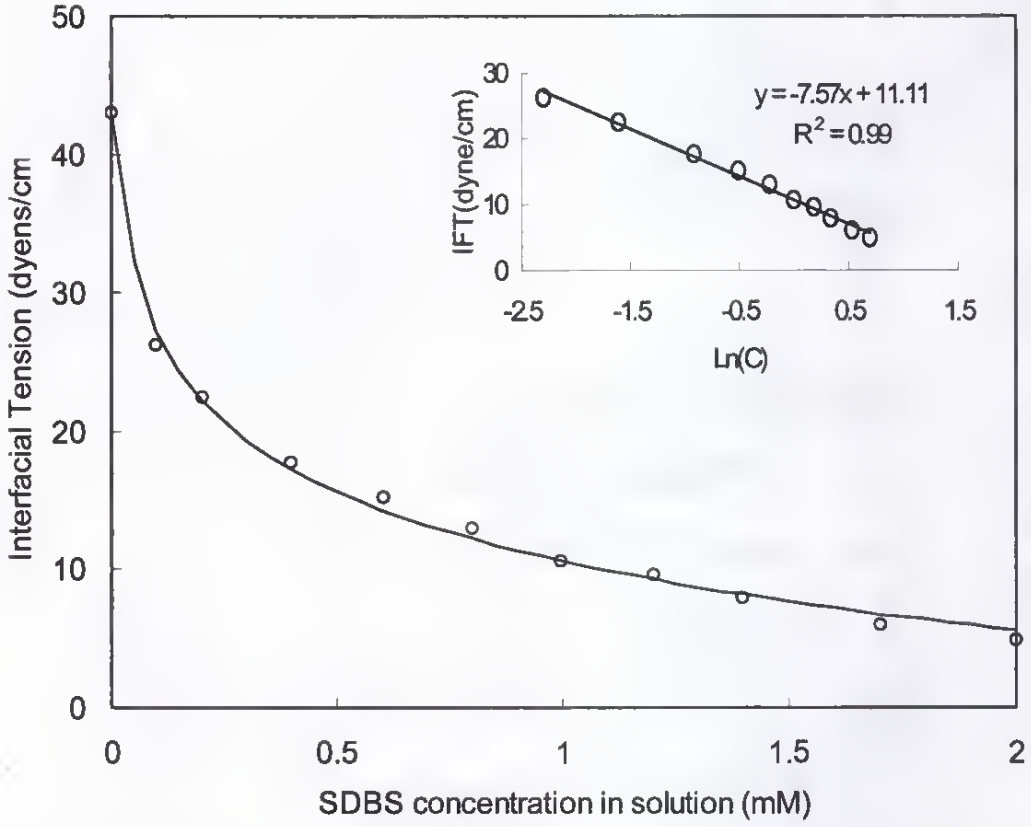

Figure 2-2. Interfacial tensions measured at NAPL-SDBS solution interfaces

equation (2-2). The interfacial tensions (γ) measured at various PCE-tracer solution interfaces are shown in Figure 2-2. The γ values decreased in log-linear fashion with increasing surfactant (SDBS) concentration. The relationship is

$$\gamma = \alpha - \beta \ln C \tag{2-10}$$

The observed α and β were 11.1 and 7.575, respectively, with a coefficient of determination (R^2) of 0.99. Using the Equation 2-2 with C_0 (= 0.14 mM) and T (= 297 °K), the estimated K_i value was 1.07×10^{-3} (cm). Note that the K_i value increases with decreasing tracer concentration (C_0), causing an increase of the tracer retardation due to interfacial adsorption. Additionally, the C_0 for the tracer solution should be below the CMC.

The partitioning coefficients (K_{nw}) for the alcohol tracers were measured in batch isotherm tests. The tracer partition equilibrium data obtained from batch tests were fit using a linear isotherm to obtain the K_{nw}. The observed K_{nw} values for 3,3 DMB and n-hexanol were 4.8 and 6.8, respectively, with R^2 of 0.998. The K_{nw} values along with retardation factors measured from column tests were used to estimate residual NAPL saturation.

NAPL-Water Interfacial Area and NAPL Saturation as a Function of Pore Size

NAPL-water specific interfacial areas and NAPL saturations were investigated through columns with various mean grain sizes ranged from 0.15 to 1.42 mm. First, tracer experiments for all the columns in the absence of NAPL were conducted to measure the background adsorption of the interfacial tracer onto sands used as porous media and the column assembly. BTCs for non-reactive (Br^-) and interfacial (SDBS) tracers are shown

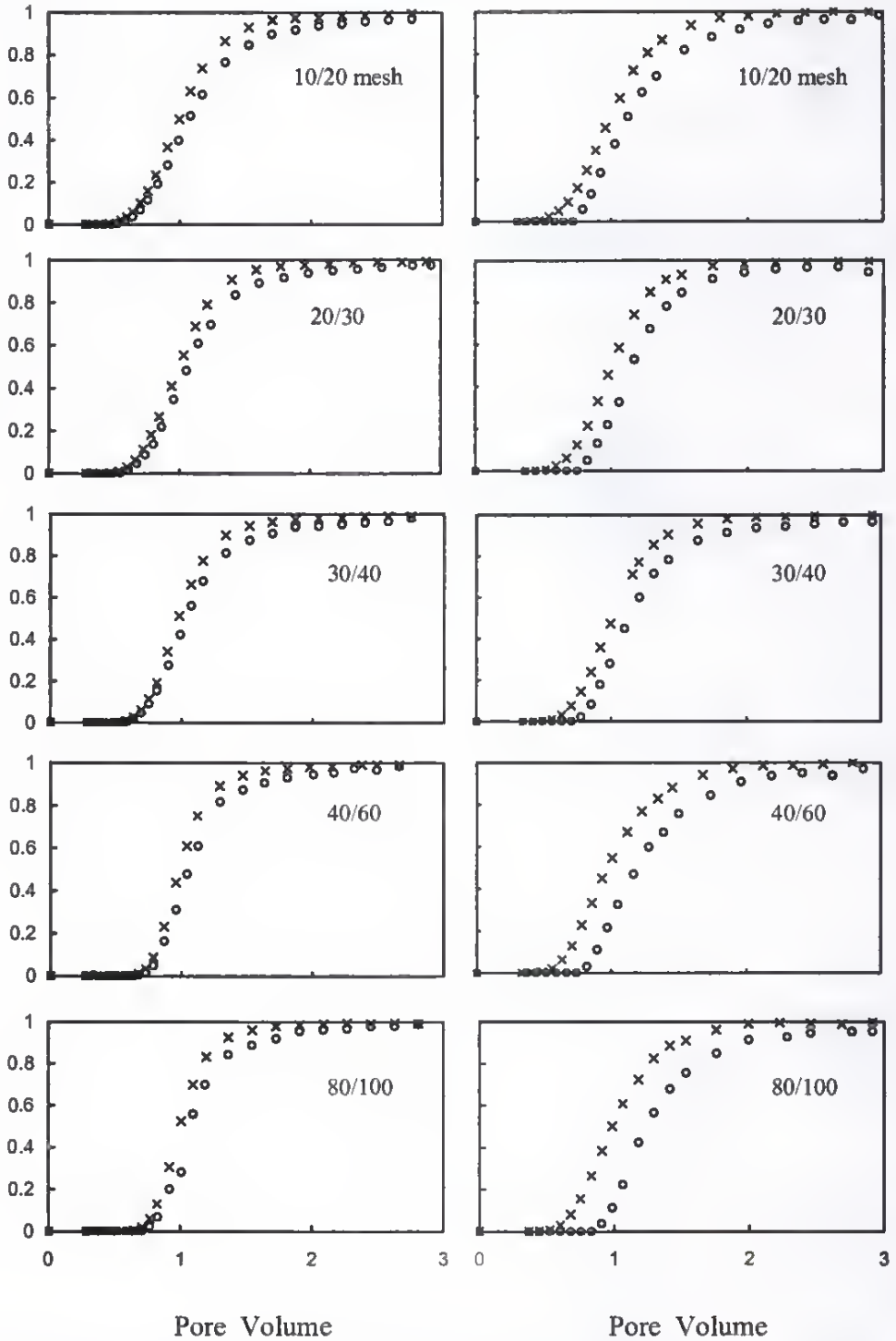

Figure 2-3. Breakthrough curves of non-reactive tracer (bromide, symbol "×") and interfacial tracer (SDBS, symbol "o") from columns with various grain sizes as porous media. Shown are the plots on left-hand side without NAPL and on right-hand side with residual NAPL (PCE).

Table 2-1. Experimental parameters and results for interfacial and partitioning tracer tests conducted with various medium sizes.

Media	d_{50} (mm)	θ_w	$R_{(back)}$	$R_{(back+ift)}$	R_{ift}	K_s cm^3/g	K_i 10^{-3}(cm)	a_{nw} (cm^2/cm^3)	R_p DMB	R_p n-hexanol	S_n	H_N (cm^{-1})
10/20	1.425	0.38	1.136	1.216	1.080	0.021	1.07	28	1.63	1.88	0.116	570
20/30	0.725	0.34	1.125	1.263	1.138	0.017	1.07	44	1.75	2.07	0.137	793
30/40	0.513	0.37	1.124	1.254	1.130	0.018	1.07	44	1.68	1.97	0.124	832
40/60	0.338	0.35	1.115	1.342	1.227	0.016	1.07	74	1.86	2.25	0.154	1129
80/100	0.165	0.34	1.119	1.462	1.343	0.016	1.07	110	1.89	2.25	0.155	1670

Table 2-2. Experimental parameters and results of column tests conducted after ethanol flushing.

Media	Flushing (etbanol 50%)	θ_w	R_{back}	$R_{(back+ift)}$	R_{ift}	K_i 10^{-3}(cm)	a_{nw} (cm^2/cm^3)	R_p DMB	R_p n-hexanol	S_n	f_D	H_N (cm^{-1})
20/30	0PV	0.34	1.125	1.263	1.138	1.07	44	1.75	2.10	0.14	0	793
20/30	4PV	0.36	1.125	1.237	1.112	1.07	38	1.56	1.81	0.11	0.23	876
20/30	8PV	0.37	1.125	1.218	1.093	1.07	32	1.41	1.59	0.08	0.41	976
20/30	12PV	0.40	1.125	1.192	1.067	1.07	25	1.25	1.37	0.05	0.62	1178

on the left-hand side in Figure 2-3. The BTCs indicated that SDBS used as interfacial tracer was retarded due to adsorption onto the sand or column assembly. The measured background retardation factor (R_{back}) for all the columns were in range of 1.12 to 1.14 and the corresponding adsorption coefficients (K_s) were estimated to be from 0.016 to 0.021 (cm^3/g) (Table 2-1). The observed background retardations are likely due to metal oxides (e.g., FeO_3, 0.02%; Al_2O_3, 0.06%; TiO_2, 0.01%, etc., US. Silica Company, 2001) present in the clean sand used. Even though the sands were washed with nitric acid to remove the metal oxides, some likely remain. The background partitioning of alcohol tracers onto the porous media (clean sand) was not observed, and thus the K_d in the Equation 2-7 was set equal to zero.

Second, tracer experiments in the presence of residual NAPL (PCE) with Oil-red-O dye (0.1×10^3 mM) were conducted to estimate the a_{nw} as well as the S_n. Since PCE saturated water was used during all the column experiments, reduction of tracer retardation by loss of PCE mass can be ignored (less than 1%). In addition, since the concentration of SDBS solution (= 0.14 mM) used was much less than the CMC (about 1.2 mM), loss of PCE mass due to enhanced solubilization or mobilization during all the experiments did not occur. Table 2-1 summaries the measured R_{ift}, a_{nw}, R_p, S_n, and H_N values along with column parameters. BTCs for Br^- and SDBS are shown on the right-hand side in Figure 2-3. The degree of retardation of SDBS relative to Br^- was evident on the sand sizes used as porous media. The measured retardation factors ($R_{back+ift}$) were subtracted from the earlier measured R_{back} to evaluate the retardation of SDBS by NAPL-water interface. Here we assume that two retardation domains are independent. The resulting R_{ift} data were then used to calculate a_{nw} using the Equation 2-6. The measured

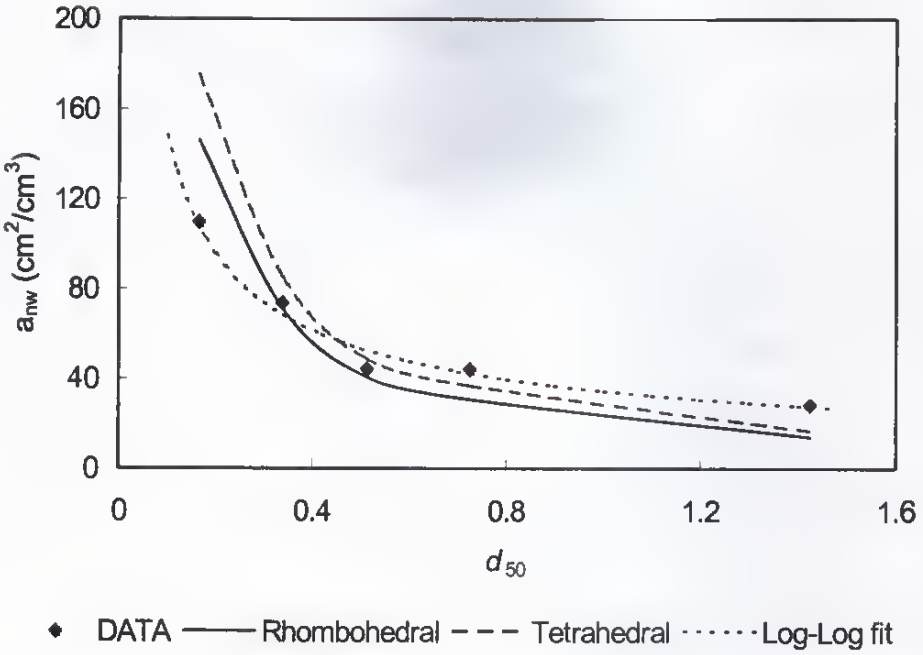

Figure 2-4. Geometric pore singlet models (Rhombohedral and Tetrahedral packing), log-log linear fit, and measured data for a_{nw} - d_{50} relationship.

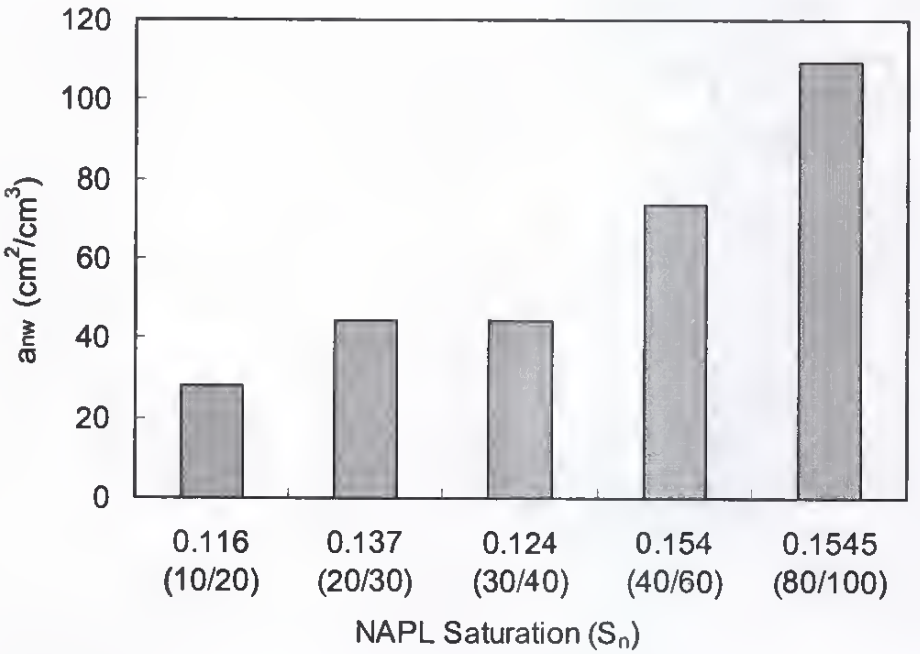

Figure 2-5. NAPL-water interfacial area (a_{nw}) and trapped NAPL saturation (S_n) for different porous media sizes.

a_{nw} values (74 to 110 cm^2/cm^3) for grain size ranging in 0.15 to 0.425 mm agreed reasonably with 77 to 91 cm^2/cm^3 for similar sand size (0.15 to 0.35 mm) observed in an earlier study (Saripalli et al, 1998). The following empirical function was fit to the a_{nw} -d_{50} data:

$$\ln(a_{nw}) = 3.54 - 0.635\ln(d_{50}) \qquad R^2 = 0.966 \qquad (2\text{-}11)$$

The a_{nw} increased exponentially with decreasing grain size used as packing media. This implies that the NAPL ganglia trapped in a finer media are smaller in size but the number of the ganglia increases exponentially, causing a corresponding increase in the a_{nw}. Such observation is likely to be more obvious by comparing to a previous prediction model. Saripalli (1997) proposed a pore singlet model to predict the specific NAPL-water interfacial area as:

For a rhombohedral packing,

$$a_{nw} = \frac{4.19\, S_n^{2/3}}{r} \qquad (2\text{-}12)$$

For a tetrahedral packing,

$$a_{nw} = \frac{5.02\, S_n^{2/3}}{r} \qquad (2\text{-}13)$$

where r is the mean radius of porous media. As shown in Figure 2-4, the trend in the measured a_{nw}-d_{50} relationship agrees with the predicted values using the pore singlet models. The measured S_n = 0.11-0.15 were lower than typical S_n = 0.15-0.2. It may be

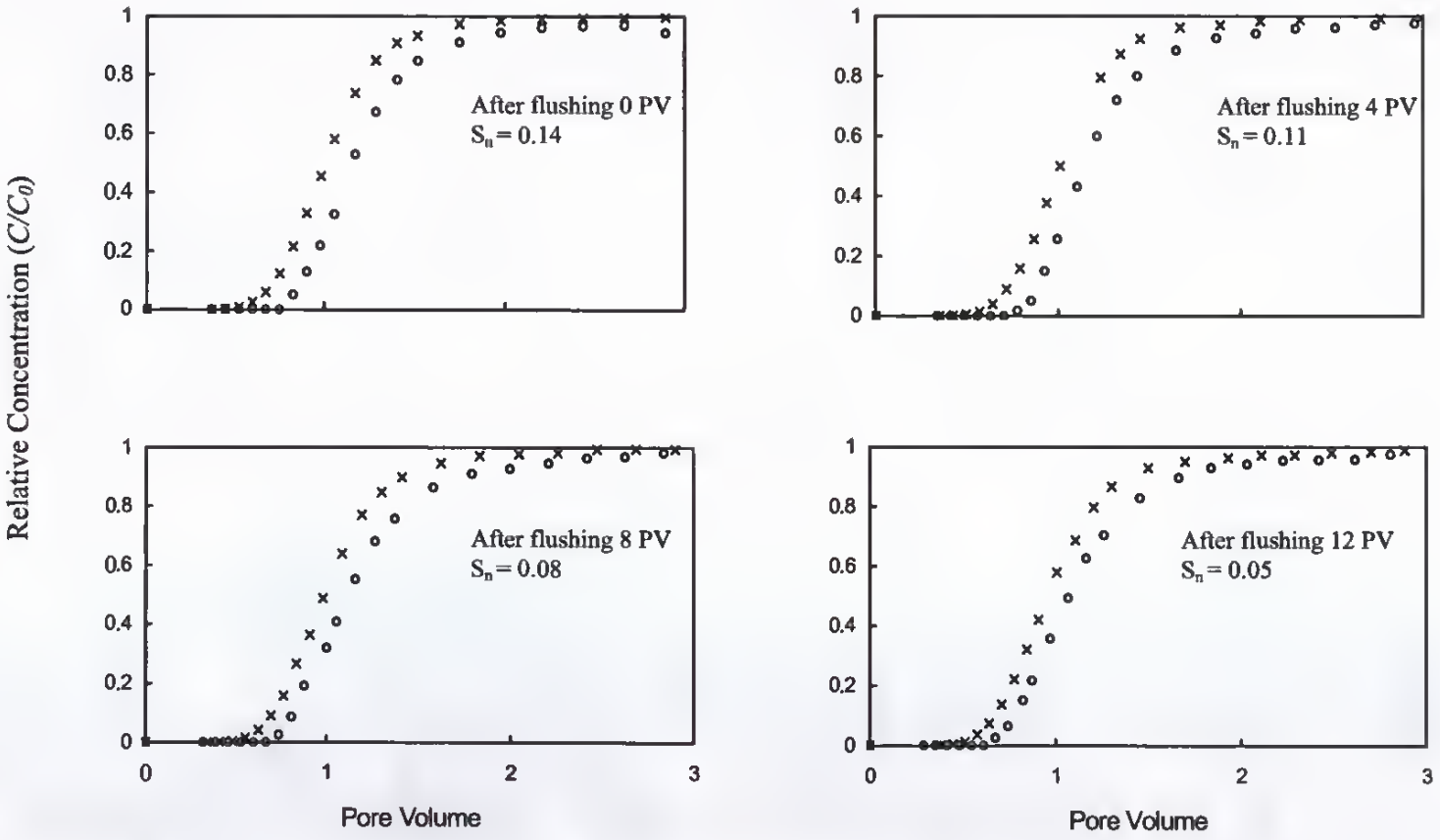

Figure 2-6. Breakthrough curves of nonreactive tracer (bromide, symbol "×") and interfacial tracer (SDBS, symbol "o") from column tests after ethanol flushing with various pore volumes (0, 4, 8, and 12 Pore volume).

due to the method used in this study to create residual NAPL, i.e., two directional flushing (up and down modes) forming a homogeneous spatial NAPL distribution (typical methods use one directional flow/flushing). The observed Sn values increased in three discrete regions with respect to coarse, medium, and fine grain sizes rather than a constantly increasing fashion. The S_n was correlated with the corresponding a_{nw} in Figure 2-5. The result shows that a_{nw} can be modeled better using the d_{50} than S_n. For example, while the S_n values for 0.725 and 1.42 mm d_{50} were nearly the same as 0.154 and 0.155, respectively, the corresponding a_{nw} values showed larger deviations of 74 and 110 cm^2/cm^3. This indicates that at a given NAPL saturation the specific interfacial area can vary greatly depending on the pore sizes. Saripalli (1997) reported that for a medium textured sand, the interfacial area was predicted to be a constant or independent of the degree of saturation, but for a finer sand, the interfacial area increased exponentially with decreasing water saturation. Moreover, interfacial area decreased sharply with increasing NAPL saturation at $S_n > 0.4$. This suggests that NAPL-water specific interfacial area is closely related to porous media size rather than residual NAPL saturation.

NAPL-Water Interfacial Area and NAPL Saturation as a Function of NAPL Dissolution

NAPL-water interfacial area as a function of residual NAPL reduction by dissolution was evaluated using the column packed with 20/30 mesh sand (d_{50} = 0.725 mm) used earlier. Sets of tracer experiments were conducted following flushing with a 4 PV ethanol solution (50 % by volume). BTCs for non-reactive (Br^-) and interfacial (SDBS) tracers are shown in Figure 2-6. Retardation of the interfacial tracers with respect to the non-reactive tracers were evident. The observed results, along with column parameters, are given in Table 2-2. NAPL-water interfacial areas decreased in a linear

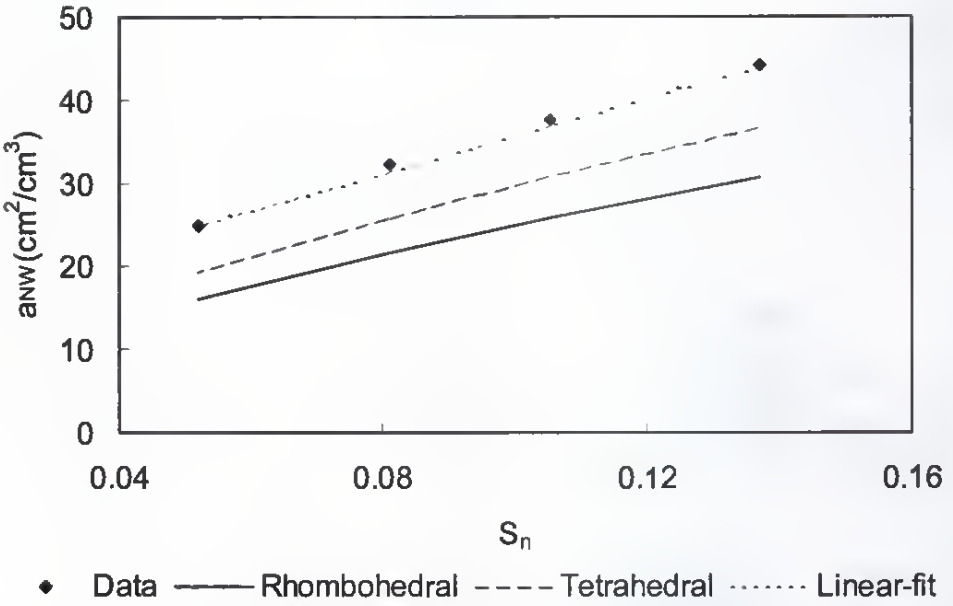

Figure 2-7. NAPL-water interfacial area (a_{NW}) as a function of remaining NAPL saturation (S_n) after ethanol flushing: Pore singlet models, linear fit, and measured data.

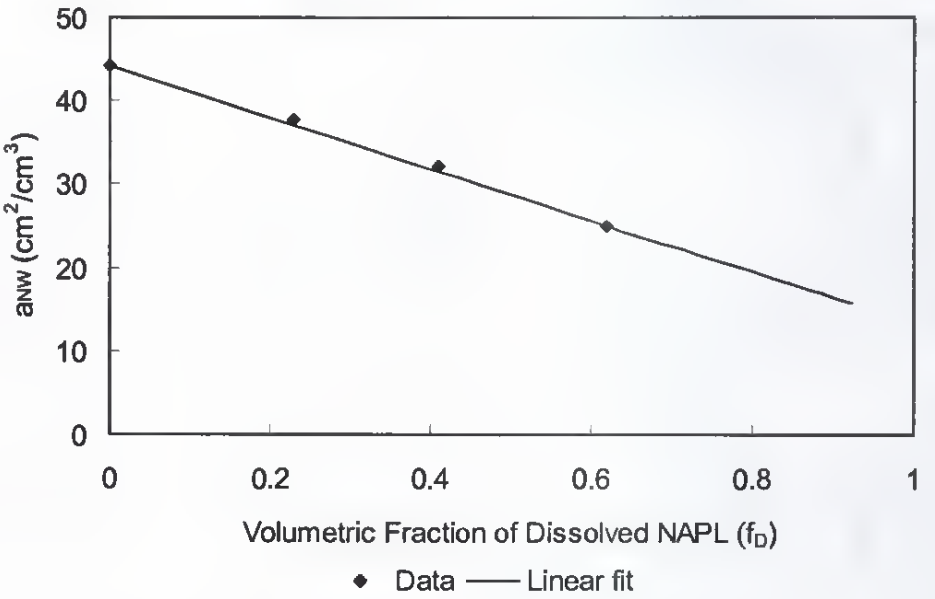

Figure 2-8. NAPL-water interfacial areas (a_{NW}) as a function of NAPL dissolution.

fashion with decreasing NAPL saturation by dissolution (Figure 2-7). The measured a_{nw} -S_n data were fit to the following function:

$$a_{nw} = 226.3 S_n + 13.55 \qquad r^2 = 0.998 \qquad (2\text{-}14)$$

Equation 2-14 can be written as a general expression for a_{nw} in terms of volumetric fraction of dissolved NAPL (f_D):

$$a_{nw} = a_o - n \cdot f_D \qquad r^2 = 0.998 \qquad (2\text{-}15)$$

where $f_D = (S_n^* - S_n) / S_n^* = 1 - (S_n / S_n^*)$ is volumetric fraction of dissolved NAPL; S_n^* is the initial NAPL saturation; S_n is the NAPL saturation remaining after reduction of NAPL by dissolution; a_o is the initial interfacial area before reduction of NAPL by dissolution; n is the dissolution factor, which is determined by the slope of the a_{nw} - f_D regression line. The n value observed for 20/30 mesh sand (d_{50} = 0.725 mm) is 30.4 with the regression coefficient (r^2) of 0.997 (Figure 2-8). As shown in Figure 2-7, although some deviation in the overall absolute values was observed, the decreasing trend and rate in the measured a_{nw}-S_n relationship agreed with the pore singlet model prediction of Saripalli (1996). The linear decrease in NAPL saturation suggests a linear decrease in the radius of the trapped NAPL blobs by dissolution. This suggests that the reduction of NAPL saturation during dissolution causes no significant change in the spatial NAPL distribution. This observation is important for NAPL distribution characterization in the presence of slow dissolution processes, given that simple monitoring of NAPL

dissolution can be used to predict changes in interfacial area. Note that the empirical model proposed in the Equation 2-15 can only be applied to predict the NAPL-water interfacial area with respect to NAPL reduction by dissolution. Recall that the experiments in this study were based on homogeneous NAPL distribution and porous media. Therefore, the proposed a_{nw}-f_D model may not be appropriate for heterogeneously distributed NAPL. In the case of heterogeneous NAPL with varying pore size distribution, the smallest ganglia are dissolved first followed gradually by the larger blobs. This results in an exponential decrease in the a_{nw} by NAPL dissolution.

NAPL Morphology Index

The NAPL saturation and interfacial area data observed earlier can be combined to calculate the morphology index to provide better NAPL characterization. The morphology index (H_N), which is the ratio of interfacial area to volumetric NAPL content, was calculated using Equation 2-9. The measured H_N values increased exponentially with decreasing mean grain size (d_{50}) (Figure 2-9). The H_N-d_{50} data were fit by the following empirical function:

$$\ln(H_N) = 6.489 - 0.496 \ln(d_{50}) \qquad r^2 = 0.981 \qquad (2\text{-}16)$$

The fact that the H_N values between a coarser sand (d_{50} = 1.425) and finer sand (d_{50} = 0.165) represent a wide range from 646 to 2079 indicates that the NAPL in the finer sand exists in much more spread out fashion. This implies that porous media size is a primary factor in characterizing spatial NAPL distribution, as determined by the magnitude of H_N.

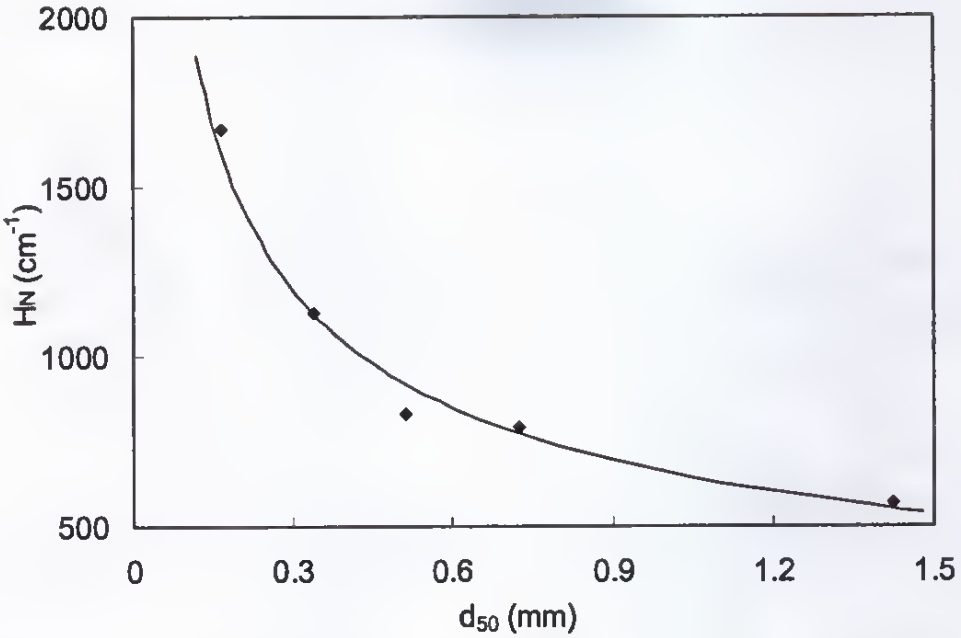

Figure 2-9. Relationship of NAPL morphology index (H_N) and porous medium size. Shown are the symbols (data: ♦; Fit data: solid line).

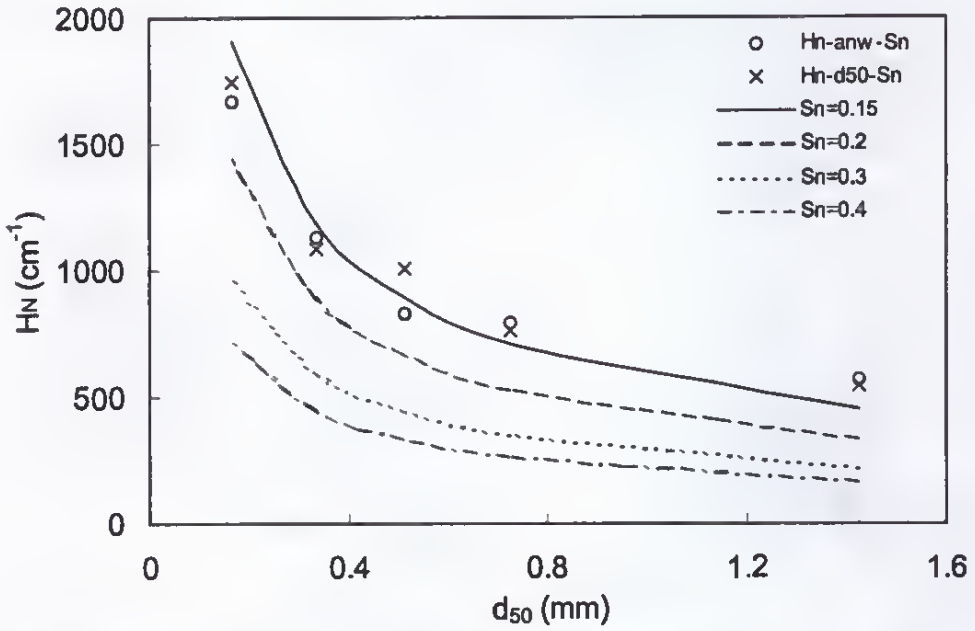

Figure 2-10. The H_N estimated using H_N-a_{nw}-S_n (Saripalli, 1997) and H_N-d_{50}-S_n relationships. Shown are also the predicted H_N with respect to varying NAPL saturation using the H_N-d_{50}-S_n relationship.

The exponential trend is similar to the a_{nw}-d_{50} relationship described earlier. Based on this relationship, the H_N function (Eq. 2-9) proposed by Saripalli et al. (1997) can be written in the terms of d_{50} instead of a_{nw} using the earlier measured a_{nw}-d_{50} functional relationship. An approximate modification of Eq. 2-11 yields:

$$a_{nw} = 34.4 \cdot d_{50}^{(-\frac{2}{3})} \tag{2-17}$$

Substituting the Equation 2-14 into Equation 2-9, the morphology index is

$$H_N = \frac{34.4 \cdot d_{50}^{(-\frac{2}{3})}}{\phi \cdot S_n} \tag{2-18}$$

As shown in Figure 2-10, the estimated H_N using Equation 2-18 agreed well with the H_N using Equation 2-9. This suggests that the proposed model provides reasonable prediction of H_N. For varying S_n (0.15, 0.2, 0.3, and 0.4) for all grain sizes used in this study, the predicted H_N values using the H_N-d_{50}-S_n relationship (Eq. 2-18) are shown in Figure 2-10. The resulting prediction shows that at a given grain size, H_N decreases with increasing the S_n and at a given saturation the H_N increases exponentially with decreasing the d_{50}. Application of the empirical model for H_N must be carefully considered, however, for characterization of a zone with a heterogeneous media size distribution. Annable et al. (1998) showed that the H_N values could be vastly based on the heterogeneity of the media. In the light of the difficulty in measuring specific interfacial area, the H_N expressed as a function of d_{50} is useful for better understanding of spatial NAPL distribution. The observed results not only supply useful information for prediction of

spatial NAPL distribution but also can provide important information for planning remedial strategies.

Conclusions

This chapter presents NAPL characterization using partitioning and interfacial tracers. A series of laboratory column experiments were conducted to investigate NAPL-water interfacial area, NAPL saturation, and morphology as a function of grain size and NAPL dissolution, which can affect spatial NAPL distribution. The specific interfacial area increased exponentially with decreasing mean grain size of the porous media, whereas the NAPL saturation showed slight increase in three discrete regions of coarse, medium, and fine grain sizes. This indicates that the interfacial area has a functional relationship with mean grain size rather than NAPL saturation. The specific interfacial area as a function of NAPL dissolution was evaluated at a grain size. The specific interfacial area decreased linearly with decreasing in NAPL saturation by dissolution. This suggests that a typical slow dissolution process causes no significant change in the spatial NAPL distribution, but a decrease in the radius of the trapped NAPL blobs by dissolution. It suggests that change of specific interfacial area by NAPL dissolution can be predicted by monitoring the effluent NAPL concentration. The morphology index (H_N), which describes the degree of spatial NAPL distribution, also increased exponentially with decreasing grain size. As a result, porous media size is an important parameter for characterizing spatial NAPL. Additionally, this study showed that the combined tracer techniques could be more useful tool for spatial NAPL characterization.

CHAPTER 3
INFLUENCE OF SPECIFIC INTERFACIAL AREA ON MASS TRANSFER: NONEQUILIBRIUM PROCESS

Introduction

Nonaqueous phase liquid (NAPL) introduced in subsurface is trapped by capillary forces that are related to the properties of the soil and the pore geometry. The trapped NAPL releases mass into the bulk aqueous phase by dissolution, acting as a potential long-term source of contamination. Removal of trapped NAPL is limited by mass transfer processes. An understanding of mass transfer process, therefore, plays an important role in efficient removal of the trapped NAPL and prediction of long term behavior.

Interphase mass transfer, which occurs in the vicinity of phase interfaces, by diffusion and advection is a function of the driving force and interfacial area between the two phases of concern. Mass transfer processes from solid or liquid spheres to a flowing fluid phase have been investigated over the last three decades. Nernst (Sherwood et al., 1975) is credited with early work on mass transfer: A stagnant film model, which is based on solute mass diffusion through a thin, stagnant boundary layer of fluid surrounding a solid particle (Sherwood et al., 1975). An application to NAPL-aqueous phase mass transfer in porous media was discussed by Pfannkuch (1984) and has been advanced by numerous studies (Hunt et al., 1988; Miller et al., 1990; Powers et al., 1991, 1992; Geller and Hunt, 1993; Imhoff et al., 1997; Cunningham et al., 1997; Soerens et al., 1998; Zhu and Skyes, 2000).

The mass transfer process between NAPL and the aqueous phase has been described using the local equilihrium assumption (Abriola and Pinder, 1985; Miller et al., 1990; Parker et al., 1990). Local equilihrium implies that if the concentration of contaminant in one phase is known, the concentration in other phase at the same spatial location can he described hy equilihrium partitioning relationships (Ahriola and Pinder, 1985). Powers et al.(1991), however, showed that the local equilihrium assumption may not he valid at higher aqueous fluid velocity. Other investigations have shown that nonequilibrium mass transfer is important in such cases (Borden and Kao, 1992; Geller, 1990; Hunt et al., 1988; Powers et al., 1992). Nonequilihrium can be expected in 1) rate limited exchange of mass from NAPL to aqueous phase (Hunt et al., 1988; Webber et al., 1991; Powers et al.,1992), 2) flow hypassing around the NAPL contaminated region (Soerens et al., 1998), and 3) nonuniform NAPL distrihution (Soerens et al., 1998) and nonuniform flow of aqueous phase due to heterogeneity of soil (Abriola and Pinder, 1985). These nonequilihrium processes have a significant role in fate and transport of contaminants and remedial strategy.

To date, most studies related to NAPL/aqueous mass transfer processes have used a lumped coefficient defined as the product of a mass transfer coefficient and the specific interfacial area (Miller et al., 1990; Powers et al., 1991, 1992; Imhoff et al., 1997; Soerens et al., 1998). To date, use of a lumped hulk mass transfer coefficient rather than an intrinsic mass transfer coefficient is done due to the difficulty in measuring specific interfacial area. Some studies have used a pore structure model closely related to specific interfacial area to explain the effect of the interfacial area on mass transfer rate (Hunter et

al., 1988; 1990; Powers et al., 1992). However, there have been no studies using measured specific interfacial area between NAPL and the aqueous phase.

The primary objective of this study was to illustrate how the specific interfacial area influences the mass transfer process. Bulk and intrinsic mass transfer coefficients were investigated as a function of specific interfacial area, pore velocity, grain size, and NAPL saturation. The impact of NAPL (or interfacial area) reduction by dissolution on mass transfer was also investigated. Models using dimensionless Sherwood number to predict steady state mass transfer rates were developed and evaluated by comparing measured and predicted values.

Theoretical Background

The mass transfer rate in a NAPL/aqueous system is a function of the driving force and the interfacial area between phases. A first-order mass transfer is often used to describe the mass flux of a solute between the phases:

$$J = \frac{1}{A_{nw}} \frac{dm}{dt} = k_i (C_s - C) \tag{3-1}$$

where J is mass flux from the non-aqueous phase to the aqueous phase [M/L^2T]; k_i, is the intrinsic mass transfer coefficient [LT^{-1}]; A_{nw} is the interfacial area between NAPL and water [L^2]; C_s is the equilibrium concentration of the solute in the aqueous phase [M/L^3]; C is the concentration of the solute in the bulk aqueous phase [M/L^3]. Equation (3-1) can be written in terms of the rate of change of mass per unit volume of porous media:

$$\frac{1}{V}\frac{dm}{dt} = \frac{dC}{dt} = \frac{A_{nw}}{V} \cdot k_i (C_s - C) = a_{nw} \cdot k_i (C_s - C) = K_i (C_s - C) \tag{3-2}$$

where V is the bulk volume of soil [L^3]; a_{nw} is the specific interfacial area [L^2/L^3]; $K_l = a_{nw} \cdot k_i$ is the bulk mass transfer rate coefficient [L/T]. A steady state mass transport equation can be written incorporating the mass flux equation (Equation 3-2). The governing equation is:

$$\frac{\partial C}{\partial t} + K_l(C - C_s) = D_L \frac{\partial^2 C}{\partial x^2} - v\frac{\partial C}{\partial x} \tag{3-3}$$

For the following boundary conditions:

$$C(0, t) = 0; \quad \left.\frac{\partial C}{\partial x}\right|_{x=\infty} = 0 \tag{3-4}$$

The solution is (Carslaw and Jaeger, 1959; Van Genuchten and Alves, 1982):

$$\frac{C(x)}{C_s} = 1 - \exp\left[\frac{v - \sqrt{v^2 + 4D_L \cdot K_l}}{2D_L} x\right] \tag{3-5}$$

where D_L is the longitudinal dispersion coefficient [L^2/T]; v is the pore water velocity (= q / ϕ) [L/T]; q is the Darcy velocity [L/T]; ϕ is the porosity; x is the length of the column [L]. This can be solved for K_l:

$$K_l = \frac{1}{4D_L}\left[\left(v - \frac{2D_L}{x} \cdot \ln\left(1 - \frac{C}{C_s}\right)\right)^2 - v^2\right] \tag{3-6}$$

The intrinsic mass transfer coefficients (k_i) can be determined using the measured a_{nw}:

$$k_i = \frac{K_l}{a_{nw}} \tag{3-7}$$

Materials and Methods

Experimental Methods

Experiments to determine mass transfer coefficients were conducted following the interfacial and partitioning tracer tests in Chapter 2. The schematic diagram of the experimental set-up is shown in Figure 2-1. The experiments were conducted at various steady flow rates (0.5, 1, 2, 3, 5, and 7 ml/min). All the experiments were prepared hy passing 10 pore volumes (PV) of DI water to reach at a steady state condition. PCE samples from the experiments were collected in 2 ml vials with a 100 μl insert and analyzed using a high performance liquid chromatography (HPLC) systyem (Perkin Elmer series LC 200) with UV detector (230nm). A HPLC pump (Shimadzu 500) was used to inject water and all experiments were conducted at room temperature (23 ± 1 °C).

Results and Discussion

Parameter Estimation

An analytical solution to the advective-dispersive equation for a saturated homogeneous porous medium was used to estimate longitudinal dispersion coefficients (Freeze and Cherry, 1997). For all grain sizes used, non-reactive tracer (Br-) experiment data at a Darcy velocity, q = 0.1 (cm/min), were fit to the analytical solution to ohtain the longitudinal dispersion (D_L) and longitudinal dispersivity (α_L). For high velocities in this study, the coefficients of longitudinal dispersion were estimated from

$$D_L = \alpha_L v + D_d \qquad (3\text{-}8)$$

where D_d is the coefficients of hulk diffusion; v is the pore water velocity in the flow direction (cm/min). Here, the coefficient of hulk diffusion can he negligihle since it is

Table 3-1. Mass transfer results and parameter values measured from column experiments with various grain sizes.

	θ	d_{50} mm	v (cm/min)	α cm	D_L (cm^2/min)	C (mg/L)	S_n	a_{nw} (cm^2/cm^3)	K_l (min^{-1})	k_t (cm/min)
10/20 mesh	0.38	1.43	0.3	0.103	0.027	119	0.116	28.3	0.17	0.006
	0.38	1.43	0.5	0.103	0.054	97	0.116	28.3	0.23	0.008
	0.38	1.43	1.0	0.103	0.108	78	0.116	28.3	0.31	0.011
	0.38	1.43	1.6	0.103	0.162	66	0.116	28.3	0.38	0.013
	0.38	1.43	2.6	0.103	0.270	50	0.116	28.3	0.43	0.015
	0.38	1.43	3.7	0.103	0.378	45	0.116	28.3	0.53	0.019
20/30	0.34	0.73	0.3	0.059	0.017	147	0.137	44.3	0.48	0.011
	0.34	0.73	0.6	0.059	0.034	143	0.137	44.3	0.75	0.017
	0.34	0.73	1.1	0.059	0.068	129	0.137	44.3	0.93	0.021
	0.34	0.73	1.7	0.059	0.102	118	0.137	44.3	1.10	0.025
	0.34	0.73	2.9	0.059	0.171	103	0.137	44.3	1.36	0.031
	0.34	0.73	4.0	0.059	0.239	91	0.137	44.3	1.53	0.035
30/40	0.37	0.51	0.3	0.055	0.015	150	0.124	44.4	0.76	0.017
	0.37	0.51	0.5	0.055	0.030	144	0.124	44.4	0.73	0.017
	0.37	0.51	1.1	0.055	0.060	132	0.124	44.4	0.95	0.021
	0.37	0.51	1.6	0.055	0.090	124	0.124	44.4	1.17	0.026
	0.37	0.51	2.7	0.055	0.149	107	0.124	44.4	1.39	0.031
	0.37	0.51	3.8	0.055	0.209	95	0.124	44.4	1.56	0.035
40/60	0.35	0.34	0.3	0.036	0.010	150	0.154	73.7	0.76	0.010
	0.35	0.34	0.6	0.036	0.021	147	0.154	73.7	0.93	0.013
	0.35	0.34	1.1	0.036	0.041	146	0.154	73.7	1.70	0.023
	0.35	0.34	1.7	0.036	0.062	143	0.154	73.7	2.19	0.030
	0.35	0.34	2.8	0.036	0.103	138	0.154	73.7	3.03	0.041
	0.35	0.34	4.0	0.036	0.145	136	0.154	73.7	3.88	0.053
80/100	0.34	0.17	0.3	0.028	0.008	150	0.155	109.6	0.84	0.008
	0.34	0.17	0.6	0.028	0.016	150	0.155	109.6	1.52	0.014
	0.34	0.17	1.2	0.028	0.032	149	0.155	109.6	2.55	0.023
	0.34	0.17	1.7	0.028	0.048	149	0.155	109.6	3.67	0.033
	0.34	0.17	2.9	0.028	0.080	149	0.155	109.6	6.33	0.058
	0.34	0.17	4.1	0.028	0.112	146	0.155	109.6	6.30	0.058

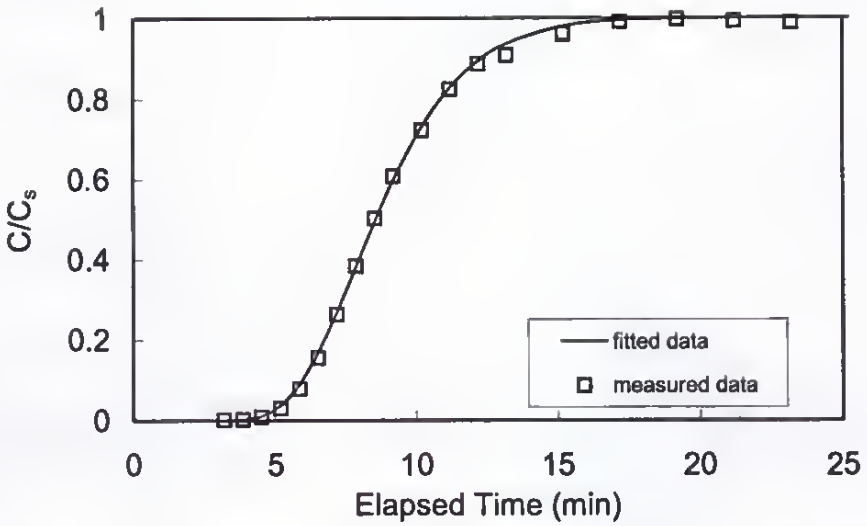

Figure 3-1 An example BTCs of non-reactive tracer (Br^-) fitted to an analytical solution to estimate longitudinal dispersion coefficient and dispersivity values.

small compared to D_L. The estimated longitudinal dispersivities for porous media with d_{50} = 0.17-1.43 mm ranged from 0.03 to 0.1 cm. An example BTC is shown in Figure 3-1. These longitudinal dispersivities were in a reasonable agreement with typical values (0.01 to 1 cm) found for longitudinal dispersivities from column experiments (Freeze and Cherry, 1979). Additionally, NAPL saturation (S_n) and specific interfacial area (a_{nw}) used in this study are the values measured using partitioning/interfacial tracers in Chapter 2. The results are given in Table 3-1 and 3-2.

Mass Transfer Coefficients

A series of dissolution experiments was conducted to investigate mass transfer between trapped NAPL in porous media and the aqueous phase. Normalized effluent concentrations (C/Cs) as a function of pore water velocity ($v = q / \phi$) are shown for individual grain sizes in Figure 3-2. The effluent PCE concentration decreased with

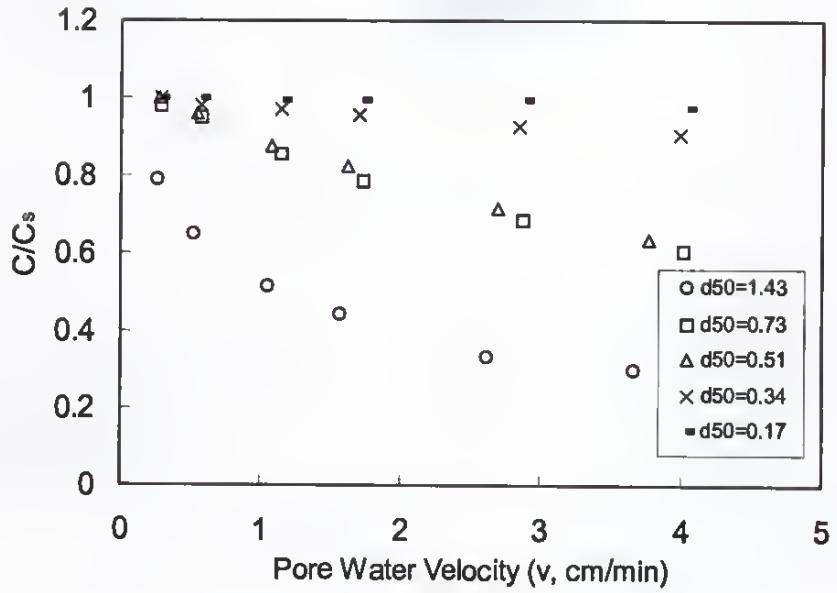

Figure 3-2. Normalized PCE effluent concentration (C/C_s) versus pore water velocity. (d_{50} units mm)

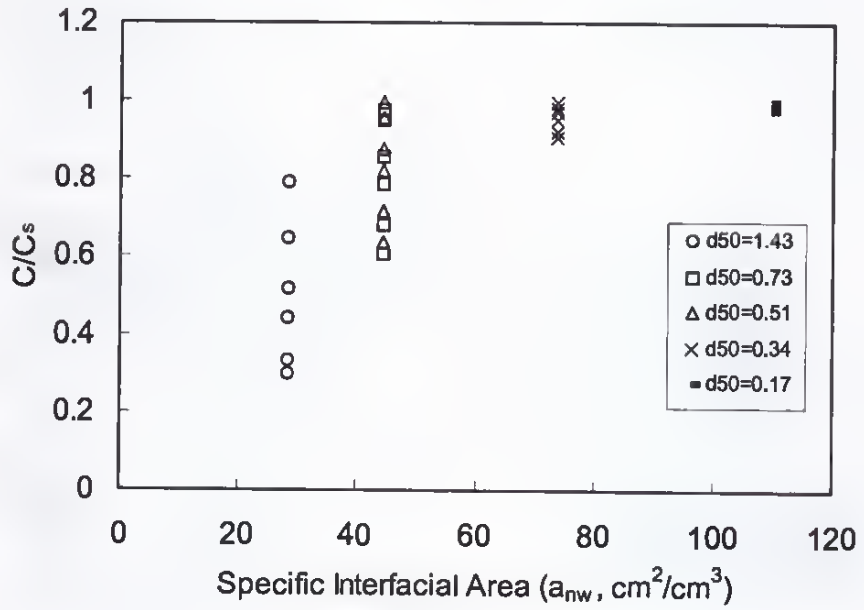

Figure 3-3. Normalized PCE effluent concentration (C/C_s) versus specific interfacial area. (d_{50} units mm)

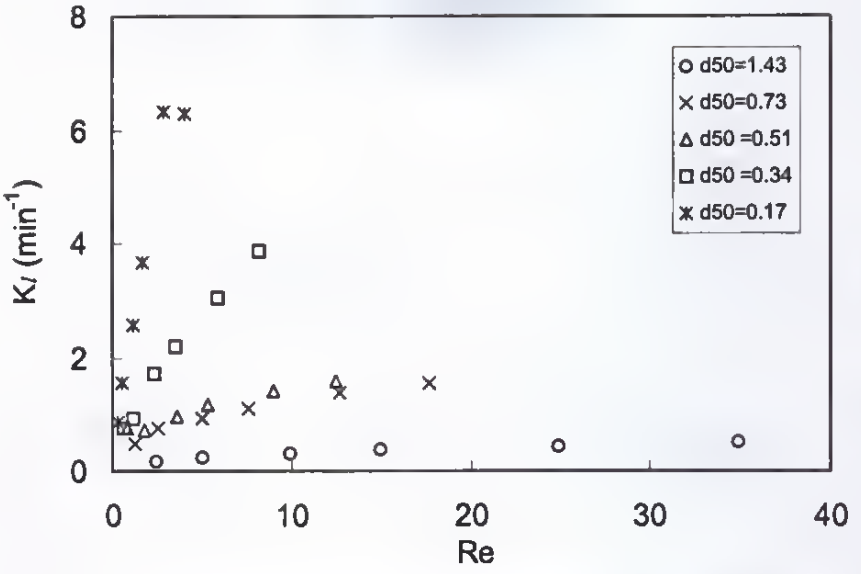

Figure 3-4. Bulk mass transfer rate coefficients (K_l) versus Reynolds number (Re) for various grain sizes. (d_{50} units mm)

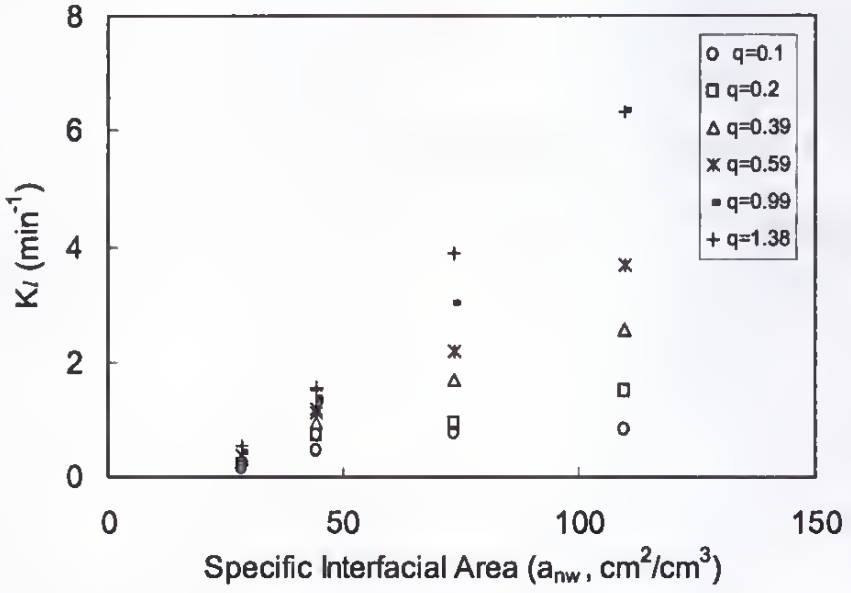

Figure 3-5. Bulk mass transfer rate coefficients (K_l) versus specific interfacial area for various velocities. (q units cm/min)

increasing pore water velocity and grain size. Typically the effluent concentrations increased with increasing NAPL saturation, but some cases did not follow this trend (Table 3-1). For example, although NAPL saturations for two different grain sizes (d_{50} = 0.17 and 0.34 cm) were nearly the same, tbe observed effluent concentrations were higher for the finer grain size, d_{50} = 0.17 cm, than for d_{50} = 0.34 cm. In addition, effluent concentrations for d_{50} = 0.51 cm were slightly higher than those for d_{50} = 0.73 cm even thougb NAPL saturation was larger. The effluent concentrations, alternatively, increased consistently with increasing interfacial areas (Figure 3-3). This means that NAPL-water mass transfer rate is well correlated with NAPL-water specific interfacial area rather than residual NAPL saturation for soil with various grain sizes or beterogeneity.

The measured results were pooled together to calculate bulk mass transfer rate coefficients ($K_l = k_i a_{nw}$) using Equation 3-6. The bulk mass transfer rate coefficients as a function of Reynolds number, whicb represents pore velocity, are sbown in Figure 3-4 and again as a function of specific interfacial area in Figure 3-5. It was evident that at the smallest grain size (largest interfacial area) small increase in Reynolds number resulted in very sbarp increases in the bulk mass transfer rate coefficients. While at low interfacial area (large grain size) the bulk mass transfer rate coefficients did not vary significantly with pore velocity. At bigb interfacial area (small grain size) mass transfer coefficients were very sensitive to pore velocity.

The bulk mass transfer rate coefficients were used to calculate intrinsic mass transfer coefficients (k_i) using specific interfacial area values. Figure 3-6 shows a plot of observed intrinsic mass transfer coefficients as a function of specific interfacial areas. The intrinsic mass transfer coefficients varied slightly or did not vary with increasing

Table 3-2. Mass transfer results with respect to reduction of NAPL saturation/interfacial area

Flushing (ethanol 50%)	θ	v (cm/min)	D_L (cm^2/min)	C (mg/L)	S_n	a_{nw} (cm^2/cm^3)	K_l (min^{-1})	k_l (cm/min)
0 PV	0.34	0.29	0.017	147	0.137	44	0.48	0.011
	0.34	0.57	0.034	143	0.137	44	0.75	0.017
	0.34	1.15	0.068	129	0.137	44	0.93	0.021
	0.34	1.72	0.102	118	0.137	44	1.10	0.025
	0.34	2.87	0.171	103	0.137	44	1.36	0.031
	0.34	4.02	0.239	91	0.137	44	1.53	0.035
4 PV	0.36	0.27	0.017	147	0.106	38	0.46	0.012
	0.36	0.55	0.034	137	0.106	38	0.57	0.015
	0.36	1.10	0.068	123	0.106	38	0.78	0.021
	0.36	1.65	0.102	112	0.106	38	0.93	0.025
	0.36	2.75	0.171	88	0.106	38	0.99	0.026
	0.36	3.85	0.239	78	0.106	38	1.16	0.031
8 PV	0.37	0.27	0.017	144	0.081	32	0.38	0.012
	0.37	0.53	0.034	133	0.081	32	0.49	0.015
	0.37	1.07	0.068	112	0.081	32	0.61	0.019
	0.37	1.60	0.102	101	0.081	32	0.73	0.023
	0.37	2.67	0.171	78	0.081	32	0.80	0.025
	0.37	3.73	0.239	69	0.081	32	0.93	0.029
12 PV	0.40	0.25	0.017	127	0.052	25	0.19	0.008
	0.40	0.49	0.034	114	0.052	25	0.29	0.012
	0.40	0.98	0.068	89	0.052	25	0.36	0.015
	0.40	1.48	0.102	73	0.052	25	0.40	0.016
	0.40	2.46	0.171	60	0.052	25	0.51	0.020
	0.40	3.44	0.239	54	0.052	25	0.62	0.025

* The dispersivity (α) used to estimate dispersion coefficients (D_L) is 0.059 cm. The grain size used is 0.73 mm (d_{50}).

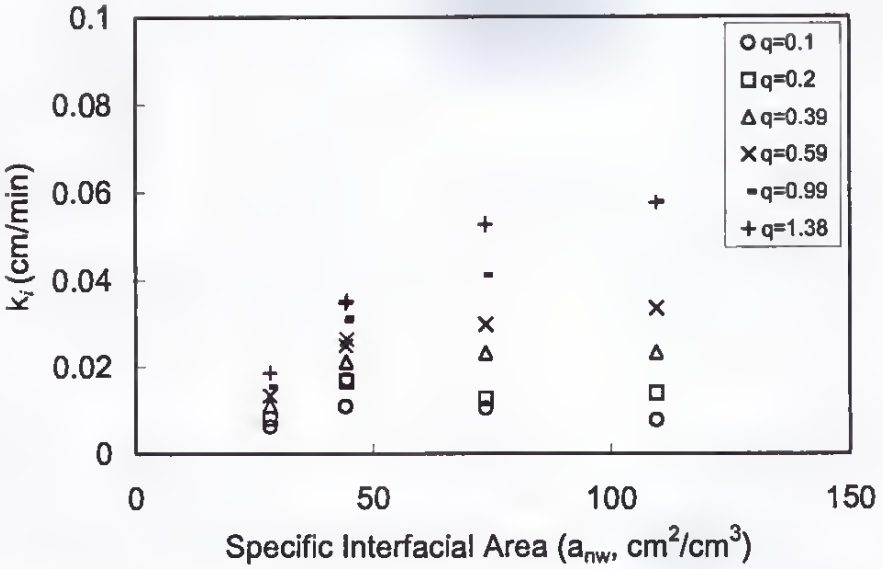

Figure 3-6. Intrinsic mass transfer coefficients versus specific interfacial area for various velocities. (q units cm/min)

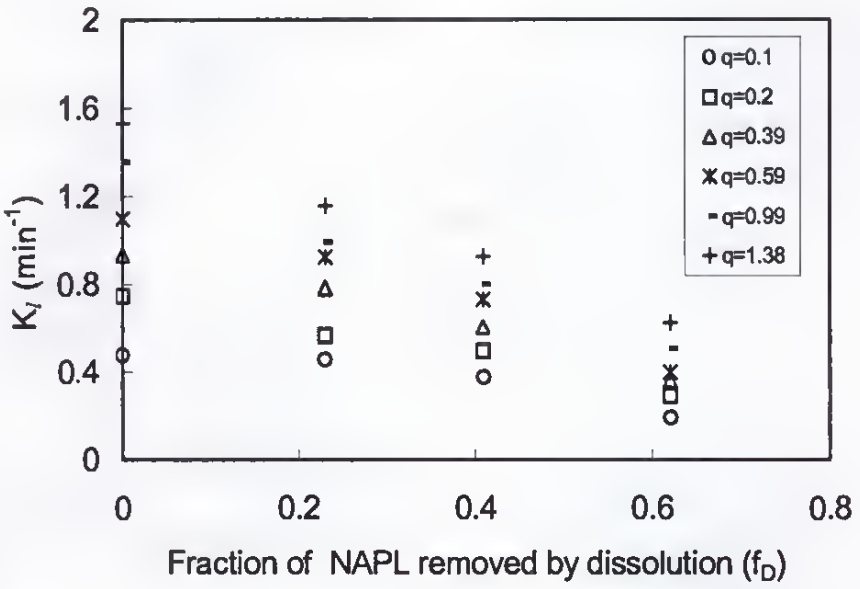

Figure 3-7. Bulk mass transfer rate coefficients (K_l) as a function of NAPL dissolution. $f_D = (S_n^* - S_n)/ S_n^* = 1 - (S_n / S_n^*)$ is volumetric fraction of dissolved NAPL; S_n^* is the initial NAPL saturation; S_n is the NAPL saturation remained after reduction of NAPL by dissolution.

specific interfacial area except for some data points at high velocity and high interfacial area. Miller et al. (1990) reported that bulk mass transfer rate coefficients were extremely sensitive at high effluent concentration. Therefore, it is likely that the observed large intrinsic mass transfer coefficients at high interfacial areas can be explained by uncertainty in system factors or potential experimental errors rather than the change of interfacial area/NAPL saturation.

Influence of NAPL Reduction by Dissolution on Mass Transfer

Mass transfer as a function of NAPL (or interfacial area) reduction by dissolution was investigated and the observed results are shown in Table 3-2. Here, all the experiments were completed in a column that started at residual saturation (S_n = 0.14). Each set of experiments was conducted following a 4PV ethanol (50 % by volume) flood, that resulted in a NAPL reduction of about 20 %. It is assumed that a change in mass transfer is only a result of NAPL saturation (or interfacial area) reduction. Figure 3-7 shows a plot of bulk mass transfer rate coefficients (K_l) versus the fraction of removed NAPL (f_D). It is apparent that bulk mass transfer rate coefficients decrease with NAPL reduction. The observed bulk mass transfer rate coefficients decreased in near linear fashion with decreasing NAPL saturation. The K_l values became less sensitive to pore velocity with decreasing NAPL saturation. This observation agreed with earlier results. These results imply that at higher NAPL saturation and interfacial area, alcohol flushing efficiency is not sensitive to flushing velocity, while at lower NAPL saturation velocity can be an important control on the efficiency of NAPL removal.

Figure 3-8 shows that while intrinsic mass transfer coefficients increase consistently with increasing velocity, they change little with reduction of NAPL. This

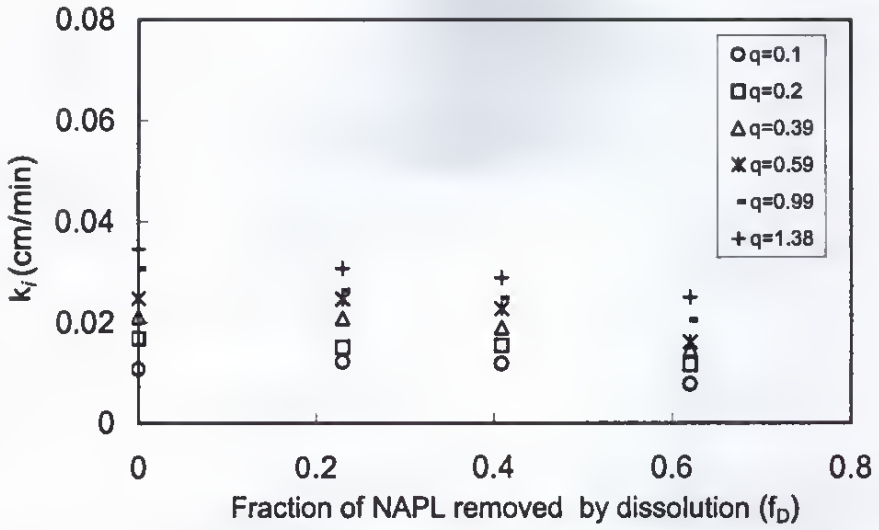

Figure 3-8. Intrinsic mass transfer coefficients (k_i) as a function of NAPL dissolution.

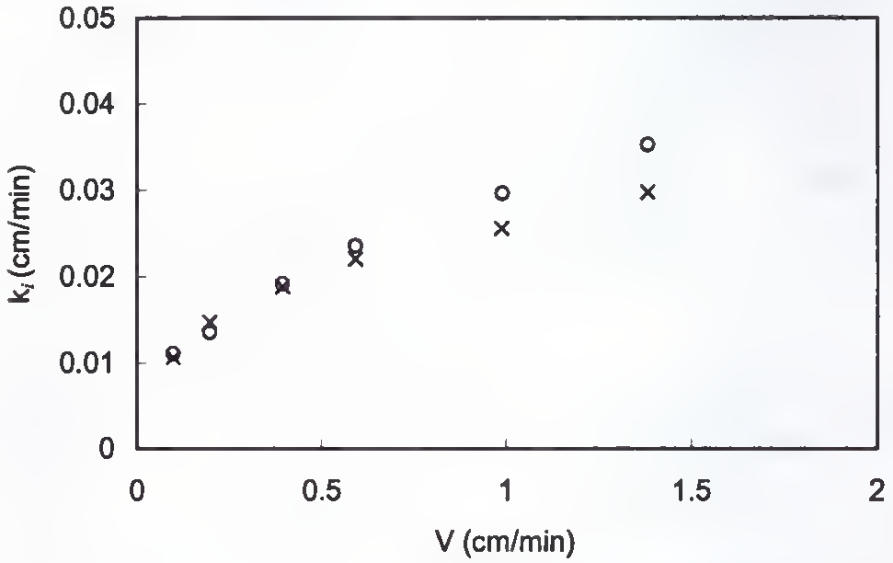

Figure 3-9. Averaged intrinsic mass transfer coefficients for various velocities. The symbol (o) and symbol (x) are the averaged k_i values from the experiments with various grain sizes and with NAPL reduction by dissolution, respectively.

Tahle 3-3. Mass Transfer Correlations.

References	Correlation	model type
Miller et al. (1990)	$Sh' = 12\ Re^{0.75}\theta_n^{0.6}Sc^{0.5}$	lumped domain
Powers et al. (1992)	$Sh' = 57.7\ Re^{0.61}d_{50}^{0.64}U_i^{0.41}$	lumped domain
Imhoff et al. (1997)	$Sh' = 1.34\ Re^{0.75}\theta_n^{0.9}Sc^{0.49}$	lumped domain

where Sh' (= $K_l d_{50}^2/D_m$) is the modified Sherwood number Miller et al., 1990); Re (= $v\rho_w d_{50}/\mu_w$) is the Reynolds numher, Sc (=$\mu_w/\rho_w D_m$) is the Schmidt numher; θ_n is ϕS_n; U_i (= d_{60}/d_{10}) is the uniformity index; D_m is the molecular diffusivity in the aqueous phase; ρ_w is the aqueous density; μ_w is the aqueous viscosity.

indicates that intrinsic mass transfer coefficients can he independent of NAPL saturation/interfacial area, hut only dependent on velocity. The ohserved results were averaged and compared with the averaged values from the experiments with various grain sizes earlier in Figure 3-9. Results from two different experimental approaches agreed well over the velocities tested.

Model Development

In general, models related to steady state mass transfer have been developed or evaluated using a dimensionless Sherwood numher (Sh). Numerous previous studies (Tahle 3-3) have shown that the Sherwood number was an appropriate tool to explain or correlate mass transfer process (Miller et al., 1990; Powers et al., 1991, 1992; Geller and Hunt, 1993, Imhoff et al., 1997). In this present work, hoth modified Sherwood number ($Sh' = K_l d_{50}^2/D_m$) (Miller et al., 1990) and Sherwood numher ($Sh = k_l L/D_m$), where L is a characteristic length which can he expressed as mean grain size, d_{50}, were used in model development. The parameters used in the correlation were Reynolds number (Re), Schmidt numher (Sc), S_n, a_{nw}, and d_{50}. Since the Sc was constant over these experiments, an exponent of 0.5 was used for Sc as suggested by Miller et al., (1990) and Imhoff et al.

(1997). The data for parameters were log-transformed and fit to multiple linear models within a SPSS statistical software package (SPSS for windows 8.0.0, SPSS Inc., 1997). The fitting was performed by stepwise regression procedures to find the optimum correlation combination of parameters. The best fit was measured with the sum of the squares defined as

$$r^2 = \sum_{i=1}^{n} \left[\frac{\log(Sh_{measured}) - \log(Sh_{estimated})}{\log(Sh_{measured})} \right]^2 \qquad (3\text{-}9)$$

where n is the number of data points for each parameter used. The first model developed used a modified Sherwood number which included lumped mass transfer rate coefficients ($K_l = k_l a_{nw}$). The model, which simutaneously incorporates all of the Re, Sc, S_n, a_{nw}, and d_{50} terms, did not offer meaningful correlation. Modified Sherwood number was also not well correlated with other multiple parameter comibations, Re/S_n, Re/a_{nw}, and $Re/d_{50}/S_n$ at the significance level. The best fit model in power law form is given as

$$Sh' = \beta_0 \, Re^{\beta 1} \, d_{50}^{\beta 2} \, Sc^{0.5} \qquad (r^2 = 0.92; \pm 95\ \%\ CI) \qquad (3\text{-}10)$$

with
$\beta 0 = 3.09 \pm 1.09$
$\beta 1 = 0.45 \pm 0.04$
$\beta 2 = 0.40 \pm 0.08$

and the best fit model including a_{nw} in power law form is

$$Sh' = \beta_0' \, Re^{\beta 1'} \, a_{nw}^{\beta 2'} \, d_{50}^{\beta 3'} \qquad (r^2 = 0.92; \pm 95\ \%\ CI) \qquad (3\text{-}11)$$

with
$\beta 0' = 3.50 \pm 2.40$
$\beta 1' = 0.45 \pm 0.04$
$\beta 2' = 0.49 \pm 0.39$
$\beta 3' = 0.70 \pm 0.25$

Powers et al. (1992) reported that the inclusion of any parameters describing pore structure sucb as the grain size distribution greatly increased r^2 values and thus can be used as representative measures of NAPL distribution and interfacial area. In this study, the modified Sherwood number is also well correlated to grain size and specific interfacial area. This indicates tbat the mass transfer rate can be correlated with pore size and NAPL specific interfacial area as well as pore velocity. This developed model (Eq. 3-10) along with the previous model (Powers et al., 1992) can be a useful tool since measurement of NAPL-water interfacial area is difficult. When an irregular spatial distribution of NAPL is considered, however, the model (Eq. 3-11), whicb includes the specific interfacial area, can be more useful in predicting the mass transfer rate between the pbases than that using (Eq. 3-10).

Comparison of the models (Eq. 3-11) developed in this study with previous investigations using the same modified Sherwood number (Miller et al., 1990; Powers et al., 1992; Imhoff et al., 1997) are sbown in Figure 3-10. The model (Eq. 3-11) was closest to that of Miller et al. (1990) but between those of Powers et al. (1992) and Imhoff et al. (1997). This deviation seems to be due to the difference in tbe measured absolute values from experiments rather than the discrepancy in the developed models. Note that while bulk mass transfer rate coefficients increased with increasing effluent concentration, modified Sherwood numbers decreased. Powers et al. (1992) conducted experiments with trichloroethylene (TCE) and the resulting effluent concentrations were lower than those using PCE in this study. This may result in larger modified Sherwood numbers. Althougb Imhoff et al. (1997) used PCE in their experiments, the observed

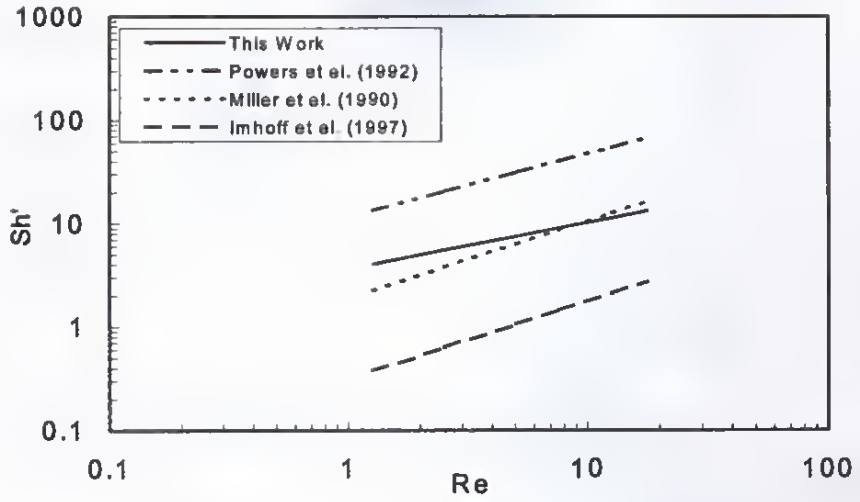

Figure 3-10. Comparison of modified Sherwood numbers (Sh') from this study with previous investigation (d_{50} = 0.073 cm, a_{nw} = 44 cm^2/cm^3. S_n = 0.14, ϕ = 0.39, UI = 1.2)

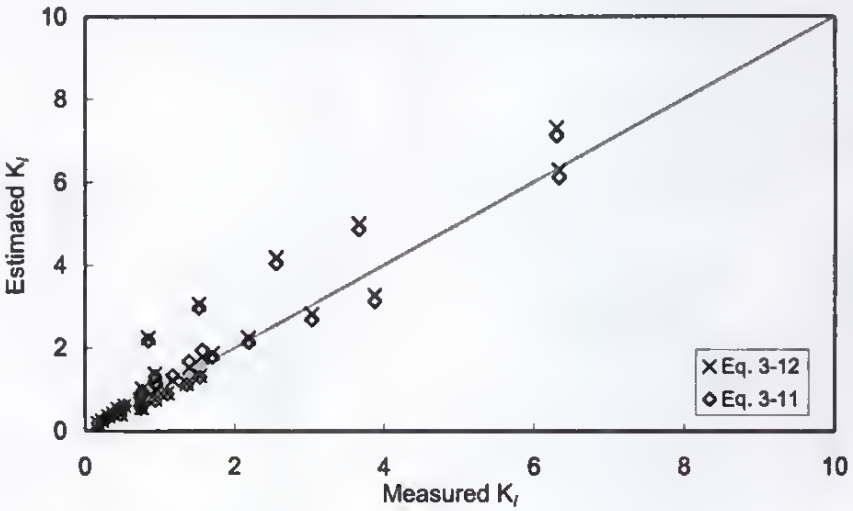

Figure 3-11. Bulk mass transfer rate coefficients measured versus those predicted from the developed model ($Re/a_{nw}/d_{50}$ model) for all data pooled together.

effluent PCE concentrations were higher than those from this work. The higher effluent concentration caused relatively smaller modified Sherwood numbers.

The Sherwood number ($Sh = k_i d_{50}/D_m$), which includes the intrinsic mass transfer coefficient (k_i) was used to develop a model for the intrinsic mass transfer coefficient. The best fit model in power law form is given as

$$Sh = \beta_0'' \, Re^{\beta 1''} \, Sc^{0.5} \qquad (r^2 = 0.87; \pm 95\ \%\ CI) \qquad (3\text{-}12)$$

with $\beta 0'' = 0.27 \pm 1.01$
$\beta 1'' = 0.57 \pm 0.04$

This best fit model had relatively lower regression constants compared to those with the modified Sherwood number. While the Sherwood number was not correlated to the S_n, a_{nw}, and d_{50} at a significant level, it was relatively well correlated to Re which includes the velocity. As described earlier, considering that the intrinsic mass transfer coefficient (k_i) can be nearly independent of S_n, a_{nw}, and d_{50} but dependent on flow velocity, the correlated model seems to be reasonable. This model (Eq. 3-12) can be valuable in the fact that it can be used to predict intrinsic mass transfer coefficients between NAPL and the aqueous phase without measuring a specific interfacial area.

Validation of the correlated models was assessed by comparison with measured data. The bulk mass transfer rate coefficients (K_i) predicted from the developed models (Eq. 3-10 and Eq. 3-11) were compared with the measured values in Figure 3-11. Although some data points scattered above the 1:1 line, most predicted values agreed with the measured data. Average predicted values for Eq. (3-10) and Eq. (3-11) were 1.13 and 1.11 times higher than the measured values from experiments, respectively. Comparison of measured and predicted values for intrinsic mass transfer coefficients (k_i) is shown in Figure 3-12. The predicted values were obtained using Eq. (3-11) and Eq. (3-

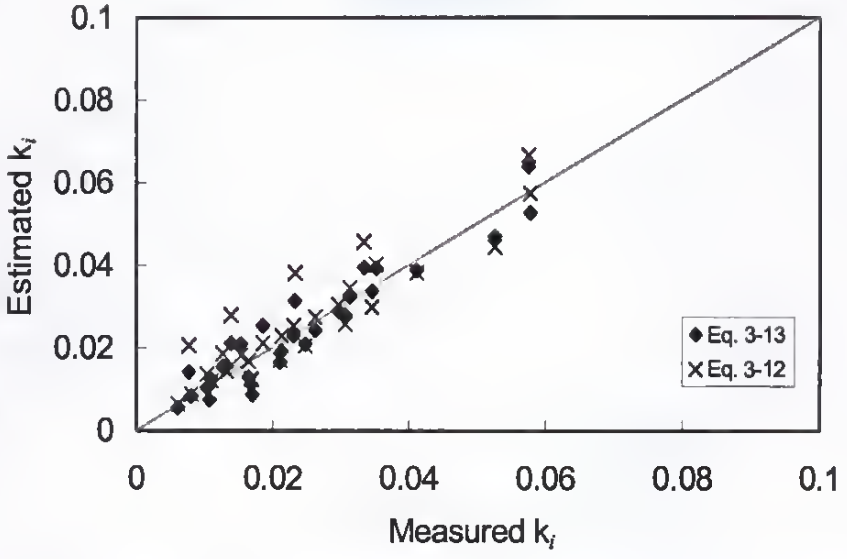

Figure 3-12. Intrinsic mass transfer coefficients measured with those predicted from the model (Re/Sc) for all data pooled together.

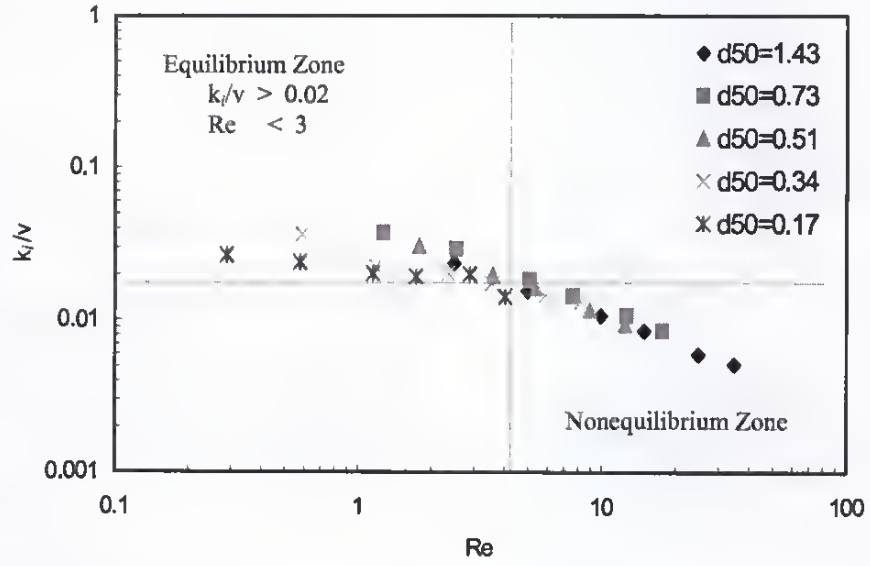

Figure 3-13. Damkohler number (Da = k_i/v) with respect to Reynolds number for various grain sizes. (d_{50} units mm)

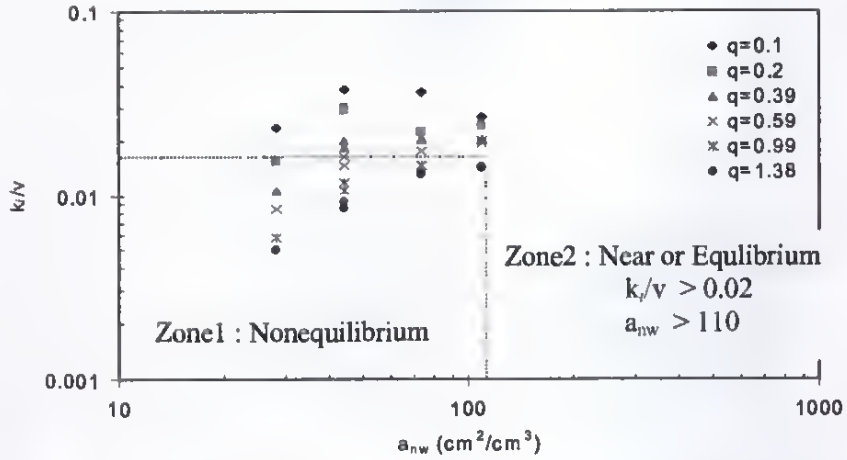

Figure 3-14. Damkohler number (Da = k_i/v) with respect to specific interfacial area for various grain sizes. (d_{50} units mm)

12). Average predicted values for Eq. (3-11) and Eq. (3-12) were 1.07 and 1.01 times higher than average measured values, respectively. The small deviations indicate that the developed models are valid as prediction models for mass transfer rate coefficients.

Nonequilibrium Mass Transfer

Equilibrium between NAPL and water reflects the conditions induced by physichemical environments such as velocity (Powers et al., 1992), temperature (Imhoff et al., 1997), contact time and concentration (Miller et al., 1990). The Damkohler number ($Da = K_i d_{50}/v = k_i a_{nw} d_{50}/v = k_i/v$), which characterizes the degree of nonequilibrium between fluids, was used to investigate how system parameters contribute to nonequilibrium conditions. Figure 3-13 shows Da (= k_i/v) versus Re, which incorporates the velocity, for a range of grain size. The higher Da numbers indicate near equilibrium conditions. That is, at k_i/v greater than about 0.02 and Re less than about 3 in systems with homogeneous grain size and NAPL distribution (present system conditions), the equilibrium assumption is appropriate. It was clear, however, that at Re > 3 the Da decreased log-linearly with increasing the Re. The decreasing trend with respect to

velocity was accelerated with increasing the grain size of porous media. Because specific interfacial area can increase exponentially with decreasing grain size, the equilibrium condition at different fluid velocity can be sensitive to the magnitude of interfacial area as well as grain size (Figure 3-14 and 3-3). This means that above a critical interfacial area ($a_{nw} \approx 110$ cm^2/cm^3 in present system conditions), effluent concentration did not vary with increasing velocity. As NAPL-water interfacial area decreased, velocity can be an important factor in determination of equilibrium conditions. In other words, below a critical velocity ($q \approx 0.01$ cm/min in present system conditions), mass transfer rate is nearly independent of the magnitude of specific interfacial area. These results indicate that above a critical interfacial area or below a critical velocity local equilibrium assumption is achieved.

Conclusions

The effect of specific NAPL-water interfacial area, along with other system parameters (e.g., grain size, velocity, and saturation), on mass transfer was investigated. Bulk mass transfer rate coefficients were found to be directly related to specific interfacial area as well as pore velocity and saturation. Particle size which was closely related to the specific interfacial area was also an important parameter in determination of bulk mass transfer rate coefficients. The bulk mass transfer rate coefficients can be correlated with NAPL-water specific interfacial area rather than residual NAPL saturation for soil with various grain sizes, and were more sensitive at high NAPL-water interfacial area than at low interfacial area. However, intrinsic mass transfer coefficients

were nearly independent of the change of NAPL saturation and specific interfacial area, but dependent on pore velocity. NAPL saturation (or interfacial area) reduction by dissolution caused a linear decrease in bulk mass transfer rate coefficients, while it caused no effect on intrinsic mass transfer coefficients. Correlation models consisting of Reynolds number, Schmidt number, interfacial area, and grain size have been developed to provide better understanding and prediction of intrinsic and bulk mass transfer coefficients using both dimensionless Sherwood number and modified Sherwood number. The developed models were verified throughout comparison of measured and predicted data. The comparison revealed that the models were robust and produced reasonable prediction for mass transfer rate.

CHAPTER 4
ESTIMATING NAPL SATURATION USING PARTITIONING TRACERS: INFLUENCE OF RESIDUAL COSOLVENTS

Introduction

The partitioning tracer technique has been used to characterize residual saturation and distribution of non-aqueous phase liquids (NAPLs) trapped in porous media (Annable et al., 1998 a, b, 1995; James et al., 1997; Dwarakanath et al., 1999; Jin et al., 1997). The technique is based on the differences in travel time of non-partitioning and partitioning tracers through a NAPL source zone (Jin et al., 1995). The tracer technique has been evaluated at both field (Annable et al., 1998a, b, 1995; James et al., 1997; Dwarakanath et al., 1999; Jin et al., 1997) and laboratory (Jin et al., 1997, 1995; Pope et al., 1994) scales. The technique has been mainly employed at sites associated with aggressive in-situ remediation, such as cosolvent or surfactant flushing (Rao et al., 1997). After a cosolvent flood, which often includes a water flood, some residual cosolvent will likely remain in the swept zone following the effort to extract NAPL from the source zone (Annable et al., 1998a). The residual cosolvent can affect the partitioning and transport behavior of tracers used during a post-flushing tracer test.

In general, cosolvents present in the aqueous phase affect chemical characteristics, such as solubility and sorption (hence, activity). In completely water-miscible solvents, the solubility of hydrophobic organic chemicals (HOCs) increases in a log-linear manner (Li et al., 1994; Pinal et al., 1990; Morris et al., 1988; Rubino et al.,

1987; Fu and Luthy, 1986; Yalkowsky and Roseman, 1986), and sorption decreases log-linearly (Bouchard, 1998b; Hermann and Powers, 1998; Kimble and Chin, 1994; Brusseau et al., 1991; Rao et al., 1990, 1985; Fu et al., 1986); as a result, the transport of HOC through soils is less retarded (Rao et al., 1985; Bouchard, 1998a; Wood et al., 1990). However, the behavior of chemicals can vary depending on type and composition. For example, Coyle et al. (1997) reported that the solubility of HOCs, such as PCB-47, PCB-153, and biphenyl, was depressed in the presence of partially miscible organic solvents (PMOS), such as methylene chloride and chloroform.

As a result, in the presence of a residual cosolvent, an estimate of NAPL saturation based on partitioning tracer test can be in error. The NAPL saturation (S_n) can be under-estimated in the presence of cosolvents such as methanol, which cause solubility enhancement of organic tracers. On the other hand, S_n can be over-estimated in the presence of other cosolvents such as methylene chloride, which cause solubility depression. Therefore, when a partitioning tracer test is conducted with a residual cosolvent present, it is important to consider the cosolvent effects. Relatively little data, however, are available on the effect of residual cosolvent on the partitioning tracer technique.

The objective of this study was to investigate the influence of residual cosolvent on the partitioning tracer technique for estimating S_n. Partitioning and solubility behavior of alcohol tracers were investigated in the presence of residual cosolvents in batch equilibrium tests. The results were verified through miscible displacement tests in packed columns. It was also examined how the magnitude of residual S_n modifies the impact of the cosolvent on the S_n estimates.

Theoretical Background

Addition of cosolvents generally increases aqueous solubility and decreases the partitioning of HOCs; bowever, not every cosolvent increases the solubility of HOCs. Most completely water-miscible organic solvents sucb as methanol, increase HOC solubility in a log-linear (Li et al., 1994; Pinal et al., 1990; Morris et al., 1988; Rubino et al., 1987; Fu et al., 1986; Yalkowsky and Roseman, 1986) fashion, since this type of cosolvent results in a decrease of the activity coefficient. However, some partially water-miscible organic solvents sucb as cbloroform decrease HOC solubility in a log-linear fashion (Coyle et al., 1997). One possible explanation is increasing activity of the PMOS into the HOC phase or a solventing-out, in whicb dissolved PMOS can occupy a significant portion of the water molecular space, rendering them unavailable for HOC dissolution. Tbe log-linear cosolvent model is one of several theoretical approacbes for predicting the organic chemical cbemodynamics. While the log-linear model is applicable over a large range of tbe volume fraction of cosolvent (f_c); at tbe low f_c (0-0.3) range, linear approximation may suffice (Pinal et al., 1990; Hermann and Powers, 1998) and the relationship can be expressed

$$S_c = S_w + a_c f_c \qquad (4\text{-}1)$$

where S_c is tbe solubility in the presence of a cosolvent; S_w is the aqueous solubility and a_c is the cosolvency factor; $a_c > 0$ for cosolvent sucb as methanol wbicb enhance HOC solubility; $a_c < 0$ for cosolvent sucb as chloroform that depress solubility; $a_c \approx 0$ for cosolvents producing minimal change in solubility.

The solubility of HOCs is inversely related to its partitioning coefficient (Rao et al., 1985). Therefore, as the volume fraction of cosolvent increases, the partitioning and

retardation of HOC decreases in a log-linear fashion Rao et al. (1985). However, over a low fc range (fc ≤ 0.3), it follows from Equation (4-2) that,

$$K_{nc} = K_{nw} - a_c f_c \qquad (4\text{-}2)$$

where the subscripts n, w, and c represent NAPL, water, and cosolvent respectively; K_{nc} is the partitioning coefficient measured in presence of a cosolvent; K_{nw} is the partitioning coefficient measured in water; a_c is an empirical constant which describes water-cosolvent interactions.

Materials and Methods

Materials

A suite of tracers was selected to examine solubility and partitioning processes over a range of retardation factors. Methanol (Fisher, 98 %) was used as a non-reactive tracer, while 4-methyl-2-pentanol (4M2P) (Acros, 99+ %), n-hexanol (Acros, 98 %), 2-methyl-3-hexanol (2M3H) (Acros, 98 %), and 2,4-dimethyl-3-pentanol (2,4DMP) (Acros, 99+ %) were used as partitioning tracers in both batch and column experiments. Ethanol (Spectrum Chemical, absolute 200 proof), Tertiary-butanol (TBA) (Aldrich, 99+ %), and Isopropanol (IPA) (Fisher, Electronic use) were used as cosolvents. Tetrachloroethylene (PCE) (Acros, 99 %) was used as a NAPL for all batch and column experiments. The laboratory temperature during the experiments was 23 ± 1 °C. A 30-40 mesh silica sand (Ottawa) was used as porous medium in all miscible displacement experiments; alcohol tracers adsorption to this solid matrix was determined to be negligibly small.

Partition Isotherm Experiments

To assess tracer partitioning in solutions with low cosolvent concentrations (≤ 10 % by volume), a series of batch equilibrium experiments were conducted. Isotherms for tracer partitioning into NAPL (PCE) were measured in aqueous/alcohol solution using three cosolvent solutions: ethanol, TBA, and IPA. The f_c used in batch equilibrium experiments were 0, 1, 3, 5, and 10 %. Each cosolvent solution was transferred to 100mL volumetric flasks, and four alcohol tracers were added with varing concentrations. Alcohol tracer mixtures prepared at each cosolvent fraction were added to an appropriate amount of PCE in 25mL vials fitted with Teflon-lined screw caps. The vials were tumbled end-over-end on a laboratory-rotator (Glas-Col model RD 4512) for 24 hr at room temperature. At the end of the equilibrium period, alcohol mixtures in supernatant solutions were analyzed by gas chromatography (Perkin Elmer GC, Autosystem XL).

Solubility Experiments

Tracer solubilities were measured using the cosolvent solutions referred to above. The prepared solutions (20mL) were transferred into 25mL vials fitted with Teflon-lined screw caps for each mixture. One alcohol tracer was added to each vial in an amount more than 3 times the maximum solubility in water. The vials were placed on a rotator for 24hr at room temperature. At the end of the equilibrium period, the vials were placed upside-down for at least 6hr to allow the remaining separate phase alcohol to rise and collect above the water. After equilibration was attained, a 5mL aliquot of liquid was collected for analysis through the Teflon-lined septum using a glass gas tight 5mL syringe (Hamilton).

Miscible Displacement Experiments

A series of column tests was conducted with various fractions of a residual cosolvent (ethanol). The glass column used was 4.8 cm in diameter and 15 cm in length (high performance liquid chromatography column from Kontes) with Teflon end pieces. Two layers of fine wire mesh and plastic screen were placed inside of the Teflon end pieces to allow for an even distribution of fluids and minimize column end effects.

Two different column packing methods were used for miscible displacement experiments. In the first method, clean sand (30-40 mesh) was wet-packed in thin layers under continuous vibration. Each layer was stirred and tamped with a rod before adding new sand. The packed column was cleaned by passing 20 pore volumes of degased DI water and weighed. Then, NAPL was introduced at a low flow rate (0.5 mL/min) using a syringe pump. Some of the NAPL was subsequently displaced by injecting water. Different levels of S_n trapped in the pores was achieved by gradually increased flow rates (1, 3, 5, and 10 mL/min steps). In the second method, sand was pre-mixed with a small amount of PCE to create very low residual saturations (S_n = 0.0056). The pre-mixed sand was prepared by adding approximately 20 % of the saturated water content (20mL) and the required amount of PCE (2 mL). The sand mixture was shaken and stirred before and after adding PCE. The mixture was wet-packed as described above. The initial residual PCE saturations of columns packed by both methods were also determined using the partitioning tracer test.

The packed columns were oriented vertically and connected to a high performance liquid chromatography (HPLC) pump (Perkin Elmer series LC 200 and Gilson model 320) through an inert valve which allowed switching among three reservoirs for the mobile phases. The first reservoir contained a mobile phase of solute-

free PCE saturated water to minimize the loss of residual PCE in the column, the second a PCE-saturated cosolvent solution, and the third an alcobol tracer solution. The residual cosolvent used in the column experiments was an etbanol/water binary mixture. The f_c used in tbe column experiments were 0, 1, 3, 5, and 10 % by volume.

The miscible displacement experiments were conducted with and without residual cosolvent present. The column was initially prepared by passing 20 pore volumes of degased-PCE-saturated water. A column with residual cosolvent was created by flushing three pore volumes of a degased-PCE-saturated cosolvent solution. Effluent breakthrough curves (BTCs) were measured under steady water flow condition with a pulse-input boundary condition. Replicate column tests for each residual cosolvent were conducted. R and S_n measured during eacb column test were used to estimate column-based partitioning coefficients.

Data Analysis

All tracer partition equilibrium data obtained from batcb tests with and without cosolvents were fitted using a linear isotherm to obtain K_{nc} and K_{nw}. The Retardation factor (R) was calculated by moment analysis of effluent BTCs. The NAPL saturation (S_n) was estimated from tbe K_{nw} from batch tests, and the R_c value measured in the presence of cosolvent. The tails of BTCs were monitored until tbe injected relative tracer concentration was less tban 10^{-2}. The measured data were log-linearly extrapolated up to 10^{-3}. For comparison with batcb test results, K_{col} values were computed using R_c and actual S_n values (i.e., S_n estimated using partitioning tracers in the absence of cosolvent) as follows:

$$K_{col} = \frac{(R_c - 1) \cdot (1 - S_n)}{S_n} \quad (4\text{-}3)$$

where K_{col} is a partitioning coefficient estimated from a column test, R_c is a retardation factor ohtained in the presence of cosolvent, and S_n is actual NAPL saturation estimated by tracers without cosolvent. The K_{col} was compared to the K_{nc} from batch tests.

Results and Discussion

Effect of Cosolvent on Soluhility

The solubilities (S_c) of three alcohols tracers were measured in the presence of low concentrations (0 to 10 %) of cosolvents (ethanol, TBA, and IPA). The ohserved results (Figure 4-1) revealed three types of hehavior depending on the cosolvent: enhancement of solubility (ethanol), reduction of solubility (TBA), and no ohservahle change (IPA).

The soluhility enhancement with ethanol is in good agreement with other studies (Li et al., 1994; Pinal et al., 1990; Morris et al., 1988; Fu and Luthy, 1986; Yalkowsky and Roseman, 1986). For instance, Yalkowsky and Roseman (1986) reported that in completely water-miscihle solvents such as methanol, the soluhility of HOCs increases log-linearly. However, the measured results showed a proportionally linear relation. It seems to be why the observed linear relation was attributed to the low concentration of cosolvent used.

Solubility reduction, as observed with TBA, was also noted by others (Coyle et al., 1997; Groves, 1988). Coyle et al. (1997) reported that the soluhility of HOCs was

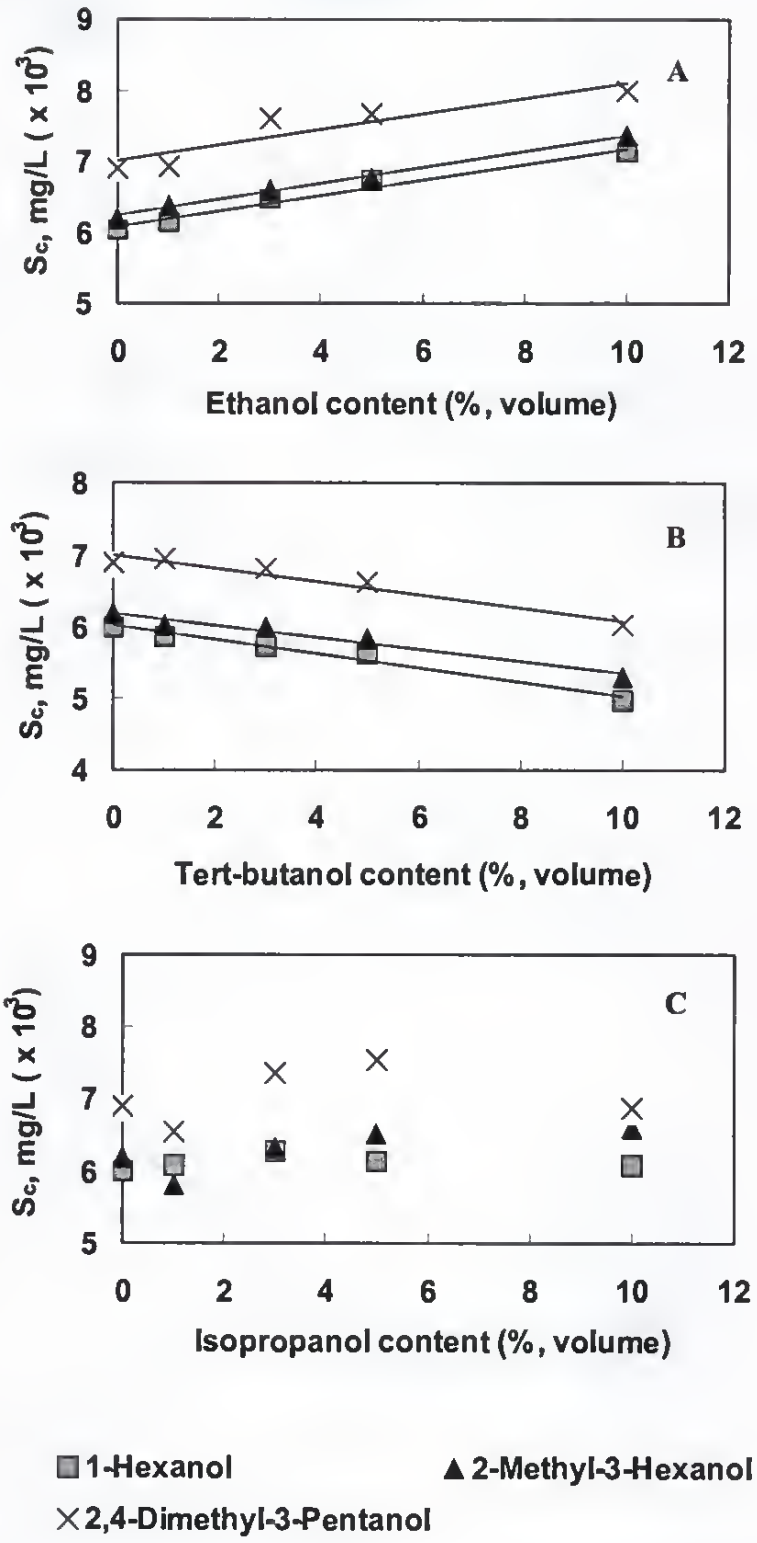

Figure 4-1. Relationship between tracer solubility (S_c) and cosolvent content (%, volume) for (A) ethanol, (B) tert-butanol, and (C) isopropanol

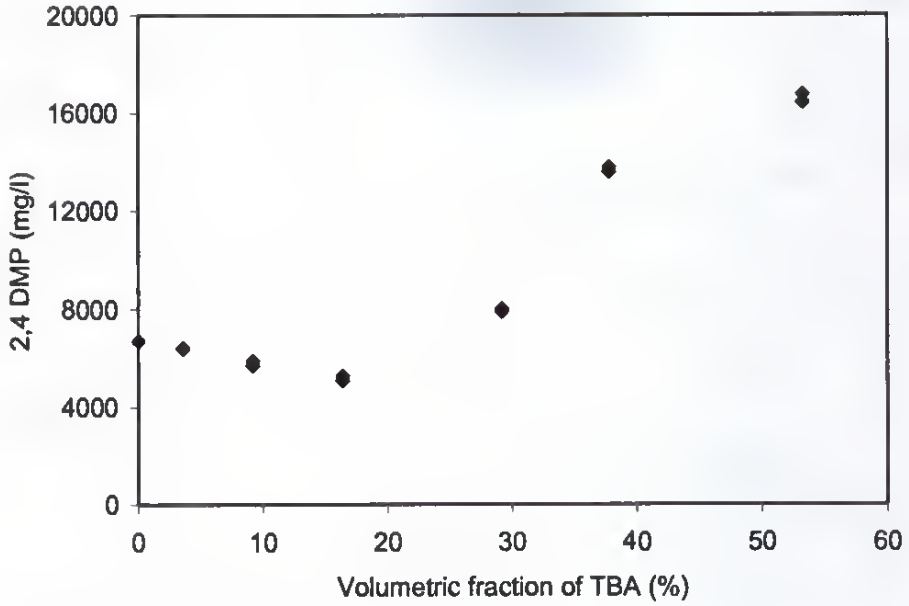

Figure 4-2. Solubility of 2,4 DMP with respect to tert-butanol content (%, volume)

decreased in the presence of PMOS, such as methylene chloride, resulting from an activity increase of the PMOS in the HOC phase (Coyle et al., 1997). Even though TBA is a CMOS such as methanol or ethanol, at low concentration the soluhility hehavior of the tracer alcohol in the TBA followed that of PMOS rather than the other CMOS. Additionally, Figure 4-2 shows that the soluhility of the alcohol tracer, 2,4 DMP, in TBA solutions decreased linearly until ahout 25 % TBA, at which point, solubility increased sharply with increasing concentration (> 25 %). The reason for the solubility reduction at low concentration is not clear, however, one possihle explanation is an activity increase of TBA-cosolvent in the tracer-alcohol phase. Ahove 25 %, however, the TBA hegan to partition into the alcohol, swelling it, and caused significant increases in soluhility.

For the IPA-cosolvent system, the solubilities did not show any ohservahle trend, with increasing volume fraction of IPA (Figure 4-1C). This was different from results

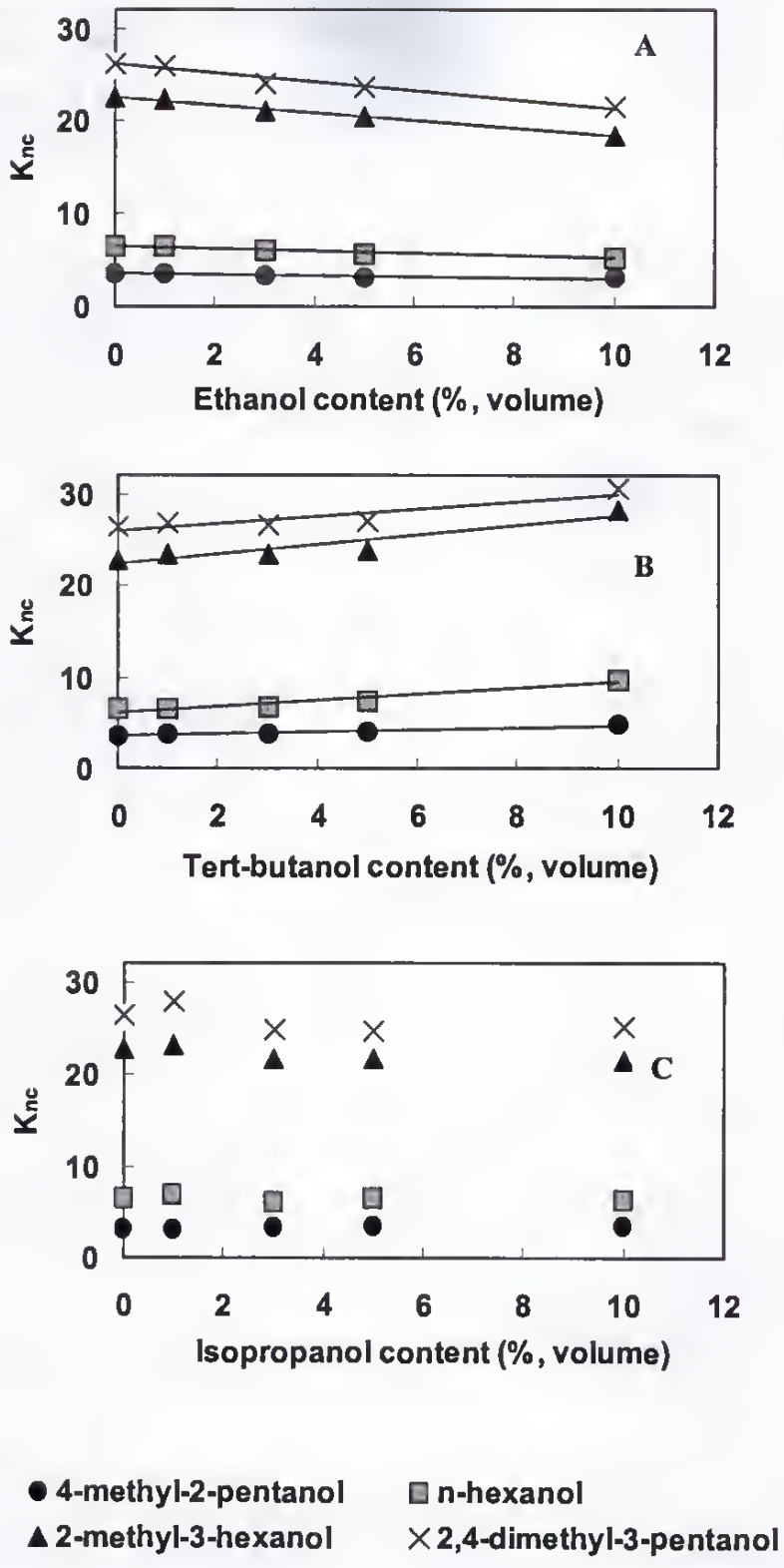

Figure 4-3. Relatioship between tracer partition coefficient (K_{nc}) and cosolvent content (%, volume) for (A) ethanol, (B) tert-butanol, and (C) isopropanol

reported in the literature. Morris et al. (1988) reported that the solubility of naphthalene increased log-linearly with increasing the fraction of IPA. Pinal et al.(1990) and Valkenburg (1999) also showed that IPA at high level (range 0-80 %) is a strong cosolvent in experiments with TCE and PCE. However, experiments in this study were conducted at low concentrations (range 0-10 %). Thus, it can be concluded that the IPA as a cosolvent has little affect on the solubility of the tracer-alcohol at low concentrations (≤ 10 %).

Effect of Cosolvent on Tracer Partitioning Isotherms

The partition coefficients, K_{nc}, determined from the batch isotherm data are shown in Figure 4-3. Based on the observed K_{nc}, three types of partitioning behavior were also found in accordance with the property of each cosolvent added in the aqueous phase.

In the presence of the ethanol, the measured K_{nc} values decreased for all alcohol tracers used in this study, as the volume fraction of ethanol ($f_{c,EtOH}$) increased (Figure 4-3A). The K_{nc} and $f_{c,EtOH}$ values were well correlated in inverse-linear relationships with $r^2 \geq 0.95$. The K_{nc} values decreased up to approximately ~15, 21, 18, and 18 % of each K_{nw} value measured in water, for 4M2P, n-hexanol, 2M3H, and 2,4DMP, respectively. Recall that the solubilities of the tracer-alcohols increased in the presence of $f_{c,EtOH}$ (Figure 4-1).

This solubility increase supports well the decrease in observed partitioning since they are inversely related to each other. Such results indicate that the residual ethanol-cosolvent can affect estimations of S_n using Equation 4-3. The S_n has a functional relationship between K_{nw} and R. The R, which is a measure of partitioning tracer mobility, becomes smaller or larger according to a degree of partitioning of the tracer into

NAPL. Reduced partitioning produces less retardation. In the presence of cosolvent such as ethanol, if the K_{nw} value determined in water is used, the S_n would be under-estimated.

In the presence of the TBA-cosolvent, the K_{nc} values increased with increasing fraction of TBA ($f_{c,TBA}$) (Figure 4-3B). The correlated results showed a linear relationship between the K_{nc} and $f_{c,TBA}$ (r^2 = 0.86-0.92). The K_{nc} values increased compared K_{nw} up to ~35, 49, 24, and 16 % for 4M2P, n-hexanol, 2M3H, and 2,4DMP, respectively. This partitioning increase has not been reported in the literature. However, we could expect a partitioning increase based on the observed solubility reduction. The results may be explained as the solventing-out effect referred by Coyle et al. (1997). The dissolved TBA causes an increased partitioning of alcohol tracers by occupying the water molecular space. In other words, an increase of cosolvent such as TBA, unlike the ethanol-cosolvent, results in a decreasing activity, producing increased partitioning. This result suggests that failing to consider the effect of residual cosolvent could result in overestimation of S_n.

In the presence of isopropanol as a cosolvent, the partitioning coefficients did not display an apparent trend (Figure 4-3C). This is consistent with the minimal affect on the solubilities of the tracer-alcohols (Figure 4-1). This suggests that residual IPA-cosolvent may not affect the tracer partitioning behavior or the estimate of S_n at low concentration ($\leq$ 10 %).

Based on above observed results, at low concentration ($\leq$ 10 %) the relationships between K_{nc} and f_c can be divided into three types according to the properties of cosolvents used. The equation to describe the relationships is as follows:

Table 4-1. Comparison of estimated a_c and b_c values from tracer solubility and partition experiments for four tracers

	Ethanol		TBA		IPA	
Tracers	solubility[a]	partition[b]	solubility[a]	partition[b]	solubility[a]	partition[b]
4M2P	nd	-0.06(0.93)	nd	+0.11(0.88)	nd	-0.01(0.00)
n-hexaol	+119(0.96)	-0.14(0.99)	-96(0.98)	+0.27(0.84)	+19(0.53)	-0.02(0.16)
2M3H	+119(0.99)	-0.43(0.99)	-83(0.96)	+0.47(0.86)	+34(0.41)	-0.13(0.61)
2,4DMP	+124(0.83)	-0.50(0.95)	-93(0.96)	+0.36(0.83)	+36(0.06)	-0.17(0.38)

[a] a_c values estimated by linear regression on solubility data for tracers-low cosolvents systems

[b] b_c values estimated by linear regression on partitioning coefficient data for tracers-low cosolvents systems

$$K_{nc} = K_{nw} + b_c f_c \qquad (4\text{-}4)$$

$b_c < 0$ for ethanol
$b_c > 0$ for TBA
$b_c \approx 0$ for IPA

where, K_{nc} is the partitioning coefficient measured in presence of a cosolvent, K_{nw} is the partitioning coefficient measured in water, b_c is an empirical constant which describes water-cosolvent interactions with the subscript $_C$ designating cosolvent. The estimated b_c values along with a_c were shown in Table 4-1.

Effect of Cosolvent on Tracer Retardation

Column miscible displacement tests were conducted to investigate the effect of residual cosolvent on tracer partitioning and transport behavior. The displacement fluid

Table 4-2. Parameter values observed from miscible displacement experiments at low volume fractions of ethanol

Tracers	Ethanol, f_c	R_c	S_n	S_n %error[a]	K_{col}[b]	K_{nc}[c]
4-methyl-2-pentanol	0	1.84	0.188		3.60	3.60
	0.01	1.82	0.185	-1.54	3.53	3.50
	0.03	1.80	0.182	-3.14	3.46	3.37
	0.05	1.78	0.178	-5.44	3.36	3.23
	0.10	1.74	0.170	-9.41	3.19	3.07
n-hexanol	0	2.47	0.184		6.56	6.56
	0.01	2.47	0.183	-0.75	6.50	6.42
	0.03	2.45	0.181	-2.00	6.40	6.13
	0.05	2.41	0.176	-4.27	6.22	5.74
	0.10	2.36	0.172	-6.82	6.02	5.18
2-methyl-3-hexanol	0	6.28	0.189		22.7	22.7
	0.01	6.15	0.185	-1.98	22.1	22.3
	0.03	6.09	0.183	-3.03	21.8	21.1
	0.05	5.96	0.180	-5.03	21.3	20.4
	0.10	5.87	0.177	-6.47	20.9	18.5
2,4 dimethyl-3-pentanol	0	7.13	0.189		26.3	26.3
	0.01	7.10	0.189	-0.40	26.1	25.9
	0.03	7.02	0.187	-1.43	25.8	23.9
	0.05	6.86	0.183	-3.55	25.1	23.7
	0.10	6.71	0.179	-5.57	24.5	21.5

[a] calculated by ((S_n measured with each f_c) - (S_n with 0 % f_c)) / (S_n with 0 % f_c) ×100
[b] Partitioning coefficients estimated from column tests in the presence of ethanol-cosolvent
[c] Partitioning coefficients measured from batch tests in the presence of ethanol-cosolvent

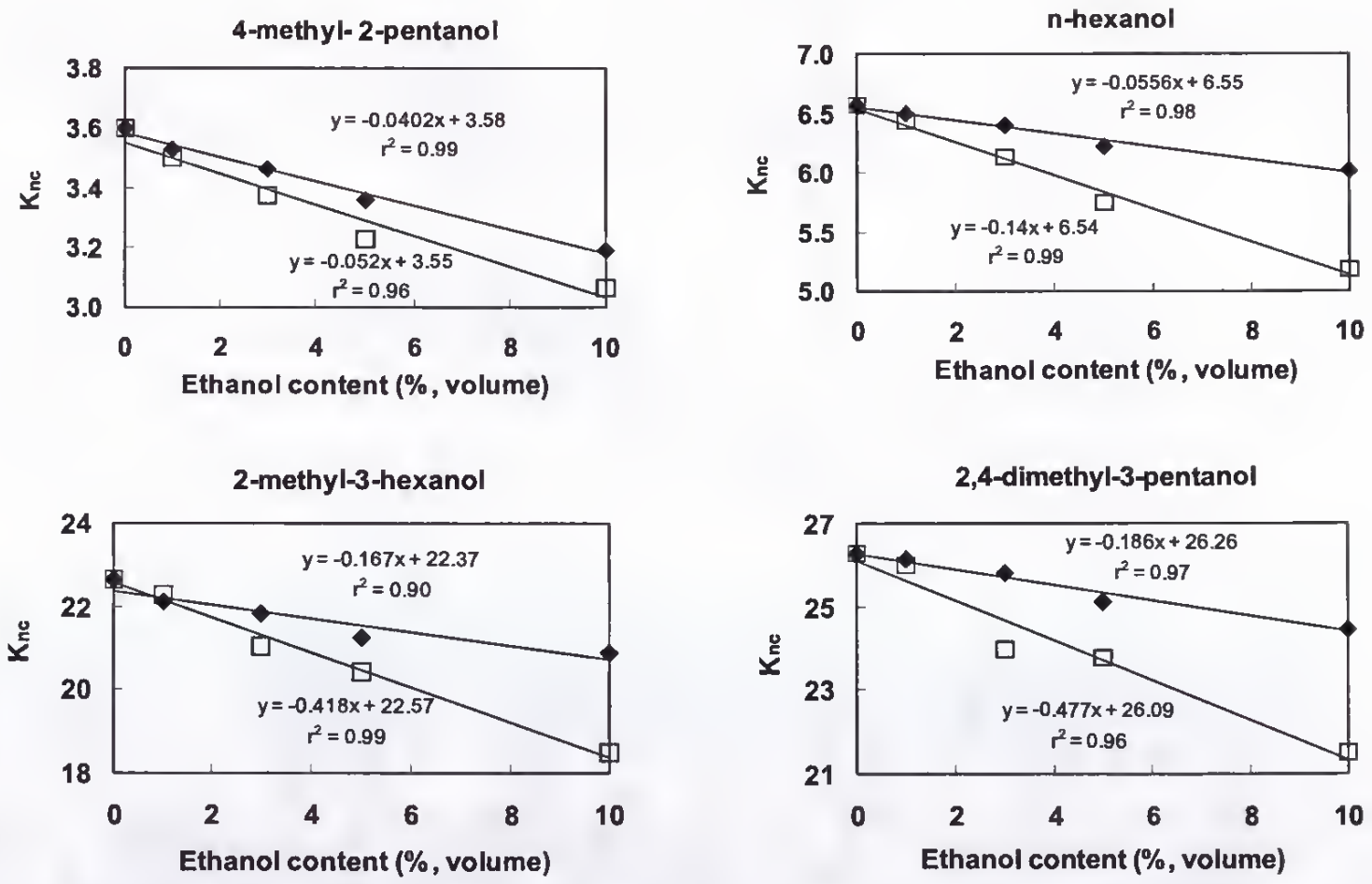

Figure 4-4. Comparison of the K_{nc} Values from batch tests to the K_{col} estimated from column tests for 4-methyl-2-pentanol, n-hexanol, 2-methyl-3-hexanol, and 2,4-dimethyl-3-pentanol in the ethanol/water system; ♦ Column test; ■ Batch test.

used is a binary ethanol/water solution, with f_c ranging from 0 to 10 %. The results are provided in Table 4-2. As expected, an increasing f_c resulted in earlier breakthrough of the tracers. Therefore, as described earlier using the K_{nw} values measured in the absence of cosolvent, lower retardation will result in lower S_n estimation.

The observed S_n values at low f_c were 1 to 10 % lower than the actual S_n, measured using tracer in the absence of ethanol(Table 4-2). While the error is fairly minor, its effect should not be neglected. The cosolvent effect can be larger depending on the magnitude of residual S_n, as discussed later.

Partitioning coefficients based on column tests (K_{col}) were calculated to compare to the batch-measured K_{nc}. The K_{col} values (Table 4-2) were computed using the R_c values measured with $f_{c,EtOH}$ and the actual S_n into Equation 4-4. Regressing K_{col} against $f_{c,EtOH}$ yielded high coefficients of determination with 0.99, 0.98, 0.90, and 0.97, respectively, for 4M2P, n-hexanol, 2M3H, and 2,4DMP. Figure 4-4 shows inverse-linear relations in good agreement with the batch results. The K_{col} values, however, were consistently higher than the K_{nc} values from batch tests. The slopes of the correlated curves for column results were lower than batch tests by the factors of about 0.2, 0.6, 0.6, and 0.6, respectively, for 4M2P, n-hexanol, 2M3H, 2,4DMP. The deviations between column and batch results are a result of two processes: cosolvent dilution and the difference in solute travel time. First, for deviation due to cosolvent dilution, recall that the column miscible displacement tests were initiated with one pore volume of the residual ethanol cosolvent without any external ethanol source. The displaced ethanol solution was diluted with the injected alcohol tracer pulse and subsequent mobile phase, PCE saturated water, which were cosolvent-free. This dilution can impact the partitioning

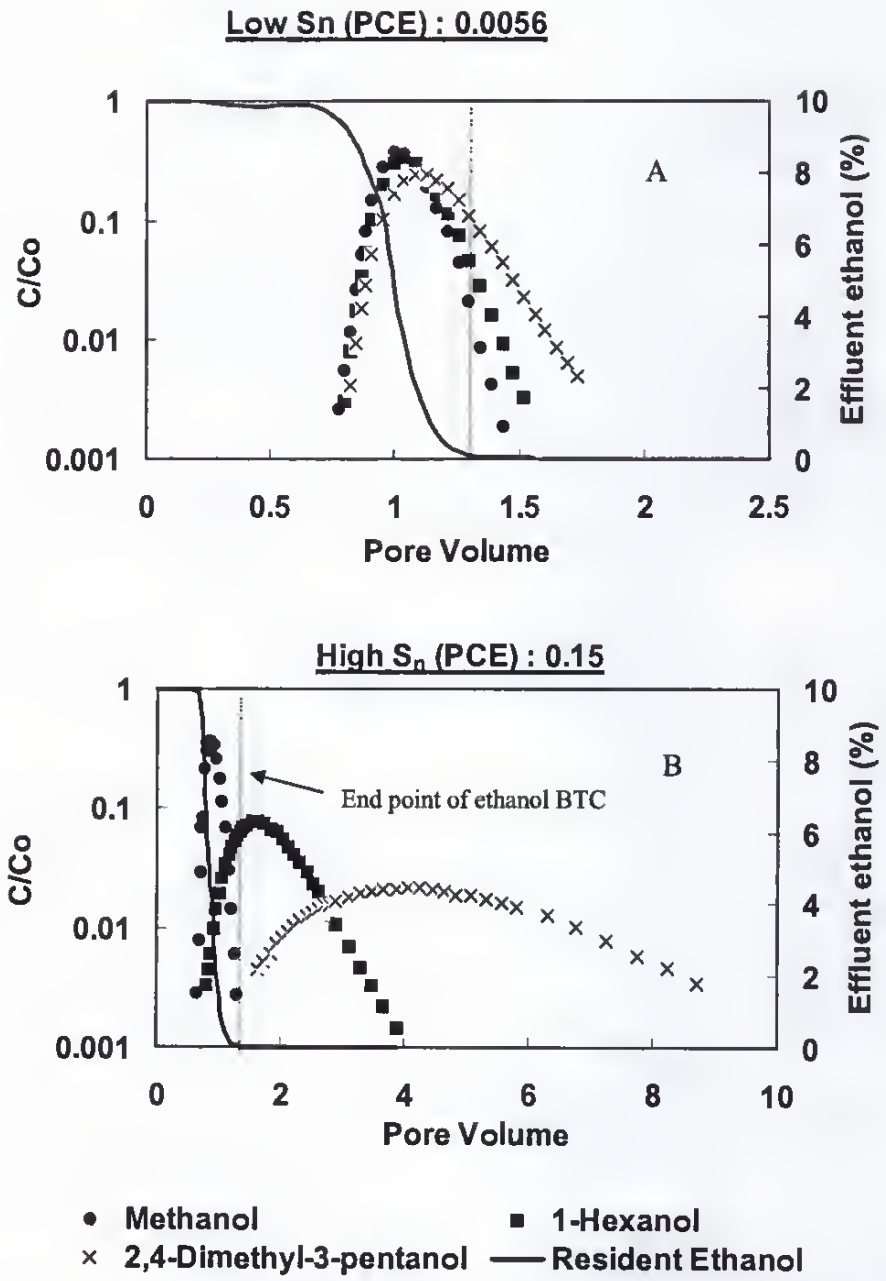

Figure 4-5. Breakthrough curves of residual ethanol cosolvent and partitioning tracers (n-hexanol and 2,4-dimethyl-3-pentanol) to display a degree of mixing, explaining the effect of residual ethanol on the NAPL saturation estimation. Initial residual ethanol content in the columns is 10 % (volume).

process by reducing local ethanol concentration. Second, deviation is caused by solute travel time of the partitioning tracers compared to the displaced ethanol front, which is essentially non-partitioning. At the tracer front, interaction with the residual cosolvent is significant. However, as the experiment proceeds, the partitioning tracers transport through the column is long, while the residual ethanol is rapidly displaced. Because of this, the influence of the residual cosolvent is reduced. Therefore, in the presence of a resident cosolvent without any additional source, the estimated K_{col} values from column tests become higher than those from batch tests.

Impact of NAPL Saturation in the Systems

As noted above, in the presence of residual cosolvent, the difference in travel times between the partitioning tracers and the cosolvent front can be a factor for estimating the residual S_n using partitioning tracers. We hypothesize that the effect of a cosolvent will be different based on the amount of S_n present in the column during a post-flushing tracer test. To verify this, column experiments were performed with low and high NAPL (PCE) saturation in the presence of ethanol-cosolvent (10 % by volume).

Effluent ethanol from the columns was monitored along with the partitioning tracers, n-hexanol and 2,4DMP. The BTCs are given in Figure 4-5A and 4-5B for the low and high NAPL saturations. The BTCs showed that the degree of mixing between residual ethanol cosolvent and the injected tracers was different between the low and high saturation columns. The BTCs of methanol and ethanol-cosolvent, which are non-partitioning solutes, followed similar trajectory for both the low and high saturation, whereas those of n-hexanol and 2,4DMP were very different for both cases as expected.

Tahle 4-3. Comparison of parameter values observed from low and high NAPL (PCE) saturation column tests using 2,4-dimethyl-3-pentanol as a partitioning tracer

	Low saturation column		High saturation column	
Cosolvent (%)	0% Ethanol	10% Ethanol	0% Ethanol	10% Ethanol
Retardation factor (R_c)	1.15	1.12	5.78	5.51
Partitioning coefficient, K_{nc}	26.3[a]	21.7[b] (21.5)[a]	26.3[a]	24.8[b](21.5)[a]
PCE saturation, S_n[c]	0.0056	0.0046	0.154	0.147
S_n % error	-17.4		-4.90	

a K_{nc} values measured by batch tests with the 0 % and 10 % ethanol-cosolvent.
b K_{col} values estimated by column tests with residual 10 % ethanol; calculated using Equation (4-3).
c calculated using Eq. (4-3); using the R_c value obtained from each column test and the K_{nw} (26.25) from the hatch test without cosolvent.

For the low S_n in Figure 4-5A, the portion of ethanol-cosolvent BTC overlapped with the frontal over ahout 60 % of the partitioning tracer BTCs (n-hexanol and 2,4DMP), indicating that over ahout 60 % of the n-hexanol and 2,4DMP traveled in the presence of the ethanol-cosolvent through the column. On the other hand, for the high S_n in Figure 4-5B, the overlapped portion between ethanol and the partitioning tracer BTCs was minimal. This suggests that the affect of residual cosolvent should be more significant in the low S_n column than in the high. As seen in Table 4-3, the S_n estimated from the low saturation column in the presence of ethanol-cosolvent (10 %) was about 17 % less for 2,4DMP than the actual S_n estimated without ethanol-cosolvent. In the high PCE saturation column, the measured S_n in the presence of 10 % ethanol was ahout 5 % less for 2,4DMP than actual.

The K_{col} values were computed to evaluate the relative effect of residual ethanol-cosolvent for hoth low and high S_n in the system. The K_{col} values (= 21.7 for 2,4DMP)

estimated from the low S_n column was very close to the K_{nc} values (21.5) from the batch test measured in the presence of same 10 % ethanol solution. However, the K_{col} values (= 24.8 for 2,4DMP) estimated from the high saturation column revealed more deviation than the K_{nc} values (21.5). This suggests that the S_n may determine the magnitude of the cosolvent effect. Typically, post-flushing tracer tests have been conducted with less than one percent of S_n in the field (Annable et al., 1998 a, b). Such a low residual S_n can result in greater cosolvent effect on S_n estimation using partitioning tracers. This suggests that in such low S_n, as a post-flushing tracer test is conducted, it is important to consider the effect of residual cosolvent.

Conclusions

Based on the results of this study, residual cosolvent can impact the estimate of NAPL (PCE) saturation using partitioning tracers. Batch test results indicated three different effects on NAPL estimation dependent on the properties of cosolvents at the low concentration ($\leq$ 10 %, vol.) used in this study: under-estimation, over-estimation, and no observable effect. Increasing the fraction of ethanol cosolvent resulted in a linear decrease in tracer alcohol partition and an increase in solubility, suggesting an under-estimation of NAPL saturation. In contrast to ethanol-cosolvent, increasing the fraction of tert-butanol cosolvent results in a linear decrease in tracer alcohol partition and decrease in its solubility, suggesting an over-estimation of NAPL saturation. In column tests, the observed S_n values in the presence of ethanol-cosolvent were under-estimated by about 1-10% with high NAPL S_n (0.15-0.18), whereas by about 17% with low NAPL S_n (0.0056). The implication from this study is that the effect of cosolvent may be significant on

estimation of NAPL saturation using a post-flushing tracer test, which is conducted in very low NAPL saturation. Consequently, a better understanding of the partition and transport of chemicals according to cosolvent types at the low level would provide valuable information for a better estimate of NAPL saturation.

CHAPTER 5
INFLUENCE OF RESIDUAL SURFACTANT ON PARTITIONING TRACERS

Introduction

Surfactants as micelle-forming surface active chemicals have been used as an enhanced subsurface flushing technology, principally in the oil industry or at organic liquid contaminated sites. The surfactants are classified, by the nature of their hydrophilic head groups as anionics, nonionics, and cationics. The anionic and nonionic surfactants have been good candidates as flushing agents since soil particles generally carry a negative charge. Their effectiveness at cleaning up contaminated sites has been demonstrated in previous studies (Abdul et al., 1990; Boving et al., 2000; Dwarakanath et al., 1999; Jawitz et al., 1998; Pennell et al., 1993; Rhue et al., 1999; Shiau et al., 1994). After remedial efforts and following a water flood, however, some amount of flushing agent is likely to remain adsorbed on the solid phase, or dissolved (as monomer or micelle) in the aqueous phase. The residual surfactants, which alter the partitioning properties of hydrophobic organic chemicals (HOCs) in the flushed zone, must be considered when the partitioning tracer technique (Pope et al., 1994; Jin et al., 1995; Annable et al., 1995) is used to characterize residual NAPL saturation.

The adsorption of surfactant at the solid-liquid or liquid-liquid interface is influenced by many factors: the nature of adsorbent structure (i.e., highly charged sites and polar or nonpolar surface), the surfactant structure (i.e., ionic or nonionic and short or

long-cbain), tbe aqueous solution condition (i.e., electrolyte content, pH, and temperature, etc) (Rosen, 1989; Abu-Zreig, 1999).

Surfactant adsorption from aqueous solution onto solid matrix

The adsorption of surfactant onto tbe solid phase is related to its orientation, concentration, and the energy change at interfaces. In general, the surface of natural soil is negatively charged, but it often bas positively charged sites whicb contains oxides sucb as alumina. The adsorption occurs mainly by ion excbange, ion pairing, and hydrogen bonding. The adsorption isotherm of ionic surfactant onto an oppositely cbarged sites is typically S-sbaped and reflects three or four distinct regions (Rosen, 1989; Holsen, 1991; and Ko, 1998a) (Figure 5-1). In region 1, the ionic surfactant sorption is low due to electrostatic repulsion and occurs mainly by ion exchange and pairing. Nonionic surfactant adsorbs mainly onto the solid surface by bydrogen bonding. The adsorbed surfactant molecules spread themselves on the surface, forming a monolayer. The cbarge density or potential at tbe stern layer of the surface remains constant. In region 2, there is a sbarp rise in adsorption, resulting from lateral interaction of tbe bydrophobic moieties of oncoming surfactant with those of tbe previously adsorbed surfactant. In region 3, the slope of the sorption isotherm is reduced and tben plateaued, indicating complete surface coverage witb a monolayer or bilayer of surfactant. This occurs mainly near tbe critical micelle concentration (CMC). When tbe concentration is above tbe CMC, any surfactant added to the solution will not increase significantly the sorption onto the solid phase and the number of monomers in solution, but rather contributes to the formation of additional micelles. The surfactant adsorption is also influenced by the pH and temperature of the solution. As the pH of the aqueous pbase decreases, the adsorption of anionic and

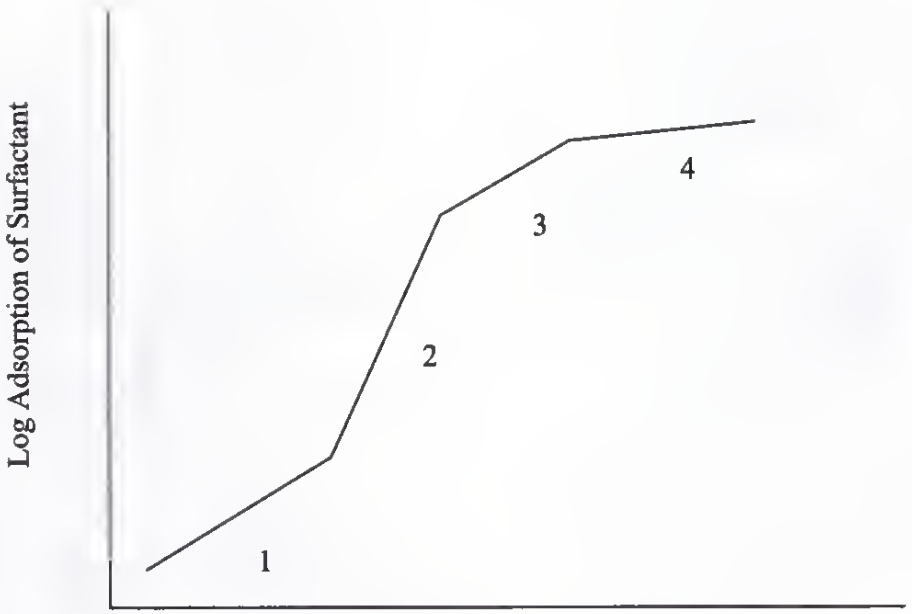

Figure 5-1. S-shaped adsorption isotherm for an ionic surfactant on an oppositely charged substrate (adapted from Rosen, 1989)

nonionic surfactants increases while that of the cationic surfactant decreases. Also, the solid phase becomes more positive, resulting from adsorption onto charged sites of proton from solution. Ko et al. (1998b) and Holsen et al. (1991) showed that the sorption of anionic surfactant (SDS) and nonionic surfactant (Tween 80) onto kaolinite increased with decreasing solution pH. Regarding temperature, as the temperature of the solution increases, even slightly, the sorption of ionic surfactant increases while that of nonionic surfactant decreases.

Surfactant adsorption from aqueous solution onto hydrophobic organic chemicals

In a system containing hydrophobic adsorbents, surfactants mainly adsorb onto the surface by dispersion forces (Rosen, 1989). The adsorption isotherms are generally of the Langmuir type. The adsorbed surfactant tail groups initially are oriented parallel to the hydrophobic surface of HOC with a slightly tilted or L-shape and the hydrophilic head groups are oriented toward the aqueous phase. As adsorption of the surfactant continues, the orientation of the adsorbed molecules is more perpendicular to the surface. The aggregation of surfactant molecules begins to form a micelle which has a hydrophobic interior where hydrophobic organic molecules can reside. John et al. (2000) reported that a low aqueous surfactant concentration, the sorption coefficient of the surfactant onto NAPL increases dramatically, but decreases with increasing surfactant concentration above the critical micelle concentration (CMC). The surfactant adsorption appears to level off near/above the CMC and this leveling off trend is attributed to the formation of micelles which limit the amount of surfactant adsorption onto the NAPL (Zimmerman, 1999; John et al., 2000).

The micelle formation significantly increases the aqueous solubility of organic chemicals. This micellar solubilization is the process used for surfactant flooding to clean up organic contaminants. In addition, an increase in the length of the hydrophobic group, and neutral electrolyte addition which decreases the electrical repulsion between the similarly charged ions and oncoming ions increase the efficiency and effectiveness of adsorption. The adsorption rate on an HOC is faster with surfactants containing the hydrophilic group in a central position because of greater a diffusion coefficient and greater CMC (Rosen, 1989).

Partitioning of hydrophobic organic chemical into residual surfactants

In a soil/water system, while anionic surfactants generally repel the negatively charged soil, nonionic surfactants adsorb onto the solid surface by hydrogen bonding. On the other hand, if the soil contains positively charged sites such as metal oxides (i.e., aluminum oxide), the anionic surfactants can adsorb strongly onto the charged sites by ionic exchange or pairing (Holsen et al., 1991; Smith et al., 1991; Rouse et al., 1993; Sun and Jaffe, 1996). The adsorbed surfactants act as good hydrophobic sites to allow partitioning of HOCs. Like the NAPL system, as the concentration of surfactants exceeds the CMC, adsorption levels off and excess surfactants form micelles which have a hydrophobic interior where hydrophobic organic molecules can reside (Holsen et al., 1991; Ko et al., 1998a,b; Sun and Jaffe, 1996).

In the aqueous phase, HOC also partition into surfactant micelles or mononers, causing a decrease in retardation. However, the retardation decrease is typically much smaller than an increase due to partitioning into the adsorbed surfactant. Sun and Jaffe (1996) reported that the partitioning of phenanthrene between the adsorbed dianionic

surfactant (DowFax) pbases (monolayers and bilayers) and water was 5 to 7 times more effective than that between the corresponding surfactants pbases (monomers and micelles) in the aqueous phase and water. This means that the adsorbed surfactant in partitioning competition dominates the corresponding surfactant micelles and monomers.

Residual surfactant as a result of remedial activities can be a concern when applying partitioning tracers (Rao et al., 1997; Annable et al., 1998a). The partitioning bebavior of tracers travelling through the porous media can be impacted by surfactants: 1) partitioning into the NAPL pbase resulting in an increase in tracer retardation, 2) forming micelles in the aqueous pbase causing a decrease in tracer retardation, and 3) adsorbing on the solid matrix resulting in increased tracer retardation.

As a result, the residual surfactants can give an erroneous NAPL indication and limit the use of partitioning tracers. This study investigates the influence of residual flushing agent (surfactants) upon residual NAPL volume estimation using partitioning tracers. The objectives were to quantify the effect of residual surfactants on the partitioning and transport behavior of alcohol tracers through batcb isotherm and column miscible tests. The effects of adsorbed surfactants on the solid matrix, including positively charged sites, were also investigated. Finally, the observed effects of residual surfactants were verified by a post-flushing column tracer test following a surfactant flood.

Materials and Metbods

Materials

Diphenyl oxide disulfonates (DowFax 8390) (Dow Chemical Co.), Sodium dihexyl sulfosuccinate (AMA-80-I) (Cytec Industries Inc.), and Polyoxyethylene (10)

oleyl ether (Brij-97) (Uniqema Industries Inc.) were the surfactants used in this study. Their physical and chemical properties are given in Table 5-1. DowFax-8390 is a di-anionic surfactant with two negatively charged hydrophilic sulfonate heads and an alkyl chain. AMA-80-I is a mono-anionic surfactant in a mixture of isopropanol and water, and Brij-97 is a nonionic surfactant. Tetrachloroethylene (PCE) (Acros, 99 %) was used as a NAPL for all batch equilibrium and column experiments. A suite of tracers was selected to examine the effects of varying retardation factors. Methanol (Fisher, 98 %) was used as a non-partitioning tracer while 4-methyl-2-pentanol (4M2P) (Acros, 99+ %), n-hexanol (Acros, 98 %), and 2,4-dimethyl-3-pentanol (2,4DMP) (Acros, 99+ %) were used as partitioning tracers. All experiments were conducted at room temperature (23 ± 1 $^{\circ}$ C). A clean silica sand (30-40 mesh, Ottawa) and a clay-silt-sandy loamy soil (Dover AFB site soil) including some metal oxides were used as porous media throughout the miscible displacement experiments. The metal oxides in the soil were extracted by an acid digestion method for soil (U.S. EPA SW-846 3050B) and quantified by an inductive coupled plasma atomic emission spectrometry (Thermo Elemental series Enviro 36).

Batch Isotherm Tests

A series of batch equilibrium experiments was conducted to evaluate the behavior of tracer partitioning in varying surfactant concentrations (≤ 0.5 % by weight). The partition isotherms were measured for three surfactant solutions (Brij 97, AMA 80, and DowFax 8390) with varying concentration (0.0, 0.05, 0.1, 0.3, and 0.5 %). Each surfactant solution was transferred to a 100 mL volumetric flask, and three alcohol tracers were added. The tracer mixtures were combined with PCE in 25 mL vials fitted with Teflon-lined screw caps. The vials were tumbled end-over-end on a Laboratory-rotator

Table 5-1. Physical and chemical properties of surfactants used in the study.

Surfactants	Mono-anionic	Di-anionic	Non-ionic
Chemical name	Dihexyl Sulfosuccinate	Diphenyl Oxide Disulfonates	Polyoxyethylene (10) Oleyl Ether
Trade name	Aerosol MA 80-1	DowFAX 8390	Brij 97
Chemical Structure	$C_{16}H_{29}O_7NaS$	$C_{16}H_{33}$ C_{12} $H_7O(SO_3Na)$	$C_{58}H_{116}O_{21}$
Mol wt.	388	642	1149
Water Solubility	Miscible	Miscible	Miscible
CMC (mM)	2.3[a]	3[b]	-
HLB	-	78.6[c]	12.4[d]

Notes : CMC is critical micelle concentration; mM is milliMolar.
[a] Lowe et al., 1999; [b] Rouse et al., 1993; [c]Dow Chemical Co.; [d] Zou and Rhue, 1999.

(model RD 4512) for 24hr at room temperature. At the end of the equilibrium period, the alcohol mixtures in the supernatant solutions were analyzed by Gas Chromatography (Perkin Elmer GC, Autosystem XL) with a flame-ionization detector.

Miscible Displacement Tests

Three series of miscible displacement tests were performed for this study. The schematic diagram of the experimental set-up is shown in Figure 5-2. The first series of tests was conducted to evaluate the effect of residual surfactants in the aqueous phase. A glass column with Teflon end pieces was used with a diameter of 4.8 cm and a length of 15 cm (high performance liquid chromatography (HPLC) column from Kontes). Two layers of a fine wire mesh and a plastic screen were placed inside of the Teflon end piece to minimize column end effects. The column was packed with pre-mixed sand containing PCE. The pre-mixed sand was prepared by adding 20 mL of water and 2 mL of PCE to 750 g ($\cong$ 300 cm^3) of sand and homogenizing. The columns used for the residual surfactant (DowFax 8390) tests were prepared for the miscible displacement experiments

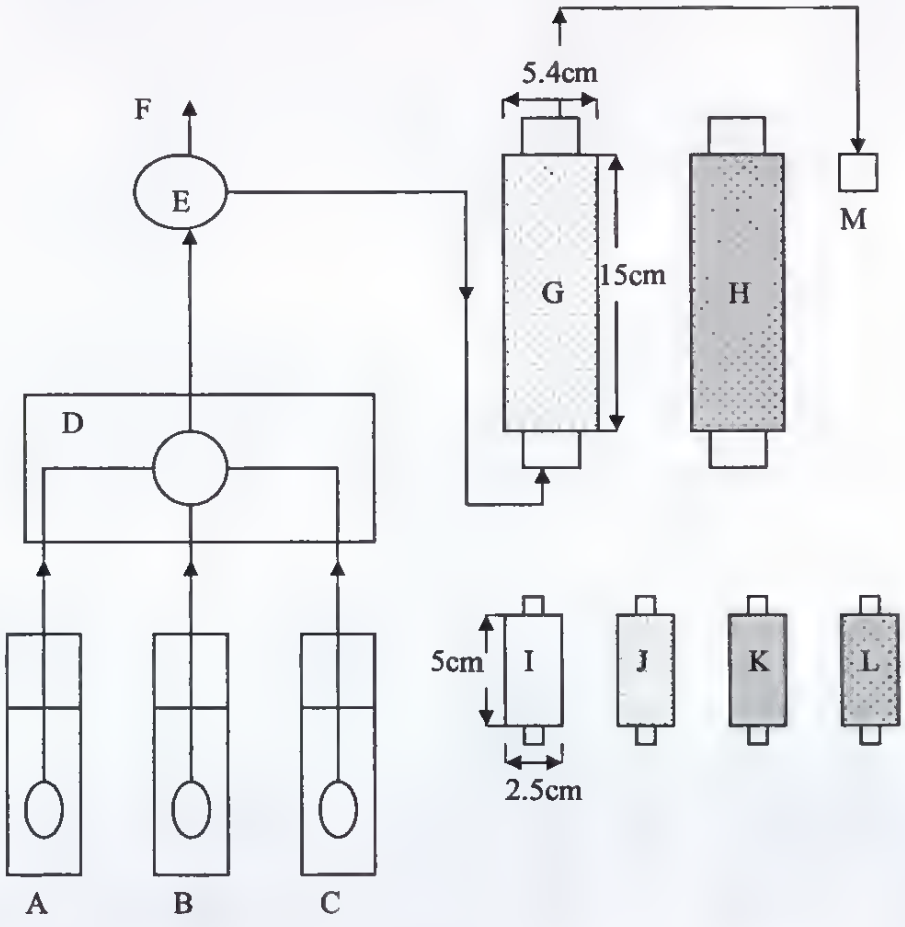

A : Tracer Reservoir

B : PCE Saturated Water Reservoir

C : Cosolvent or Surfactant Solution Reservoir

D : HPLC Pump

E : Switching Valve

F : Waste

G : Sand /PCE Column

H : Sand /PCE/ Cosolvent or Surfactant Column

I : Dover Soil Column

J : Dover Soil/PCE Column

K : Dover Soil/ Surfactant Column

L : Dover Soil/ Surfactant/ PCE Column

M : Sampling Vial

Figure 5-2. Schematic diagram of the experimental set-up

by flushing 3 pore volumes (PV) of DowFax solution through the column. The mobile phase and DowFax solution used PCE saturated water to minimize loss of residual PCE in the column. The partitioning tracer tests were conducted hoth with and without DowFax solution at varying concentrations (0.05, 0.1, 0.3, and 0.5 % hy weight). The retardation factor and PCE saturation measured from each column test were used to estimate column hased partitioning coefficients (K_{col}).

The second series of miscihle displacement tests was conducted to assess residual surfactant adsorhed on the solid matrix without NAPL. The column used was a glass column, 2.54 cm in diameter and 5 cm in length (HPLC column, Kontes) with Teflon end pieces and a fine wire mesh and a plastic screen. Silt-sandy loamy soil (Dover AFB site soil) was wet-packed and cleaned hy passing 20 PV of degased DI water. The silt-sandy loamy soil contained some metal oxides which can exchange with a negative charged surfactant (i.e., DowFax 8390). Brij 97 (5 %), AMA 80(5 %), and DowFax 8390 (5 %) solutions were used as surfactants. The column tests for adsorhed surfactants were prepared hy flushing 5 PV of each surfactant solution, followed hy 5 PV of water through the column. Partitioning tracer tests were conducted in the columns containing adsorhed surfactant and the results were used to quantify false indications of PCE.

The third series of miscihle displacement tests was conducted to demonstrate the impact of the adsorbed surfactant using a surfactant flushing test. The column, media, and packing method used were the same as those descrihed for the second series of experiments. Column test 1 was conducted using a surfactant mixture (5 % DowFax 8390/ 3 % AMA 80/ 3 % NaCl / 3 % $CaCl_2$, wt.) as the flushing agent, but without the presence of PCE. The column was prepared by flushing 5 PV of the surfactant mixture,

followed by 5 PV of water. The retardation factor from column test 1 was used to calculate a false indication of PCE.

The column test 2 was conducted witb a residual PCE present (S_{PCE} = 0.16). The PCE was introduced in the initially water saturated column using a syringe pump at 0.2 mL/min. Some of the PCE was displaced by injecting water to create residual PCE trapped in tbe pores. A pre-flushing partitioning tracer test was conducted to quantify the residual PCE volume trapped in the column. The trapped PCE in the column was flushed out with 20 PV of the same surfactant mixture used in column 1. The effluent was collected and analyzed for PCE to calculate tbe flushed and remaining PCE volume. The column was then flusbed with 5 PV of degased DI water. Finally, a post-flushing tracer test was conducted to estimate the residual PCE volume. The estimated PCE volume was compared with that obtained from mass balance ("initial PCE volume" minus "the recovered PCE volume" = residual PCE).

Results and Discussion

Effect of Surfactants on Batcb Isotherms

In the presence of three surfactants (AMA 80, Brij 97, and DowFax 8390) ranging in concentration from 0 to 0.5 % by wt., alcobol tracer NAPL-water partitioning coefficients (K_{ns}) were measured by batch isotherm experiments. The partitioning coefficients were determined by linear-least-square curve fitting. The K_{ns} values and regression coefficients, R^2, are shown in Table 5-2. The dependence of tracer partitioning coefficients on the surfactant type was observed for the range of concentrations used in this study. The partitioning of alcohol tracers into NAPL (PCE) decreased in the presence

Table 5-2. Partitioning coefficients (K_{ns}) of alcohol tracers measured on various surfactant contents (% by weight).

Surfactants	contents (%, wt.)	4M2P	n-hexanol	2,4DMP
water	0	3.6(0.994)	6.56(0.999)	26.52(0.999)
AMA 80 I	0.05	3.48(0.998)	6.56(0.999)	25.69(0.999)
	0.1	3.40(0.998)	6.43(0.999)	25.43(0.999)
	0.3	3.30(0.997)	6.38(0.999)	25.32(0.999)
	0.5	3.08(0.999)	6.59(0.996)	25.54(0.999)
DowFax 8390	0.05	3.51(0.999)	6.45(0.999)	26.23(0.999)
	0.1	3.47(0.999)	6.19(0.999)	24.98(0.999)
	0.3	3.36(0.999)	5.76(0.999)	23.22(0.999)
	0.5	3.17(0.999)	5.19(0.999)	20.95(0.999)
Brij 97	0.05	3.49(0.999)	7.13(0.998)	26.07(0.999)
	0.1	3.68(0.996)	7.49(0.995)	26.94(0.999)
	0.3	3.90(0.989)	8.07(0.986)	27.31(0.999)
	0.5	4.01(0.982)	8.17(0.987)	26.96(0.999)

of anionic surfactants (AMA 80 and DowFax 8390), but increased in the presence of the nonionic surfactant (Brij 97) (Figure 5-3).

Unlike a NAPL/water system, the tracer partitioning behavior in a NAPL/ surfactant system is a complex process involving the partitioning of the tracer into NAPL, sorbed surfactant, and surfactant micelles. At low concentrations, below the CMC, surfactant molecules adsorb to the NAPL-water interface or reside in aqueous phase as monomers. The alcohol tracers in the aqueous phase partition into the NAPL and the hydrophobic portion of the adsorbed surfactant. At high concentrations above the CMC, however, the surfactants generally form micelles with a hydrophobic inner core, allowing partitioning of alcohol tracers. In this system, partitioning of the alcohol tracers

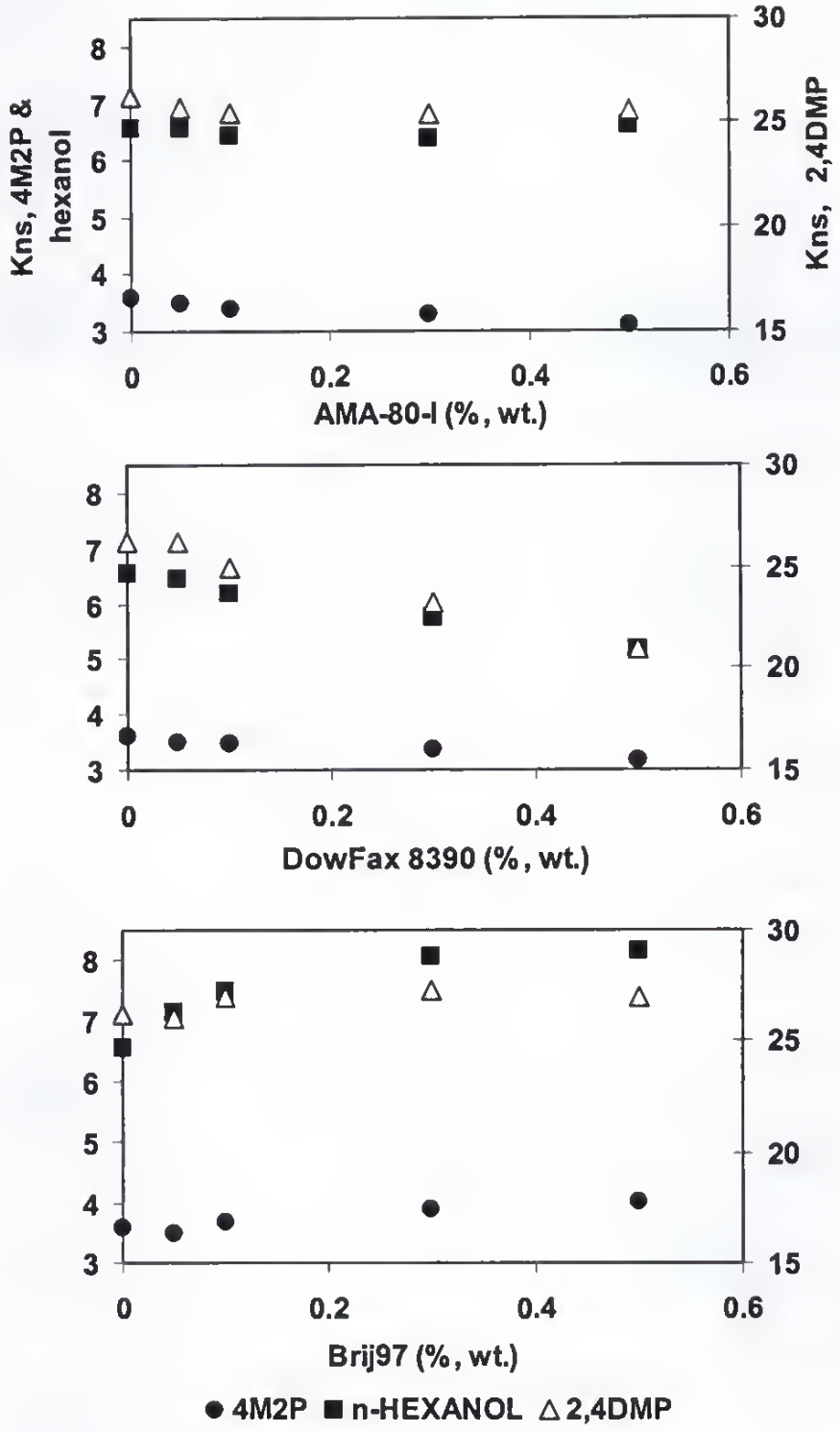

Figure 5-3. Relationship between tracer partition coefficients (K_{ns}) and surfactant [(A) AMA-80, (B) DowFax 8390, and (C) Brij97] contents (%, weight).

into NAPL with adsorhed surfactant competes with partitioning into surfactant micelles. Therefore, the micelles in the aqueous phase cause a decrease in NAPL partitioning of the alcohol tracers. The decrease of K_{ns} of HOCs resulting from micellar partitioning in a solid-water system has heen reported (Sun et al., 1995, 1996; Ko et al., 1998 a, h). For the nonionic surfactant (Brij 97), however, the partitioning of the alcohol tracers increased with increasing surfactant concentration. For anionic surfactants, the hydrophohic tail groups adsorb onto the hydrophobic NAPL, hut are only slightly soluhle in hydrocarbons (Rosen, 1989). The NAPL surface with the hydrophilic head groups oriented toward the aqueous phase may he less hydrophohic than the original NAPL (PCE). The lower hydrophobicity of the NAPL surface and the competition with micelles in the aqueous phase can hoth cause a decrease in partitioning of the alcohol tracers into the NAPL phase. For Dowfax 8390 with twin hydrophilic heads, the partitioning coefficients (K_{ns}) decreased in a linear fashion with increasing DowFax concentration:

$$K_{ns} = K_{nw} - b_s \cdot C_s \tag{5-1}$$

where K_{nw} is the partitioning coefficient in water; C_s is the surfactant concentration (% by weight); b_s is an empirical constant; the suhscripts, *n, w, s* denote NAPL, water, and surfactant. For AMA 80, however, the decrease was slight and some values were relatively uncertain at high concentrations. For Brij 97, the K_{ns} values increased and plateaued with increasing the surfactant concentration (≤ 0.5 % hy weight). The increasing trend is of a Langmuir type:

$$K_{ns} = \frac{a \cdot b \cdot C_s}{1 + a \cdot C_s} + K_{nw} \tag{5-2}$$

wbere *a* and *b* are empirical constants. Unlike anionic surfactants, for polyoxyethylenated (POE) nonionics sucb as Brij 97, the surfactant not only adsorbs onto the bydrocarbon, but is also soluble in the hydrocarbon (Rosen, 1989). The NAPL phase tends to become more bydrophobic because the surfactant is adsorbed onto and dissolved into the NAPL. Even though partitioning of alcobol tracers into the NAPL phase competes with that into the micelles, the increase of the tracer partitioning due to higher hydrophobicity of the NAPL witb the adsorbed nonionic surfactant may dominate the expected decrease of the partitioning due to the micelles. The otber possible explanation for the observed bebavior is a significant increase in interfacial area for the partitioning of alcobol tracers by formation of a macroemulsion, whicb is a stable suspension of particles. Alcobol tracers can partition into or be mixed with the macroemulsion pbase (which is a single-phase mixture of surfactant, NAPL (PCE), and water), and then be separated from the aqueous pbase. The separation means a decrease of the tracer partitioning in the aqueous pbase wbile an increase into the NAPL. The Brij 97 used in tbis study formed an opaque macroemusion phase with the NAPL (PCE)/alcobol tracers, and its stability also was longer (several days to several weeks) without any additives, resulting in an increase of tbe partitioning of the alcohol tracers. However, for the range of concentrations used in tbis study (0.05 to 0.5 % by weight), the DowFax 8390 did not form a macroemulsion, and the AMA 80 formed a slight macroemulsion wbile its lifetime was very sbort (a few minutes to a few hours). These observations suggest that the surfactant macroemusion formation and its lifetime may also contribute to an increase in tbe partitioning of alcobol tracers.

Table 5-3. Parameter values observed from column miscible experiments with PCE / DowFax 8390.

Tracers	Content (%, wt.)	R_s	S_{PCE}	S_{PCE} % error	K_{col}
n-hexanol	0	1.111	0.0166		6.56[a]
	0.05	1.106	0.0159	-4.3	6.27[b]
	0	1.099	0.0149		6.56[a]
	0.1	1.086	0.0129	-12.9	5.70[b]
	0	1.055	0.0084		6.56[a]
	0.5	1.043	0.0066	-21.7	5.13[b]
2,4DMP	0	1.435	0.0163		26.25[a]
	0.05	1.434	0.0163	-0.2	26.14[b]
	0	1.378	0.0142		26.25[a]
	0.1	1.338	0.0127	-10.42	23.44[b]
	0	1.055	0.0084		26.25[a]
	0.5	1.167	0.0063	-24.71	19.96[b]

[a] Partitioning coefficients (K_{nw}) measured in water by the batch isotherm tests.
[b] Partitioning coefficients (K_{col}) values estimated by the column tests in the presence of residual surfactants.

Effect of Residual Surfactants on Tracer Transport

A series of column tests were conducted to verify the observations from the batch equilibrium tests on partitioning and transport of alcohol tracers. The columns contained very low PCE saturation (S_{PCE} = 0.0125) trapped in a clean sandy medium, and DowFax 8390 ranging from 0 to 0.5 % wt. was used as a residual surfactant. The observed results showed decreasing retardation with increasing residual surfactant concentration (Table 5-3). Here, it is assumed that adsorption of surfactant on the solid media (which causes an increase in tracer retardation) is negligible since the doubly negative charged DowFax is

not attracted to the negative charged clean sand. A comparison of partitioning coefficients between batch and column tests provides a better understanding of the observed results. The partitioning coefficients from the column miscible test (K_{col}) can be estimated using Equation (5-3):

$$K_{col} = \frac{(R_s - 1) \cdot (1 - S_{PCE})}{S_{PCE}} \tag{5-3}$$

where R_s is a retardation factor obtained in the presence of residual surfactant, and S_{PCE} is a PCE saturation estimated from a tracer test without residual surfactant. The estimated K_{col} values from the column tests were compared with the K_{ns} from batch tests in Figure 5-4. Although showing slight deviation at high concentrations, the decreased partitioning behavior with increasing DowFax concentration is in good agreement with the K_{ns} from batch tests. Based on Equation (5-3), the larger the partitioning coefficient, the smaller the NAPL saturation. Recall that in the presence of residual DowFax 8390, the K_{ns} was smaller than the K_{nw} in water. This means that as the larger partitioning coefficient (K_{nw}) is used with the smaller R_s measured in the presence of residual surfactant, the PCE saturations (S_{PCE}) is underestimated. The observed results showed that the S_{PCE} values were under-estimated from 4.3 to 21.7 % for n-hexanol and 0.2 to 24.7 % for 2,4DMP using varying residual concentrations (0.05 to 0.5 % by weight). Assuming about 10 % (≈ 0.4 to 0.8 % wt.) or lower residual for typical surfactant concentrations (≈ 4 to 8 % wt.) (Dwarakanath et al., 1999) at post-flushing field sites, the observed results in this study show a potential for significant error in S_n estimation in the presence of a residual surfactant.

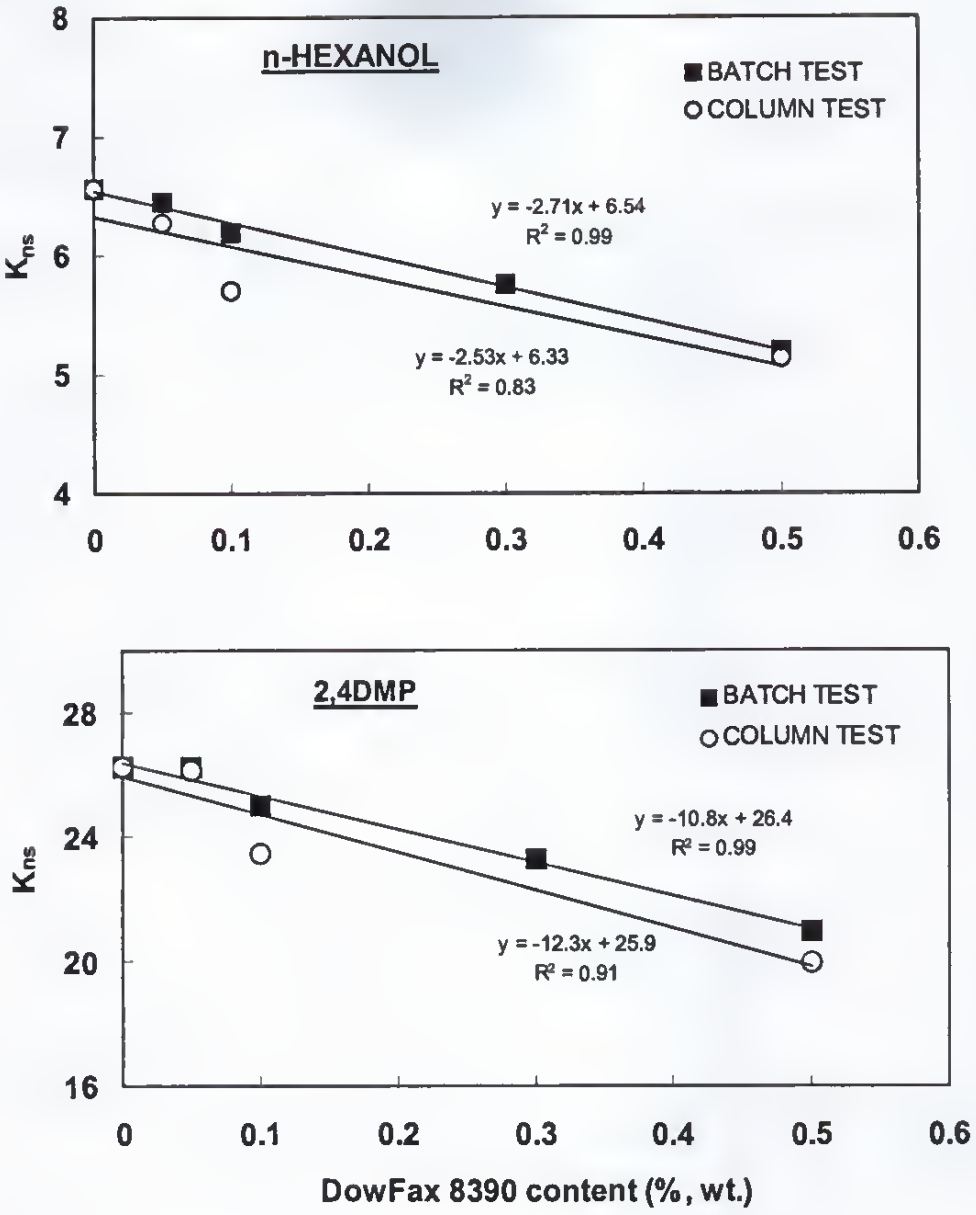

Figure 5-4. Comparison of the K_{ns} values measured by batch tests to the K_{col} estimated by column tests for (A) n-hexanol and (B) 2,4-dimethyl-3-pentanol in the PCE / DowFax 8390 system.

Effect of Adsorhed Surfactants on the Solid Matrix

Alcohol tracer partitioning to adsorhed surfactant on a solid matrix was evaluated with a field site soil from Dover AFB containing ahundant metal oxides which have a strong positive charges. The main oxides in the soil consist of iron (9800 mg/ kg soil) and aluminum (4600 mg/ kg soil). Tracer hreakthrough curves (BTCs) from the column tests with residual sorhed surfactant are shown in Figure 5-5. The retardation of the tracers showed a significant deviation depending upon the structure of the surfactants used. The ohserved retardation factors (R_s) for n-hexanol are 1.003 for no surfactant (background soil), 1.016 for AMA 80, 1.303 for Brij 97, and 3.016 for DowFax 8390.

In general, anionic surfactants are repelled by negatively charged surfaces, hut if the soil contains positively charged oxides, the anionic surfactants are adsorhed to the surface through interactions such as ion exchange. Adsorption isotherms of ionic surfactants onto a charged sites are typically S-shaped (Rosen et al., 1989; Holsen et al., 1991; and Ko et al., 1998a). The distrihution coefficients (K_d) at low concentration increase with increasing surfactant concentration, and at high concentration (ahove the CMC) decrease since surfactant micelles in the aqueous phase hegin to compete with the adsorbed surfactant (Sun et al., 1995; Ko et al., 1998a).

In this study water flooding (which typically has conducted hefore a post-flushing tracer test) (e.g., Rao et al., 1997) followed surfactant flooding. The suhsequent water flooding would remove most of the adsorbed surfactants existing as monolayers or hilayers and most of the residual surfactants as micelles in the aqueous phase. The remaining surfactant is likely to be adsorbed as a monolayer. The adsorbed surfactants with hydrophobic tail groups oriented toward the aqueous solution act as a highly

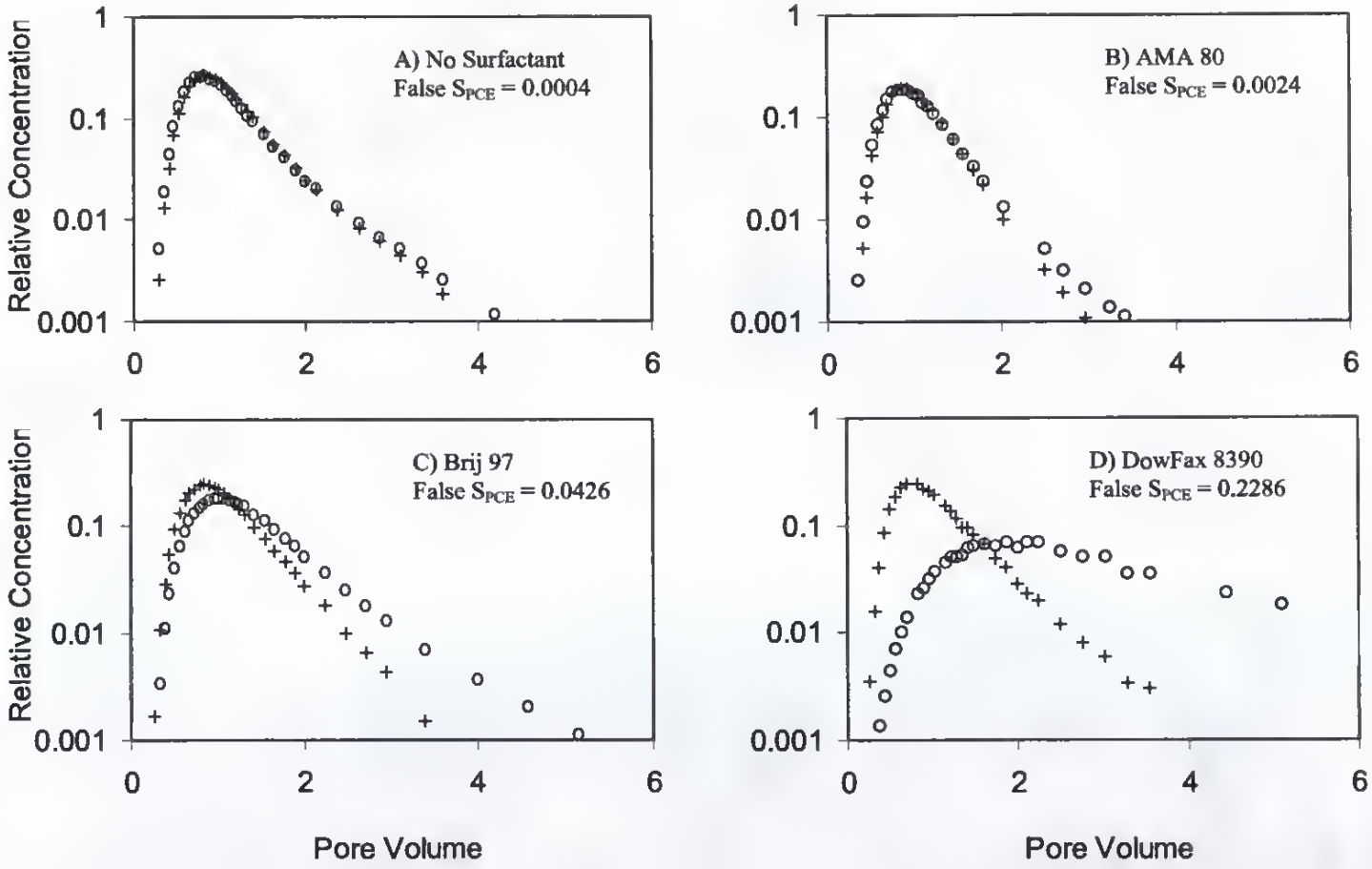

Figure 5-5. Results from column experiments with A) no surfactant, B) AMA 80, C) Brij 97, and D) DowFax 8390 adsorbed surfactants and no NAPL. Shown are BTCs for nonpartitioning tracer (methanol, plus symbols) and partitioning tracer (n-hexanol, circles).

efficient hydrophohic medium into which alcohol tracers can partition (Holsen et al., 1991).

For AMA 80, while the R_s value (=1.016) is larger than the R_s (= 1.003) for hackground soil (no surfactant), the degree of retardation was not significant (Figure 5-5 A, B). This implies AMA 80 may he a good candidate for a surfactant remediation effort requiring a post-flushing tracer test. This may he due to less hydrophobicity of the short carbon chain (dihexyl groups) or the less residual amount due to weak adsorption binding which can he displaced easily hy water.

However, for DowFax 8390, an extremely large R_s value (= 3.016) was ohserved (Figure 5-5 D). This retardation seems to he attrihuted to its special chemical structure. The douhly charged sulfonate groups of DowFax 8390 adsorh strongly onto the positively charged oxides as compared to mono-anionics such as AMA 80. Therefore, the adsorbed hydrophilic moieties on the strong positive sites are likely to resist water flooding; that is, DowFax 8390 can not he displaced easily hy water flooding. This indicates that the adsorhed DowFax 8390 can cause a serious error in estimation of residual NAPL saturation during a post-flushing tracer test.

The adsorption behavior of nonionic surfactants will he different from the anionic surfactants. In general, nonionic surfactants such as Brij 97 adsorh onto surfaces with either hydrophilic or the hydrophohic group oriented toward the surface. Polyoxyethlenated surfactants adsorb onto a silica surface through hydrogen bonding

between SiOH groups on the surface and the oxygens of the oxyethylene groups (Rosen, 1989). This adsorption has been explained as the electrostatic interaction between the oxygens of the POE chain and the negatively charged soil surface by picking up protons from the water and acquiring positive charges.

Retardation resulting from the adsorbed surfactants causes a false PCE saturation (False S_{PCE}) using post flushing tracer tests. The false S_{PCE} values can be calculated by Equation (5-3) with K_{nw} (= 6.56) for n-hexanol and the observed R_s values. The false S_{PCE} values were 0.0004, 0.0024, 0.0426, and 0.2286 for no surfactant (background soil), for AMA 80, Brij 97, and DowFax 8390, respectively. Considering that typical post flushing tracer tests have been conducted with low NAPL saturation (approximately ranging 0.005 to 0.02)(Rao et. al., 1997), the impact of the residual surfactant on soil with the positively charged sites can be significant.

Demonstration through a Flushing Test

The effect of residual surfactant on partitioning tracer tests was demonstrated through a surfactant flood using columns packed with the Dover AFB soil used previously. The surfactant mixture used was 5 % DowFax 8390 / 3 % AMA 80 / 3% NaCl / 3 % $CaCl_2$. The solubility of PCE in this mixture was approximately 70000 mg/l. Partitioning tracer tests were conducted before and after the surfactant flooding test. BTCs for the pre- and post-flushing tracers are shown in Figure 5-6. The observed BTCs from the post-flushing tracer test with low S_{PCE} (0.0125 based on PCE mass balance) (Figure 5-7) showed a similar trend to those from the pre-flushing tracer test with high S_{PCE} (0.16 by tracers). The estimated S_{PCE} values were 0.16 (1.27 mL PCE) and 0.16 (1.27 mL) for the pre flushing tracer test, and 0.13 (1.05 mL) and 0.15 (1.22 mL) for the

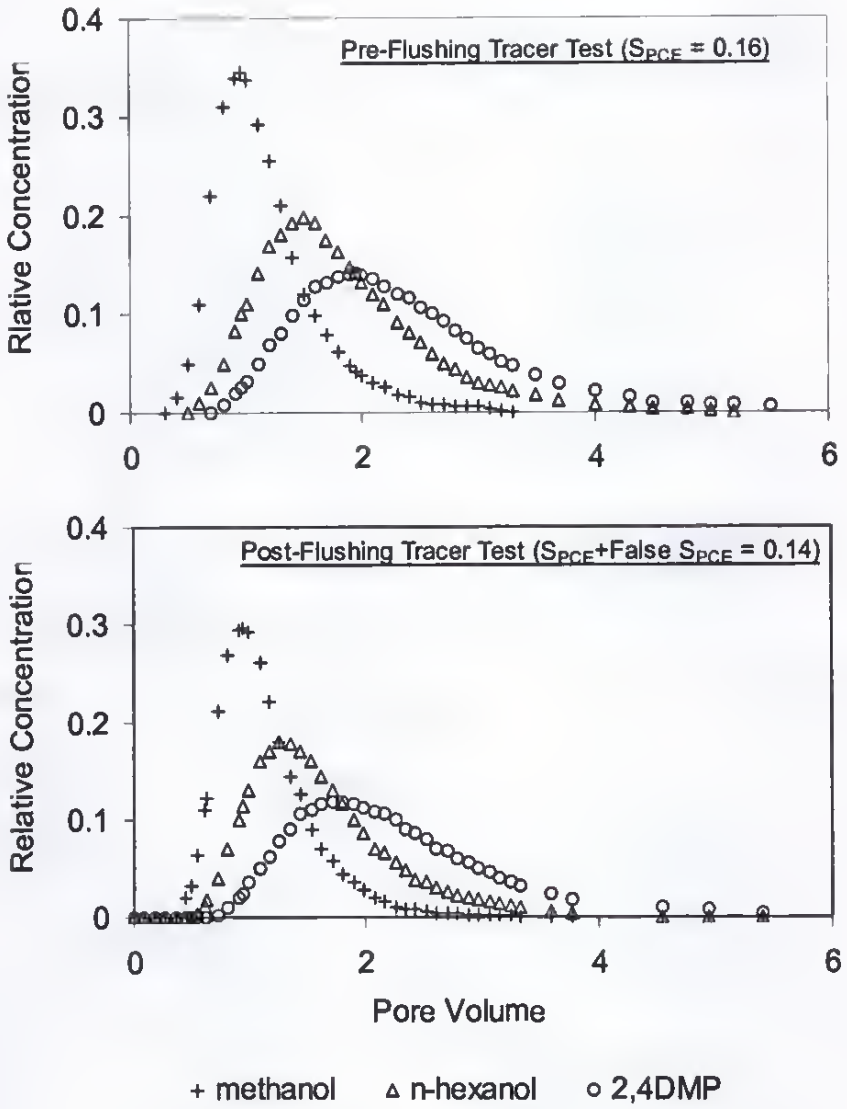

Figure 5-6. BTCs of pre-flushing tracer test with only residual NAPL (S_{PCE} = 0.16), and post-flushing tracer test with residual NAPL (S_{PCE} = 0.0125) and surfactant (DowFax 8390).

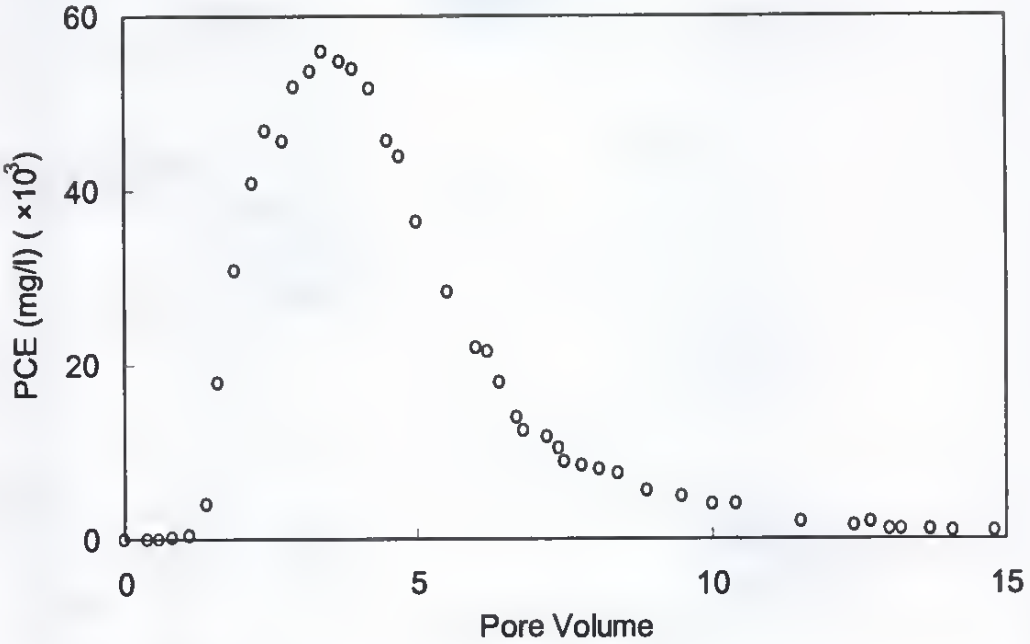

Figure 5-7. BTC of removed PCE during the surfactant mixture flooding

post flushing tracer test after the surfactant flooding based on 4M2P and n-bexanol, respectively. As calculated using only the results of pre- and post-flusbing tracer tests, the removal percentage of PCE by the surfactant flooding should be about 10 %. Based on a mass balance between injected and extracted PCE (Table 5-4), bowever, the removal percentage of PCE was about 92% (1.17 mL / 1.27mL). This deviation between the S_{PCE} estimations based on tbe tracer tests and PCE mass balance is due to the residual adsorbed flooding agent. The results from column 1 quantified the false S_{PCE} caused by the adsorbed surfactant mixture. This false S_{PCE} (= 0.12 and 0.14 for 4m2p and n-bexanol, respectively) can be subtracted from the estimated S_{PCE} (= 0.13 and 0.15 for

4m2p and n-bexanol, respectively) from the post-flushing tracer test, resulting in $S_{PCE} \approx$ 0.01 whicb is approximately tbe S_{PCE} based on mass balance.

Table 5-4. Results observed from pre- and post-flushing tracer tests and PCE mass balance from tbe flooding test with DowFax 8390 5%/ AMA 80 3%/NaCl 3%/ $CaCl_2$ 3%.

Column	Test type	PV (mL)	4-methyl-2-pentanol		n-hexanol	
			R_s	S_{PCE}	R_s	S_{PCE}
1	Tracer test for only adsorbed surfactant	8	1.46	0.12	2.06	0.14
2	Preflushing tracer test	8.1	1.68	0.16	2.27	0.16
2	Postflushing tracer test	8.1	1.55	0.13	2.17	0.15

	Trapped PCE before flooding		Removed PCE during flooding	Residual PCE after flooding	
	volume(mL)	S_{PCE}	volume(mL)	volume(mL)	S_{PCE}
2	1.27	0.16	1.17	0.1	0.0125

Conclusions

The results of tbis study indicate that NAPL volume estimates using a post-flushing partitioning tracer test can be influenced by the residual surfactant flushing agent. The surfactants remain adsorbed on the solid pbase (causing an increase in retardation of alcohol tracers) and dissolved (as monomers and micelles) in aqueous phase (causing a decrease in retardation). In the PCE/surfactant system (≤ 0.5 % by weight), the partitioning coefficients of alcohol tracers into PCE decrease linearly with increasing concentration of anionic surfactants (AMA 80 and DowFax 8390), whereas

they increase and then plateau with increasing concentration of nonionic surfactant (Brij 97). Results based on column tests with DowFax 8390 showed less retardation which was in good agreement with the lower partitioning coefficient. The lower retardation resulted in an under-estimation of the PCE saturation up to 20 %. In a soil system that included abundant metal oxides which have strongly positive charges, surfactants were adsorbed weakly or strongly depending upon the structure of the surfactants used. The adsorbed surfactants with hydrophobic tail groups oriented toward aqueous solution would act as a hydrophobic medium into which alcohol tracer can partition. The resulting partitioning of the tracers into the hydrophobic medium caused a false S_{PCE} based on post-flushing partitioning tracer tests. The false S_{PCE} values were 0.0024, 0.0426, and 0.2286 for AMA 80, Brij 97, and DowFax 8390, respectively. Considering that post-flushing tracer tests have been typically conducted with low NAPL saturation, the adsorbed surfactants can cause significant over-estimation of NAPL saturation.

CHAPTER 6
CONCLUSIONS

In this dissertation, as a part of pre-remediation characterization of NAPL source zones, NAPL-water interfacial area as a function of pore geometry and NAPL dissolution, and mass transfer between NAPL and water were discussed. As a part of post-remediation characterization, the influence of residual flushing agents on estimating NAPL saturation using partitioning tracers was investigated.

Characterization of source zones requires information about where and how the trapped NAPL is distributed. The NAPL distribution typically depends on soil properties such as grain size distribution in the target zone as well as the NAPL type. Here, characterization of spatial NAPL distribution was investigated with relationships between NAPL saturation and the corresponding NAPL-water interfacial area measured using combined (partitioning and interfacial) tracer techniques. The observed NAPL-water interfacial area increased exponentially with decreasing grain size, but it did not show a clear trend with residual NAPL saturation formed in different porous media sizes. For a given grain size, in contrast, the interfacial area decreased linearly with reduced NAPL saturation by dissolution. This indicates that in soils with different grain size distributions, specific interfacial area plays a primary role in spatial NAPL distribution rather than the magnitude of residual NAPL saturation. It was evident that the estimated morphology indices, which describe the degree of spatial NAPL distribution, increased exponentially with decreasing grain size, resulting in an exponential increase in

interfacial area.

It is well known that the specific interfacial area, which represents contact area between NAPL and the aqueous phase, is closely related to interphase mass transfer. Evaluating this dependence has been limited because of the difficulty measuring specific interfacial area. Here, steady state mass transfer across the NAPL-water interface was investigated with measured specific interfacial areas using tracers. The observed bulk mass transfer rate coefficients increased linearly with specific interfacial area and increased with increasing pore water velocity. It was also determined that grain size is an important parameter for interphase mass transfer since it is a controling factor in the magnitude of specific interfacial area. The intrinsic mass transfer coefficient was nearly independent of specific interfacial area, but dependent on pore water velocity. NAPL saturation (or interfacial area) reduction by dissolution at a given grain size caused a linear decrease in bulk mass transfer coefficients. This indicates that as NAPL dissolution proceeds, the flushing efficiency may decrease with decreasing NAPL saturation and interfacial area. Correlation models using dimensionless Sherwood number were developed to predict mass transfer rates under steady state conditions. The models were well correlated with Reynolds number (including flow velocity), Schmidt number (including molecular diffusivity), interfacial area, and grain size. The developed models were robust and produced reasonable predictions. In addition, results showed that NAPL-water interfacial area along with flow velocity can be a significant factor in determination of equilibrium conditions. This implies that interfacial area is an important factor in determining the efficiency of flushing efforts.

Partitioning tracer tests, before and after a flushing effort, have heen performed to quantify NAPL saturation residing in the target zone. Some of the flushing agent is typically left hehind in the flushed zone. It is likely that the influence of residual flushing agents can interfere in quantifying residual NAPL using tracers. Use of cosolvents and surfactants as primary flushing agents was investigated. The hatch isotherm results showed that as the volume fraction of cosolvents (≤10 %, vol.) increased, partitioning coefficients for the alcohol tracers linearly decreased for ethanol, linearly increased for tert-butanol, and did not exhihit an evident relationship for isopropanol. In the presence of ethanol, the decrease of tracer partitioning coefficients means an earlier tracer hreakthrough, resulting in an under-estimate of NAPL saturation. The results also showed that residual tert-hutanol can cause an over-estimate of NAPL saturation. The ohserved NAPL saturation from column tests, in the presence of ethanol (≤10 %, vol.) was under-estimated up to10 % under a typical residual NAPL saturation (18 % in this study). The other finding revealed that the effect of residual cosolvent was different depending on the amount of NAPL in the column. The effect of residual cosolvent at low NAPL saturation was higher than that at high saturation. Considering that typical NAPL saturation in the field site is very low, this implies that the effect of residual cosolvents can produce a significant error.

Unlike cosolvents, surfactants can remain on the solid matrix as well as in the aqueous phase. The effect of residual surfactants in the aqueous phase was investigated through hatch and column tests. The hatch equilihrium results showed that as the concentrations of the surfactants (< 0.5 %) increased, the tracer partitioning coefficients linearly decreased for DowFax 8390, increased for Brij 97, and decreased slightly or

exhibit no observable trend for AMA 80. This result indicates that NAPL saturation can be under- or over-estimated depending on the type of surfactants. Results from column tests using clear sand media with residual DowFax 8390 sbowed that the NAPL saturations were under-estimated by up to 20 %. It may be reasonable to assume that most of the residual surfactant existed in aqueous pbase because of the property of dual negative charged DowFax. This indicates that residual amount of sucb anionic surfactant in aqueous phase cause an earlier tracer breakthrough, resulting in an under-estimate of NAPL saturation. However, in the presence of residual-adsorbed surfactants, the result was reversed. The adsorbed surfactant (DowFax) on a loamy sand soil with strongly positive charged oxides caused false indications of PCE saturation. In the absence of NAPL, the observed false PCE saturations were 0.0024, 0.043, and 0.229 for AMA 80, Brij 97, and DowFax 8390, respectively. This means that the adsorbed surfactant provided an additional bydrophobic sorbent, allowing for increased tracer partitioning. Sucb results indicate that tbe adsorbed surfactant can cause a significant overestimation of NAPL saturation. As a result, both residual flushing agents showed possibilities for error in NAPL estimates. This suggests tbat wben conducting post-flushing tracer tests, the effect of residual flushing agents should be considered for a successful estimate based on partitioning tracers.

APPENDIX A

INTERFACIAL TENSION: SDBS SOLUTION-PCE WITH OIL-RED DYE

Concentration (mM)	Interfacial Tension (dynes/cm)
0.0	43.0
0.1	26.3
0.2	22.6
0.4	17.7
0.6	15.2
0.8	13.0
1.0	10.7
1.2	9.6
1.4	7.9
1.7	6.0
2.0	4.9

APPENDIX B
DERIVATION FOR MASS TRANSFER COEFFICIENT AT THE STEADY STATE CONDITION

An approximation of Fick's law is often used to describe the mass flux of a solute between phases:

$$J = K_l(Cs - C) \tag{B-1}$$

where J is the mass flux from the non-aqueous phase to the aqueous phase, the constant of proportionality; K_l, is the mass transfer rate coefficient [T^{-1}]; C_s is the equilibrium concentration of the solute in the aqueous phase [M/L^3]; C_s is the concentration of the solute in the bulk aqueous phase. Equation (B-1) can be written in terms of the rate of change of mass per unit volume of porous media:

$$\frac{dC}{dt} = K_l(C_s - C) = \frac{A_{nw}}{V} \cdot k_l(C_s - C) = a_{nw} \cdot k_l(C_s - C) \tag{B-2}$$

where A_{nw} is the interfacial area between NAPL and water [L^2], V is the unit volume of soil [L^3], a_{nw} is the specific interfacial area [L^2/L^3], and k_l is the mass transfer coefficient [$(L^3)/(TL^2)$]. The steady state mass transport equation for experimental system can be written incorporating the mass flux equation (Equation B-2). The governing equation is:

$$\frac{\partial C}{\partial t} + K_l(C - C_s) = D_L \frac{\partial^2 C}{\partial x^2} - v\frac{\partial C}{\partial x} \tag{B-3}$$

where D_L is the longitudinal dispersion coefficient; v is the pore water velocity; x is the length of the column. At the steady state condition, the term, $\partial C/\partial t$, in Equation (B-3) must be zero, $\partial C/\partial t = 0$. Equation (B-3) becomes an ordinary differential equation:

$$D_L \frac{d^2C}{dx^2} - v\frac{dC}{dx} - K_l C = -C_s \tag{B-4}$$

Find the general solution of Equation (B-4):

$$D_L C'' - vC' - K_l C = -C_S \tag{B-5}$$

$$C = C_C + C_P \tag{B-6}$$

where $C = -C_s$ is a solution of Equation (B-5). Therefore, the C_p in Equation (B-5) is taken to be C_s. The homogeneous equation is:

$$D_L C'' - vC' - K_l C = 0 \tag{B-7}$$

Using an auxiliary equation:

$$D_L r^2 - vr - K_l r = 0 \tag{B-8}$$

$$r_1 = \frac{v - \sqrt{v^2 + 4D_L \cdot K_l}}{2D_L}, \quad r_2 = \frac{v + \sqrt{v^2 + 4D_L \cdot K_l}}{2D_L} \tag{B-9}$$

The homogeneous equation (B-7) has as its general solution:

$$C_C = C_1 \exp^{r_1 \cdot x} + C_2 \exp^{r_2 \cdot x} \tag{B-10}$$

Thus the complementary function for Equation (B-5) is $C_c + C_p$. Hence the general solution of Equation (B-7) is:

$$C = C_1 \exp^{r_1 \cdot x} + C_2 \exp^{r_2 \cdot x} + C_s \tag{B-11}$$

in which C_1 and C_2 are arbitrary constants. Evaluate C_1 and C_2 from boundary conditions to get a particular solution. Boundary conditions are:

$$C(0,t) = 0, \quad \frac{dc}{dx}\Big|_{x=\infty} = 0 \tag{B-12}$$

C (0, t) = 0, that is, C = 0 at x = 0.

$$0 = C_1 + C_2 + C_s \tag{B-13}$$

$dC / dx = 0$ at $x = \infty$. The derivative of Equation (B-11) is

$$\frac{dC}{dx} = C_1 \cdot r_1 \cdot \exp^{r_1 \cdot x} + C_2 \cdot r_2 \cdot \exp^{r_2 \cdot x} = 0 \tag{B-14}$$

Since the v, D_L, and K_l are positive,

$$r_1 = \frac{v - \sqrt{v^2 + 4D_L \cdot K_l}}{2D_L} < 0,\ r_2 = \frac{v + \sqrt{v^2 + 4D_L \cdot K_l}}{2D_L} > 0 \tag{B-15}$$

Therefore, at $x = \infty$, the first term in Equation (B-14), $C_1 \cdot r_1 \cdot \exp^{r1 \cdot X}$, must be negligible. Equation (B-14) becomes:

$$C^2 \cdot r^2 \cdot \exp^{r_2 x} = 0 \tag{B-16}$$

where since $r^2 > 0$ and $x = \infty$, the arbitrary constant, C_2, must be zero.

$$C_2 = 0 \tag{B-17}$$

Substituting the Equation (B-17) into Equation (B-13),

$$C_1 = - C_s \tag{B-18}$$

Substituting the Equation (B-17) and (B-18) into Equation (B-11), The particular solution is:

$$C = -C_s \exp\left[\frac{v - \sqrt{v^2 + 4D_L \cdot K_l}}{2D_L}\right] x + C_s \tag{B-19}$$

$$\frac{C}{C_s} = 1 - \exp\left[\frac{v - \sqrt{v^2 + 4D_L \cdot K_l}}{2D_L} x\right] \tag{B-20}$$

This can be solved for K_l:

$$K_l = \frac{1}{4D_L}\left[\left(v - \frac{2D_L}{x} \cdot \ln\left(1 - \frac{C}{C_s}\right)\right)^2 - v^2\right] \tag{B-21}$$

The mass transfer coefficients (k_l) can be determined using measured a_{nw}:

$$k_l = \frac{K_l}{a_{nw}} \qquad \text{(B-22)}$$

APPENDIX C
EQUILIBRIUM ISORTHERMS OF PARTITIONING TRACERS IN THE PRESENCE OF COSOLVENTS WITH VARYING CONCENTRATIONS

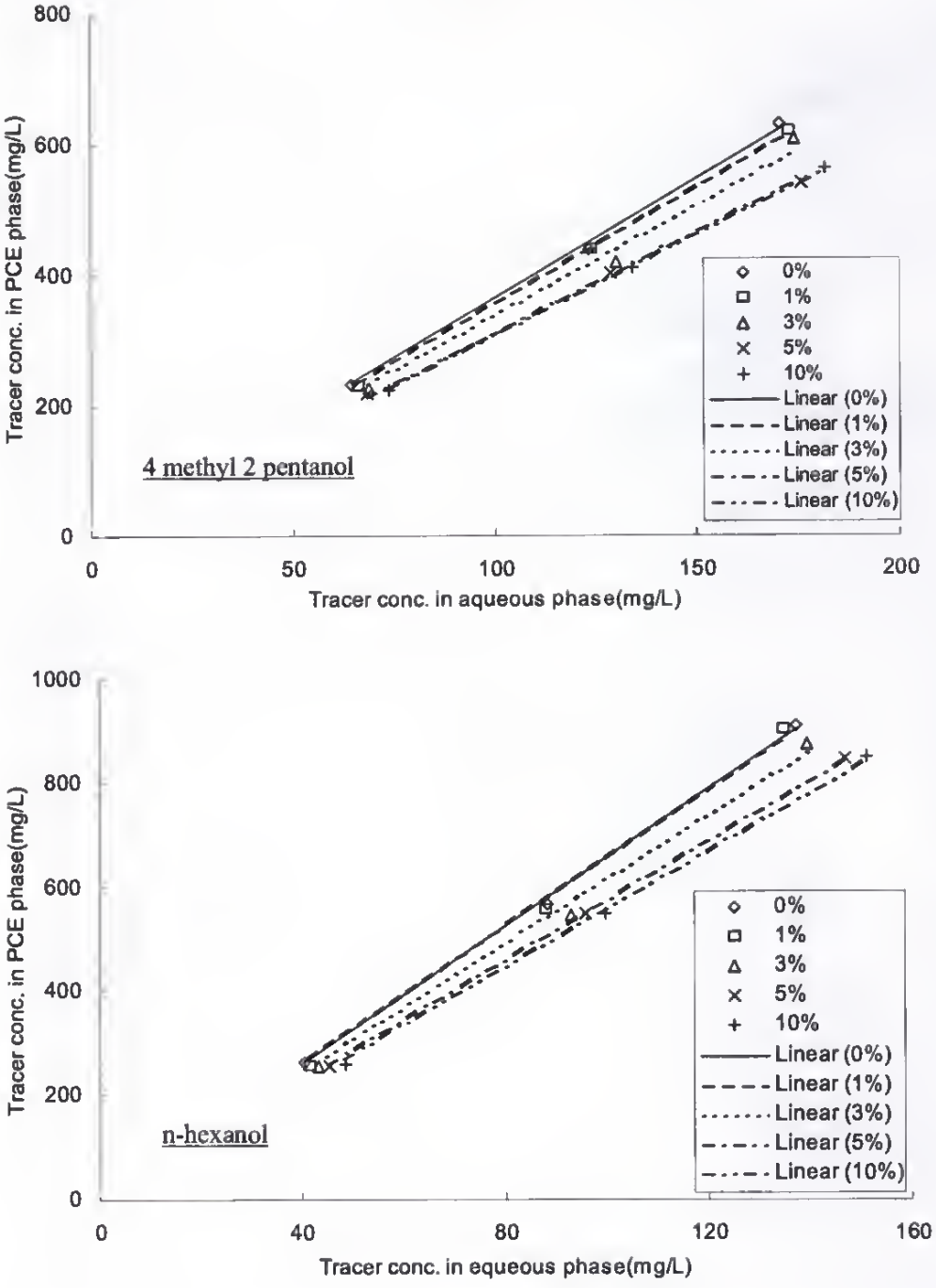

Figure C-1. PCE/water partitioning isotherms in volume fraction of ethanol solution

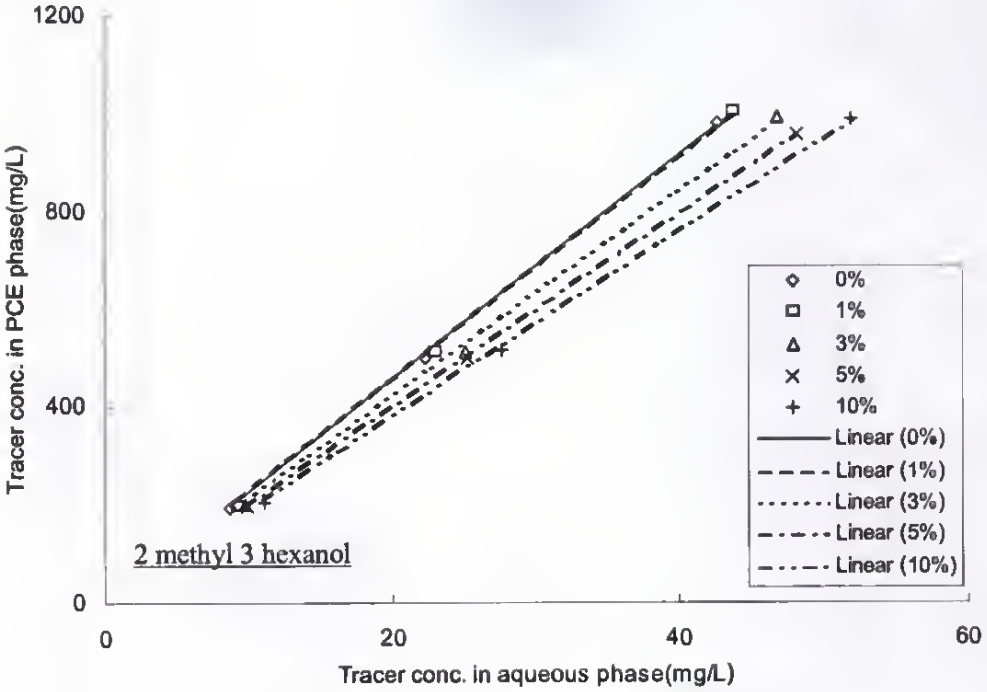

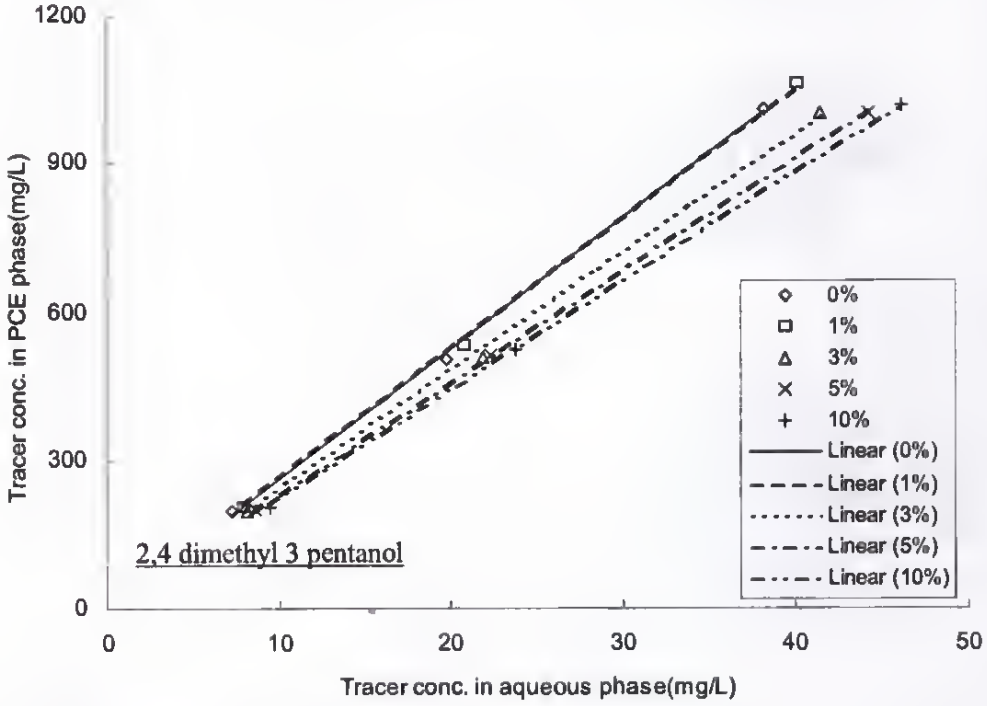

Figure C-2. PCE/water partitioning isotherms in volume fraction of ethanol solution

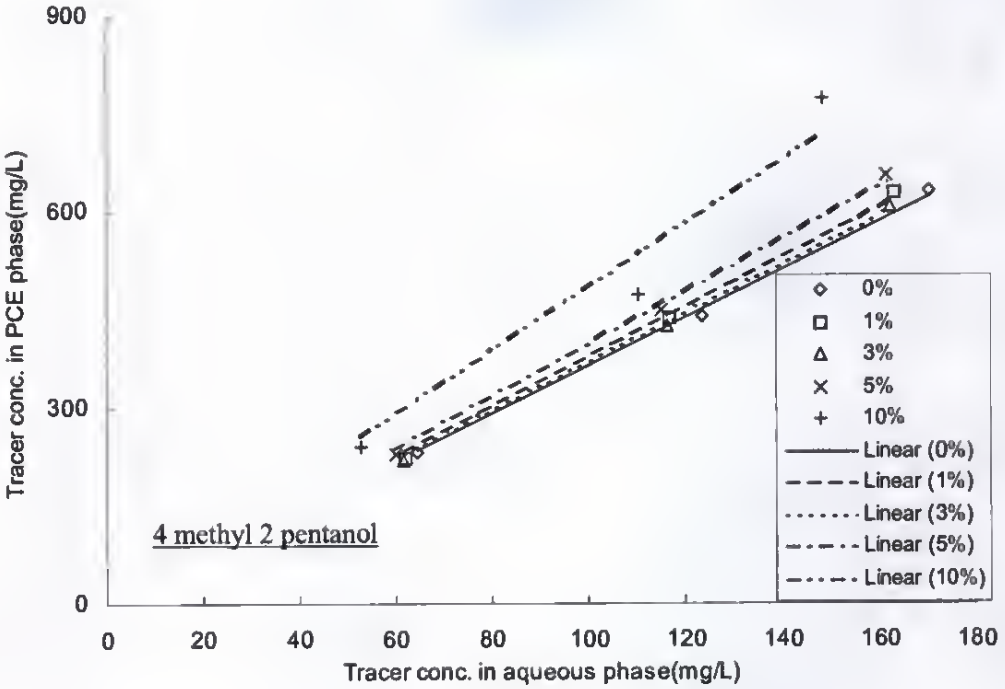

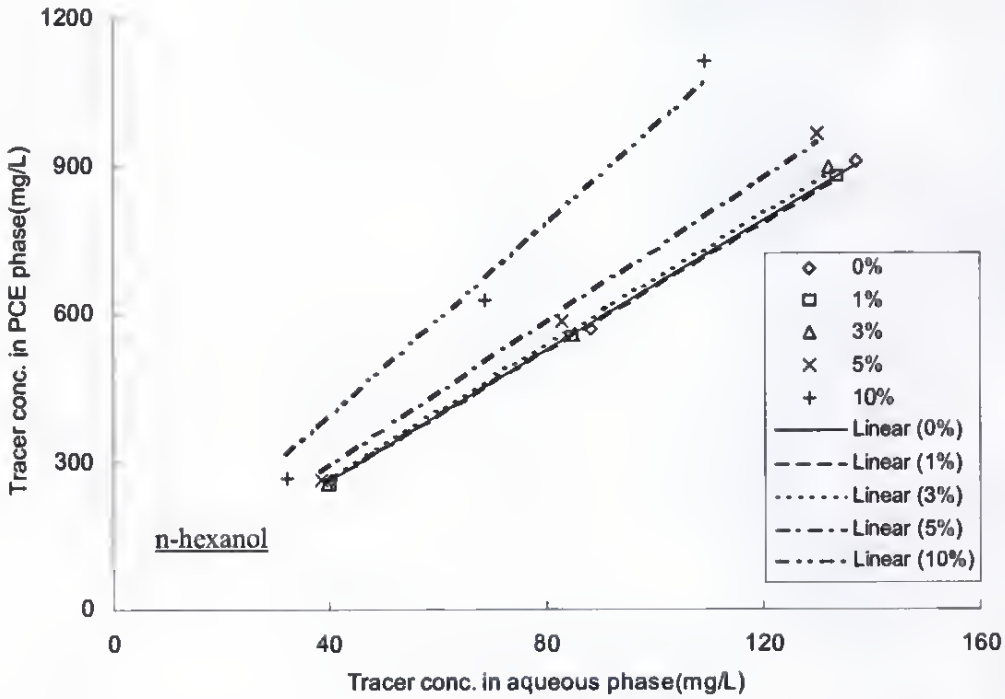

Figure C-3. PCE/water partitioning isotherms in volume fraction of tert-butanol solution

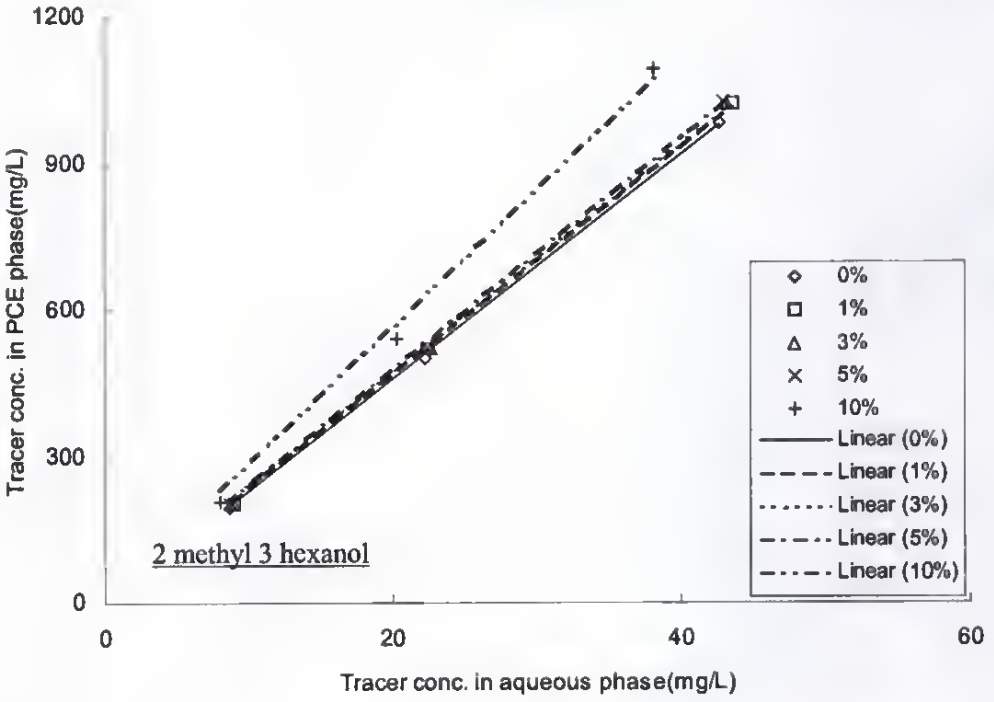

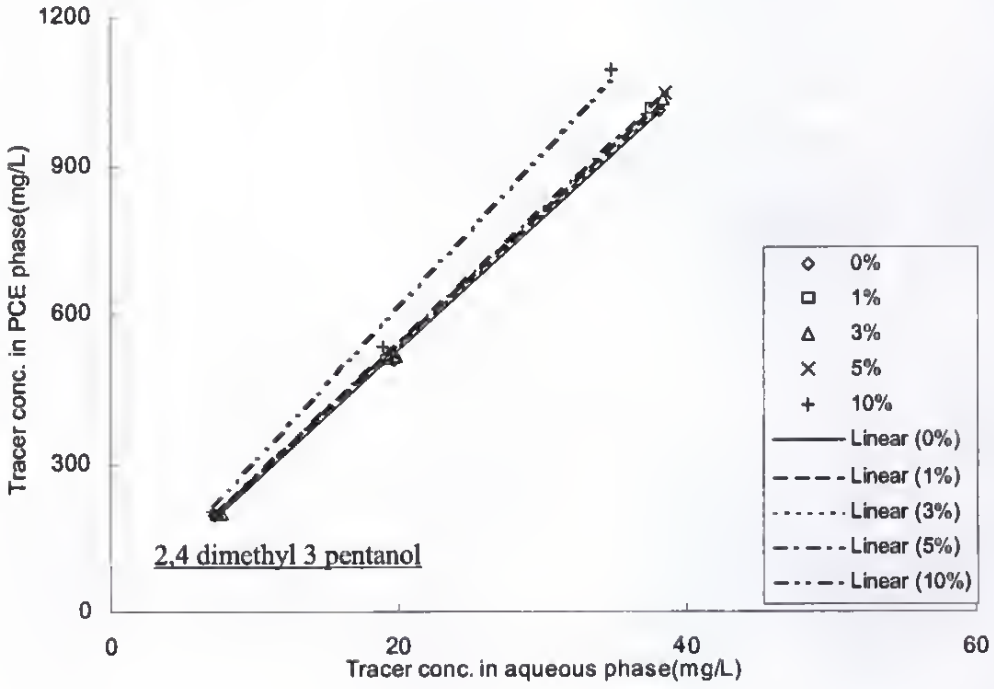

Figure C-4. PCE/water partitioning isotherms in volume fraction of tert-butanol solution

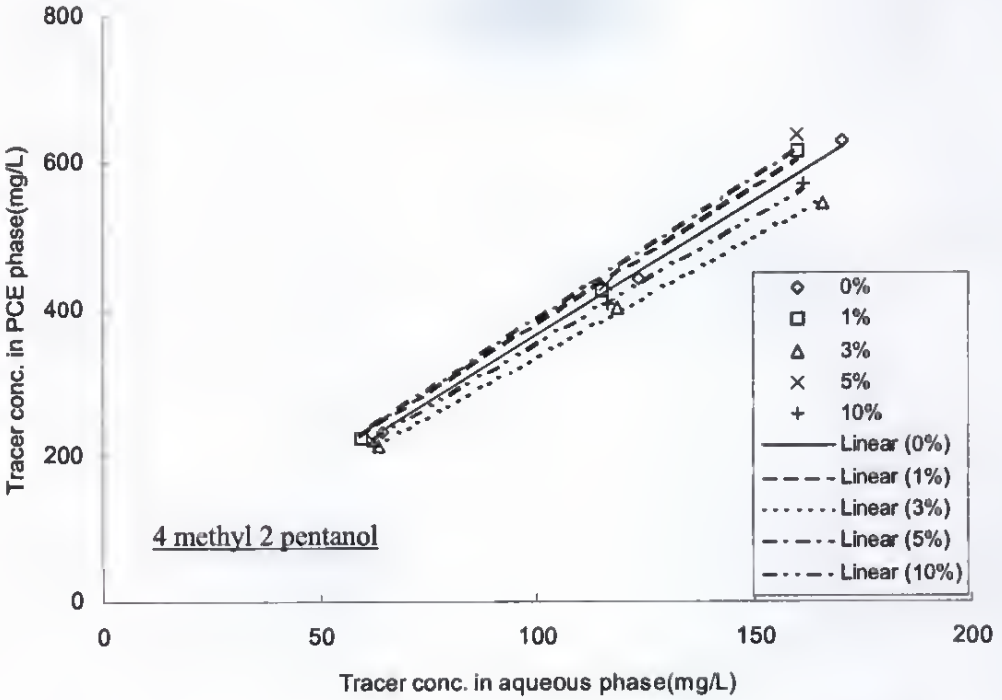

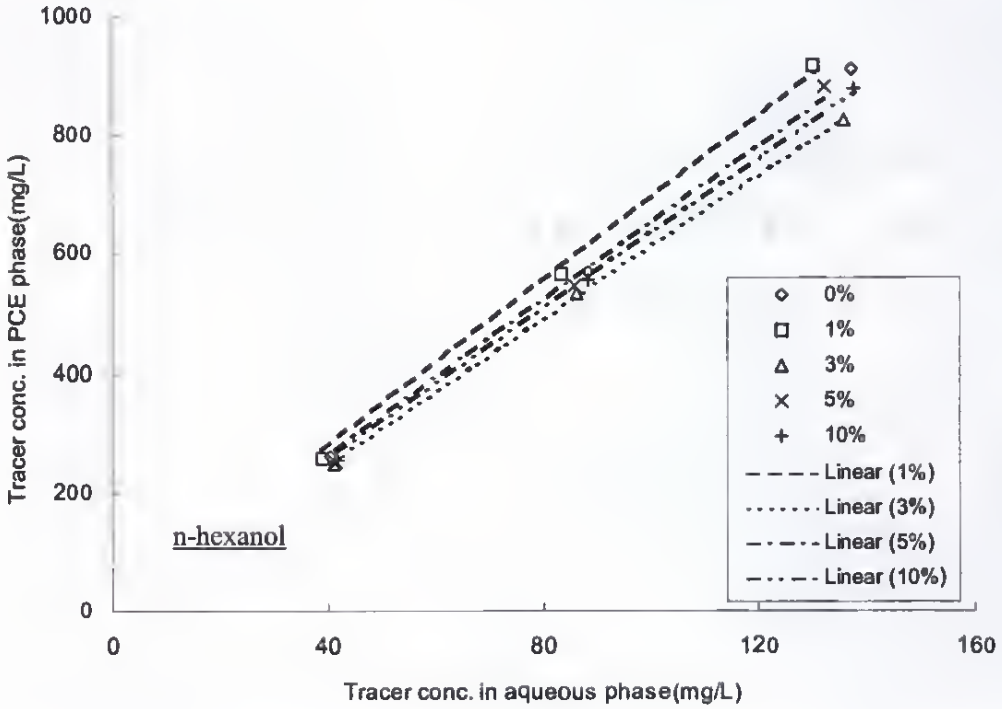

Figure C-5. PCE/water partitioning isotherms in volume fraction of isopropanol solution

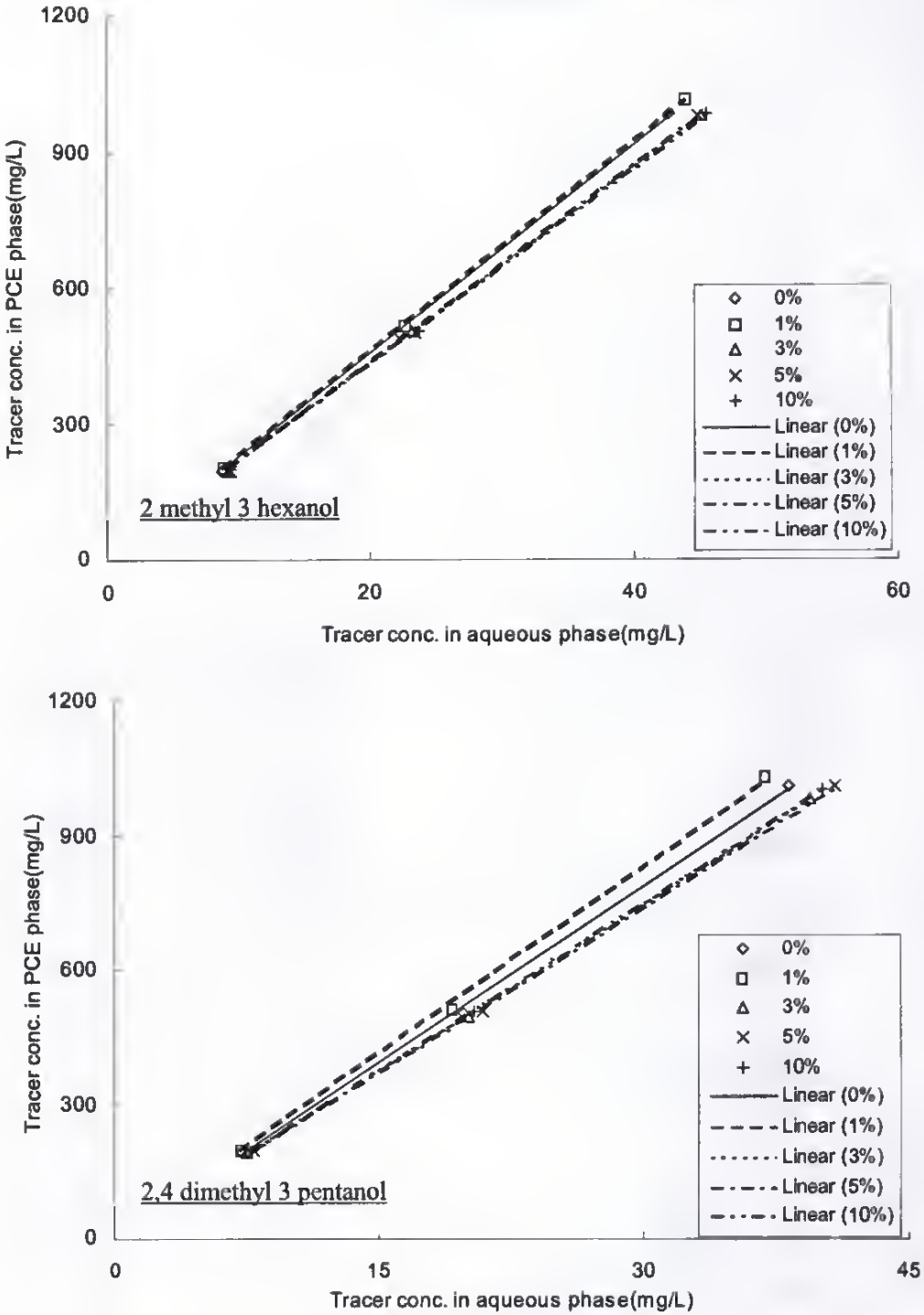

Figure C-6. PCE/water partitioning isotherms in volume fraction of isopropanol solution

APPENDIX D
EQUILIBRIUM ISORTHERMS OF PARTITIONING TRACERS IN THE PRESENCE OF SURFACTANTS WITH VARYING CONCENTRATIONS

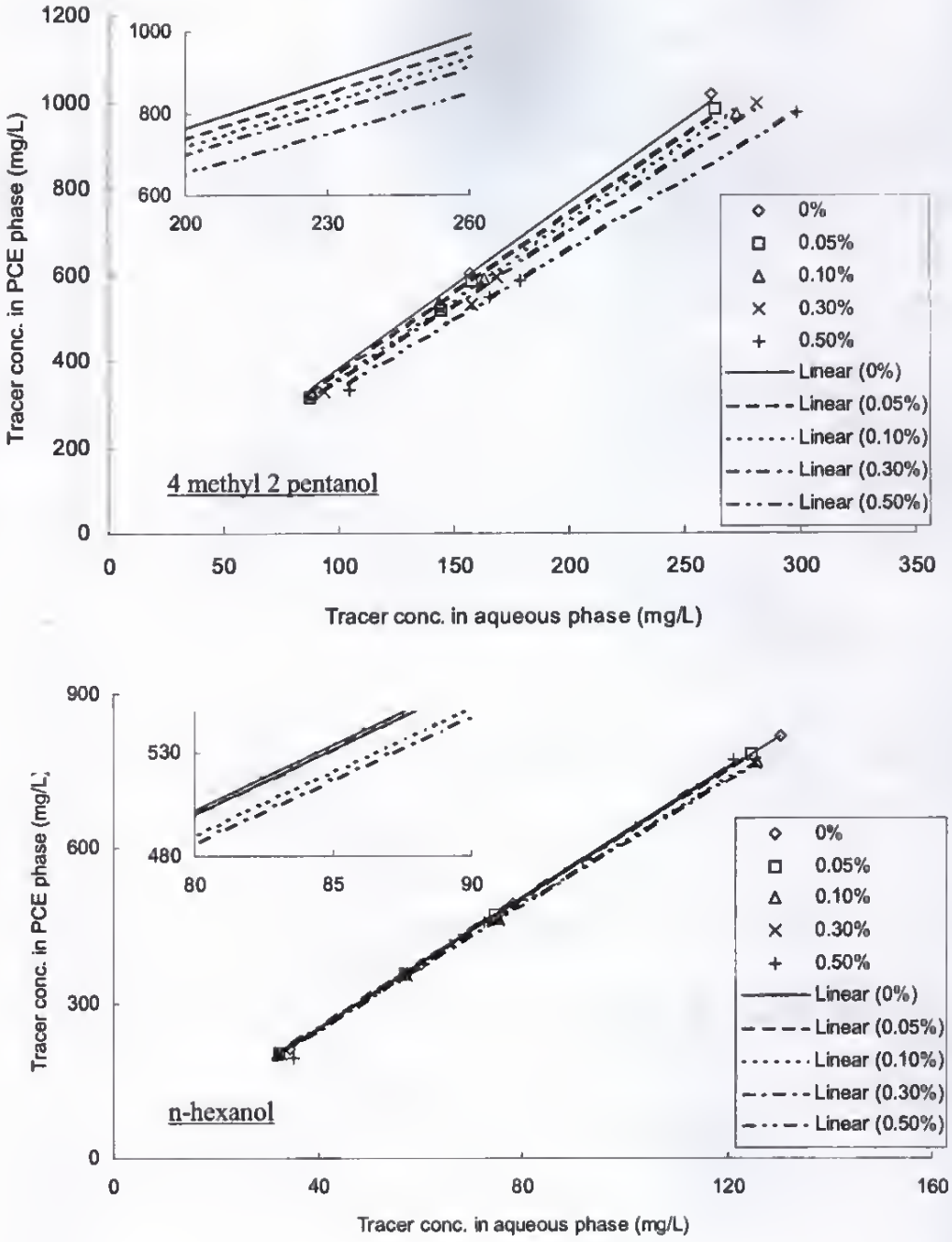

Figure D-1. PCE/water partitioning isotherms in varying AMA-80 concentration (%, weight)

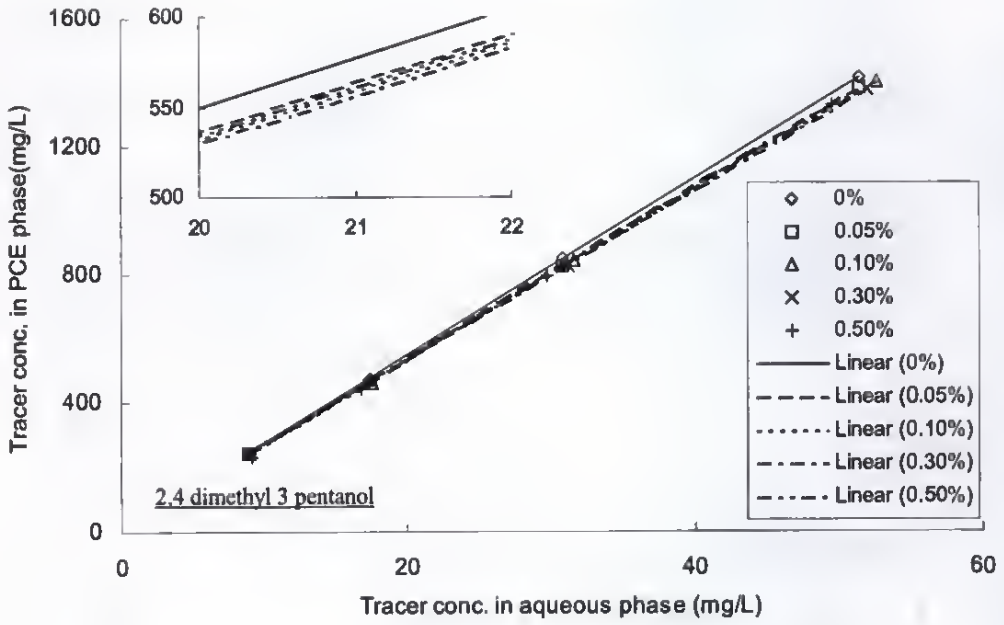

Figure D-2. PCE/water partitioning isotherms in varying AMA-80 concentration (%, weight)

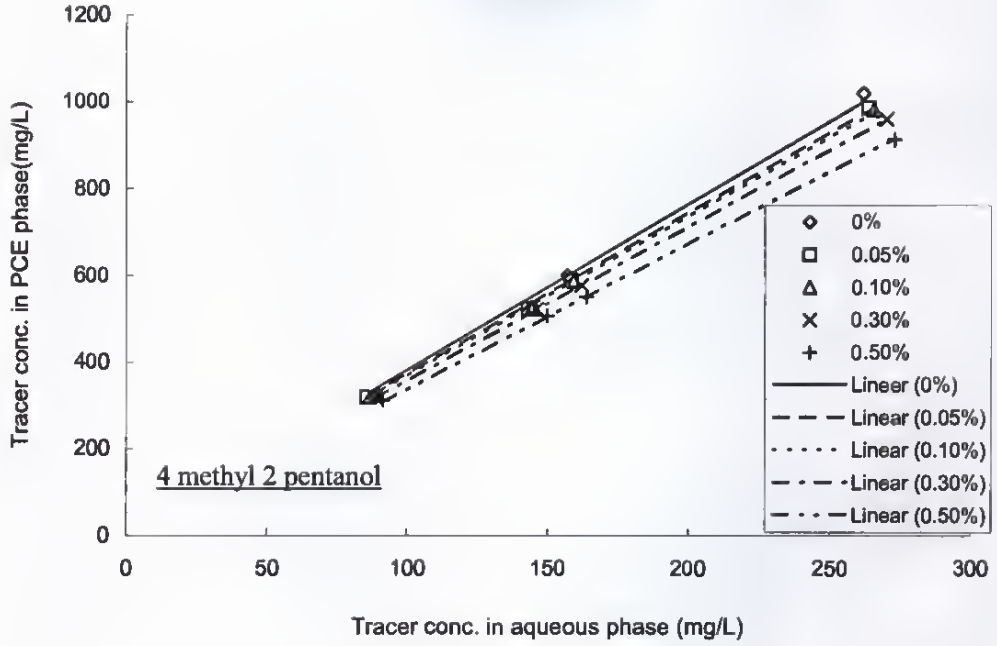

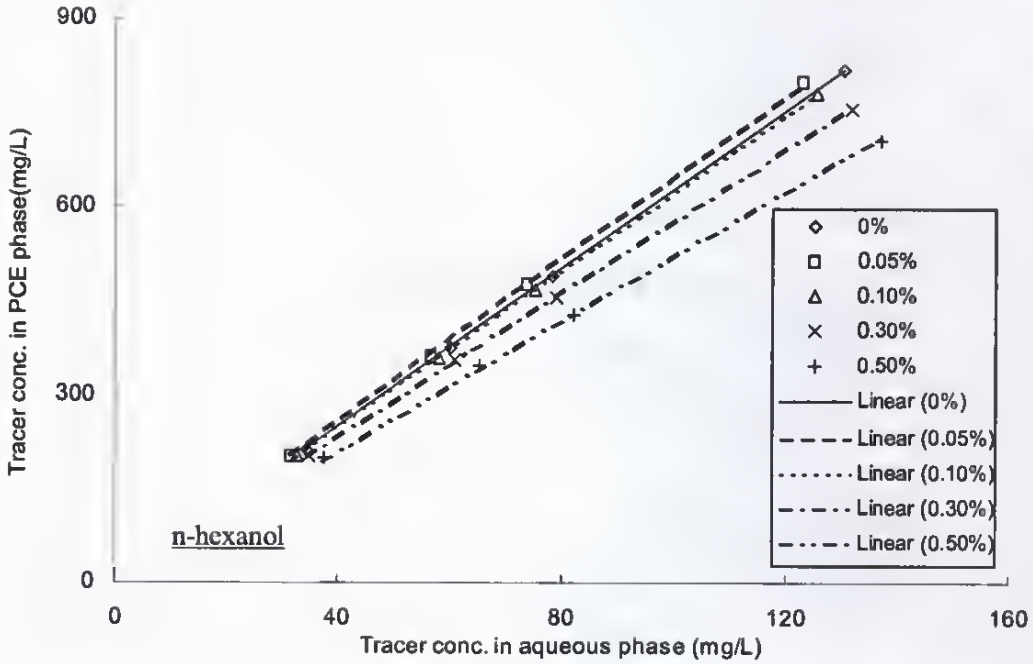

Figure D-3. PCE/water partitioning isotherms in varying DowFax 8390 concentration (%, weight)

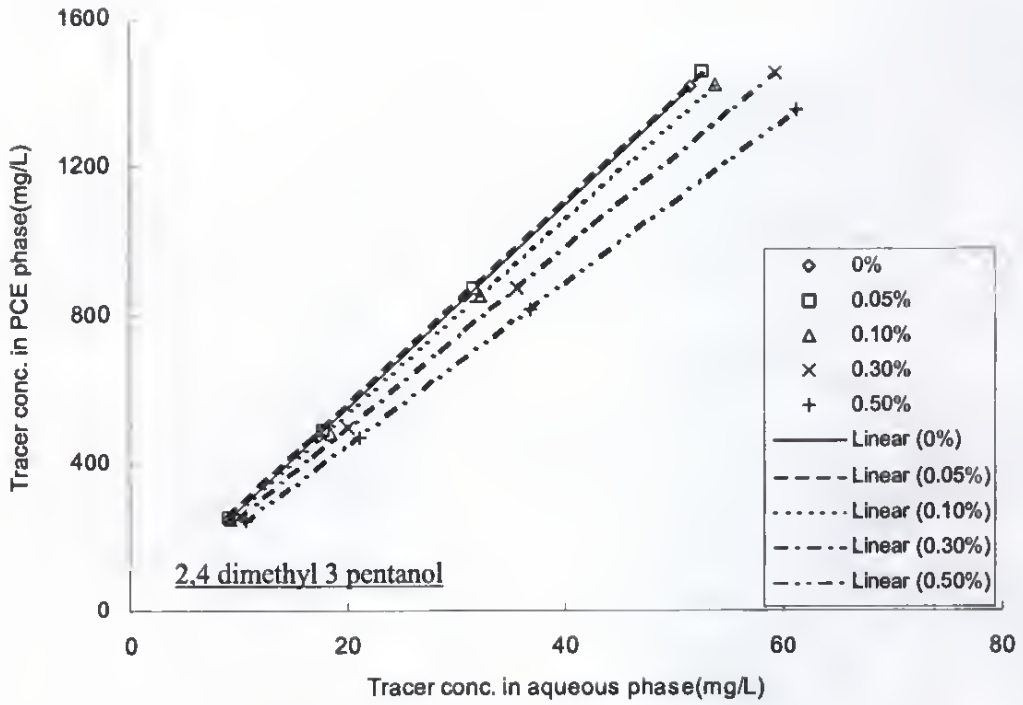

Figure D-4. PCE/water partitioning isotherms in varying DowFax 8390 concentration (%, weight)

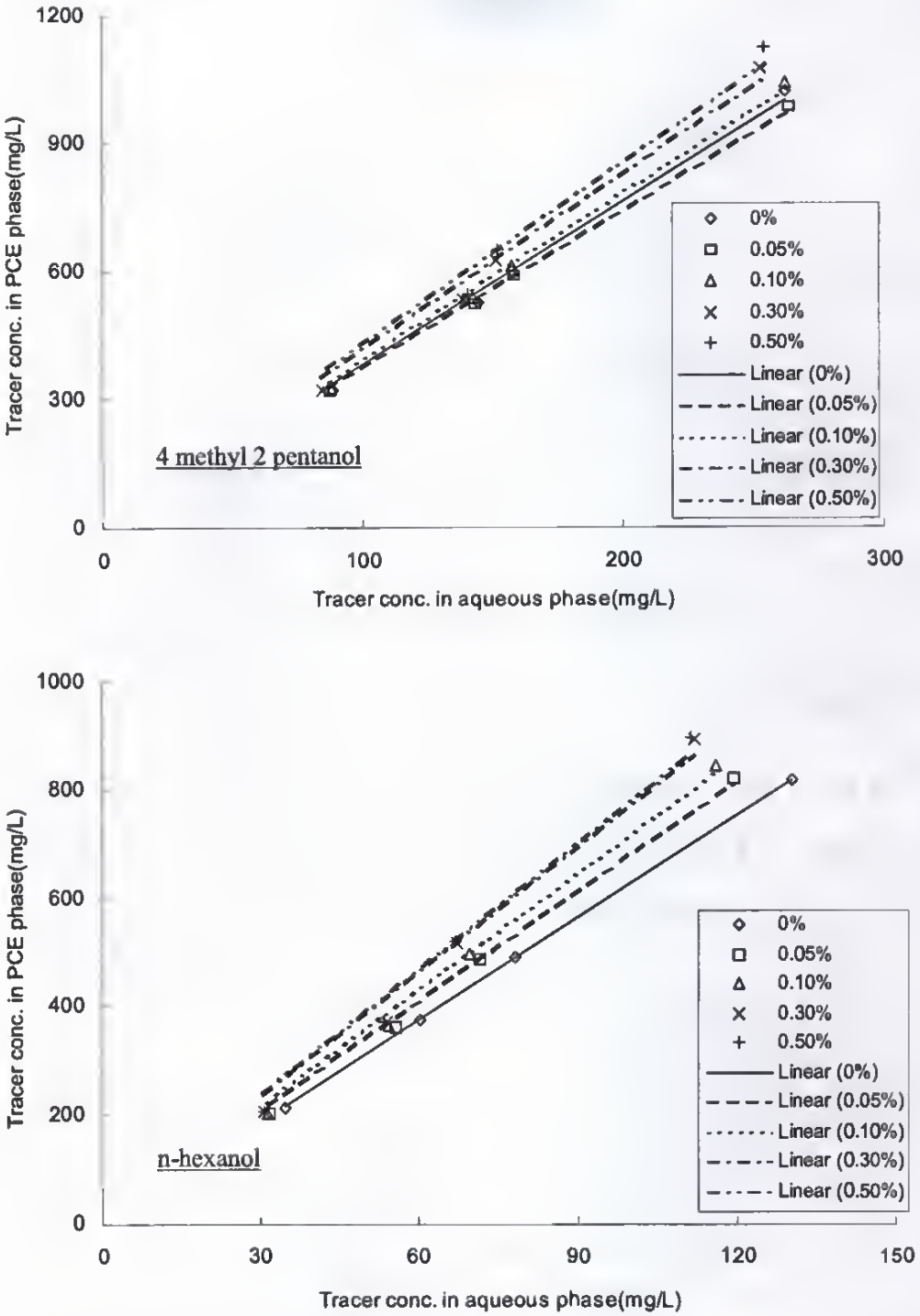

Figure D-5. PCE/water partitioning isotherms in varying Brij 97 concentration (%, weight)

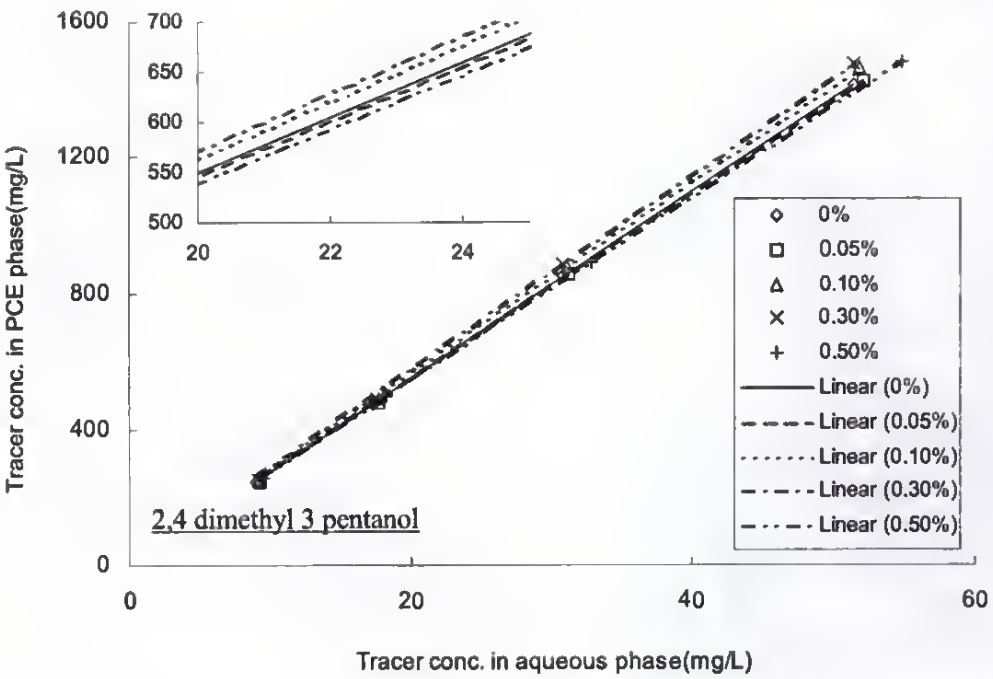

Figure D-6. PCE/water partitioning isotherms in varying Brij 97 concentration (%, weight)

REFERENCES

Ahdul, A.S., Gihson, T.L., and Rai, D.N., 1990. Selection of surfactant for the removal of petroleum products from shallow sandy aquifers. Ground Water, 28: 920-926.

Ahriola, L.M., and Pinder, G.F., 1985. A multiphase approach to the modeling of porous media contamination hy organic compounds. 1. Equation development. Water Resour. Res., 21: 11-18.

Abu-Zreig, M., Rudra, R.P., Dickinson, W.T., and Evans, L.J., 1999. Effect of surfactants on sorption of atrazine hy soil. J. Contam. Hydrol., 36: 249-263.

Adamson, A.W., 1982. Physical chemistry of surfaces, John Wiley & Sons, New York.

Annahle, M.D., Rao, P.S.C., Hatfield, K., Graham, W.D., and Wood, A.L., 1995. Use of partitioning tracer for measuring residual NAPL distrihution in a contaminated aquifer: Preliminary results from a field-scale test. Proc. 2nd Annual tracers workshop, Univ. of Texas, Austin, TX.

Annahle, M.D., Jawitz, J.W., Rao, P.S.C., Dai, D.P., Kim, H., and Wood, A.L., 1998a. Field evaluation of interfacial and partitioning tracers for characterization of effective NAPL-water contact areas. Ground Water, 36: 495-502.

Annahle, M.D., Rao, P.S.C., Hatfield, K., Graham, W.D., Wood, A.L., and Enfield, C.G., 1998h. Partitioning tracers for measuring residual NAPL: Field-scale test results. J. Env.Eng.,124: 498-503.

Borden, R.C., and Kao, C.M., 1992. Environmental groundwater extraction for remediation of petroleum contaminated groundwater. Water Environ. Res., 64: 28-36.

Bouchard, D.C., 1998a. Organic cosolvent effects on the sorption and transport of neutral organic chemicals. Chemosphere, 36:1883-1892.

Bouchard, D.C.,1998h. Sorption kinetics of PAHs in methanol-water systems. J. Contam. Hydrol., 34:107-120.

Boving, T.B., and Brusseau, M.L., 2000. Solubilization and removal of residual trichloroethene from porous media: comparison of several soluhilization agents. J. Contam. Hydrol., 42:51-67.

Bradford, S.A., and Leij, F.J., 1997. Estimating interfacial areas for multi-fluid soil systems. J. Contam. Hydrol., 27: 83-105.

Brusseau, M.L., Wood, A.L., and Rao, P.S.C., 1991. Influence of organic cosolvents on the sorption kinetics of hydrophobic organic chemicals. Environ. Sci. Technol., 25: 903-910.

Carslaw, H.S. and Jaeger, J.C., 1959. Conduction of heat in solids. Oxford university press, New York.

Cary, J.W., 1994. Estimating the surface area of fluids phase interfaces in porous Media. J. Contam. Hydrol.,15: 243-248.

Chatzis, I., Morrow, N.R., and Lim, H.T., 1983. Magnitude and detailed structure of residual oil saturation. SPEJ Soc. Pet. Eng. J., 23: 311-326.

Cooke, C. E., Jr., 1971. Method for determining residual oil saturation, U.S. Patent 3,590,923., U.S. Patent Office, Washington, D.C.

Coyle, G.T., Harmon, T.C., and Suffet, I.H., 1997. Aqueous solubility depression for hydrophobic organic chemicals in the presence of partially miscible organic solvents. Environ. Sci. Technol., 31: 384-389.

Cunningham, J.A., Werth, C.J., Reinhard, M., and Roberts, P.V., 1997. Effects of grain-scale mass transfer on the transport of volatile organics through sediments. 1. Model development. Water Resour. Res., 33: 2713-2726.

Dean, H. A., 1971. Method for determining fluid saturation in reservoirs, U.S. Patent 3,623,842., U.S. Patent Office, Washington, D.C.

Dwarakanath, V., Kostarelos, K., Pope, G.A., Shotts, D., and Wade, W.H., 1999. Anionic surfactant remediation of soil columns contaminated by nonaqueous phase liquids. J. Contam. Hydrol., 38: 465-488.

Freeze, R.A., and Cherry, J.A., 1979. Groundwater. Prentice Hall, Inc.

Fu, J.K., and Luthy, R.G., 1986. Aromatic compound solubility in solvent/water mixtures. J. Env.Eng., 112: 328-345.

Geller, J.T., and Hunt, J.R., 1993. Mass transfer from nonaqueous phase organic liquids in water-saturated porous media. Water Resour. Res., 29: 833-845.

Groves, F.R., Jr., 1988. Effect of cosolvents on the solubility of hydrocarbons in water. Environ. Sci. Technol., 22: 282-286.

Gvirtzman, H., and Roberts, P.V., 1991. Pore scale spatial analysis of two immiscible

fluids in porous media. Water Resour. Res., 27: 1165-1176.

Hermann, S.E., and Powers, S.E., 1998. Modeling the partitioning of BTEX in water-reformulated gasoline systems containing ethanol. J. Contam. Hydrol., 34: 315-341.

Holsen, T.M., Taylor, E.R., Seo, Y., and Anderson, P.R., 1991. Removal of sparingly soluble organic chemicals from aqueous solutions with surfactant-coated ferrihydrite. Environ. Sci. Technol., 25: 1585-1589.

Hunt, J.R., Sitar ,N., and Udell, K.S., 1988. Nonaqueous phase liquid transport and cleanup, 2, Experimental studies. Water Resour. Res., 24: 1259-1269.

Imhoff, P.T., Frizzell, A., and Miller, C.T., 1997. Evaluation of thermal effects on the dissolution of a nonaqueous phase liquid in porous media. Environ. Sci. Technol., 31: 1615-1622.

Imhoff, P.T., Jaffe ,P.R., and Pinder ,G.F., 1990. Dissolution of organic liquids in groundwater, paper presented at specialty conference, Am. Soc. of Civ. Eng., Arlinton, Va.

James, A.I., Graham, W.D., Hatfield, K., Rao, P.S.C., and Annable, M.D., 1997. Optimal estimation of residual non-aqueous phase liquid saturations using partitioning tracer concentration data. Water Resour. Res., 33: 2621-2636.

Zhang Y, Graham WD., 2001 Partitioning tracer transport in a hydrogeochemically heterogeneous aquifer. Water Resour. Res., 37 (8): 2037-2048.

Jawitz, J.W., 1999. Aquifer contaminent source zone characterization with partitioning tracers and remediation with single-phase microemulsoin flushing. Ph D dissertation, University of Florida, Gainesville, FL.

Jawitz, J.W., Annable, M.D., Rao, P.S.C., and Rhue, R.D. 1998. Field implementation of a Winsor Type I surfactant/alcohol mixture for in situ solubilization of a complex LNAPL as a single-phase macroemulsion. Environ. Sci. Technol., 32: 523-530.

Jawitz JW, Sillan RK, Annable MD, Rao PSC, Warner K, 2000. In situ alcohol flushing of a DNAPL source zone at a dry cleaner site. Environ. Sci. Technol., 34 (17): 3722-3729.

Jin, M., Butler, G.W., Jackson, R.E., Mariner, J.F., Pickens, G.A., Pope, Brown, C.L., and McKinney, D.C. 1997. Sensitivity models and design protocol for partitioning tracer test in alluvial aquifers. Ground Water, 35: 964-972.

Jin, M., Delsbad, M., Dwarakanath, V., McKinney, D.C., Pope, G.A., Sepehrnoori, K., and Tilburg, C.E., 1995. Partitioning tracer test for detection, estimation, and remediation performance assessment of subsurface nonaqueous pbase liquids. Water Resour. Res., 31: 1202-1211.

John, W.W., Bao, G., Johnson, W.P., and Stauffer, T.B., 2000. Sorption of nonionic surfactant oligomers to sediment and PCE DNAPL: Effects on PCE distribution between water and sediment. Environ. Sci. Technol., 34: 672-679.

Kim H, Annable MD, Rao PSC., 2001. Gaseous transport of volatile organic cbemicals in unsaturated porous media: Effect of water-partitioning and air-water interfacial adsorption. Environ. Sci. Technol., 35 (22): 4457-4462.

Kim, H., Annable, M.D., and Rao, P.S.C., 1998. Influence of air-water interfacial adsorption and gas-pbase partitioning on tbe transport of organic cbemical in unsaturated porous media. Environ. Sci. Technol., 32: 1253-1259.

Kim, H., Rao, P.S.C., and Annable, M.D., 1997. Determination of effective air-water interfacial area in partially saturated porous media using surfactant adsorption. Water Resour. Res., 33: 2705-2711.

Kim, H., Rao, P.S.C., and Annable, M.D., 1999. Consistency of interfacial tracer technique: Experimental evaluation. J. Contam. Hydrol., 40: 79-94.

Kimble, K.D., and Cbin, Y.P. 1994.The sorption of polycyclic aromatic bydrocarbons by soils in low-methanol/water mixtures. J. Contam. Hydrol., 17: 129-143.

Ko, S., Schlautman, M.A., and Carraway, E.R., 1998a. Effects of solution cbemistry on the partitioning of phenanthrene to sorbed surfactants. Environ. Sci. Technol., 32: 3542-3548.

Ko, S., Schlautman, M.A., and Carraway, E.R., 1998b. Partitioning of hydropbobic organic compouns to sorbed surfactants. 1. Experimental Studies. Environ. Sci. Technol., 32: 2769-2775.

Leverett, M.C., 1941. Capillary bebavior in porous solids. Trans. Am. Inst. Min. Metall. Pet. Eng., 142: 152-169.

Li, A., and Anderson, A.W., 1994. Solubility of polychlorinated biphenyls in water/alcohol mixtures: 1. Experimental data. Environ. Sci. Technol., 28: 47-52.

Lowe, D.F., Oubre, C.L., and Ward, C.H., 1999. Reuse of surfactants and cosolvents for NAPL remediation. Lewis publisbers, New York.

Miller, C.T., Poirier-McNeill, M.M., amd Mayer, A.S., 1990. Dissolution of trapped nonaqueous phase liquids: Mass transfer characteristics. Water Resour.Res.,

26: 2783-2796.

Morris, K.R., Abramowitz, R., Pinal R., Davis, P., and Yalkowaky, S.H. 1988. Solubility of aromatic pollution in mixed solvents. Chemosphere, 17: 285-298.

Morrow, N.R. and Heller, J.P., 1985. Fundamentals of enhanced oil recovery, in enhanced oil recovery, 1: Fundamental and analyses. Elsevier publishing Co., New York.

Parker, J.C.,et al., 1990. Modeling multiphase organic chemical transport in soils and groundwater, final report submitted to U.S. Environmental Protection Agency Project CR-814320, Washington, D.C.

Pennell, K.D., Abriola, L.M., and Weber Jr., W.J., 1993. Surfactant-enhanced solubilization of residual dodecane in soil columns. 1. Experimental investigation. Eviron. Sci. Technol., 27: 2332-2340.

Pfannkuch, H.O., 1984. Groundwater contamination by crude oil at the Bemidji, Minnesota, research site: U.S. Geological survey toxic waste groundwater contamination study, U.S. Geological survey.

Pinal, R., Rao, P.S.C., Lee, L.S., and Cline, P.V., 1990. Cosolvency of partially miscible organic solvents on solubility of hudrophobic organic chemicals. Environ. Sci. Technol., 24: 639-647.

Pope, G.A., Jin, M., Dwarakanath, V., Rouse, B., and Sepehrnoori, K., 1994. Partitioning tracer tests to characterize organic contaminants.2nd Tracer Workshop. Univ. of Texas at Austin.

Powers, S.E., Abriola, L.M., and Weber, Jr., W.J., 1992. An experimental investigation of nonaqueous phase liquid dissolution in saturated subsurface systems: steady state mass transfer rates. Water Resour. Res., 28: 2691-2705.

Powers, S.E., Loureiro, C.O., Abriola, L.M., and Weber, Jr., W.J., 1991. Theoretical study of the significance of nonequilibrium dissolution of nonaqueous phase liquid in subsurface systems. Water Resour. Res., 27: 463-477.

Rao, P.S.C., Annable, M.D., Sillan, R.K., Dai, D., Hatfield, K., Graham, W.D., Wood, A.L., and Enfield, C.G., 1997. Field-scale evaluation of in situ cosolvent flushing for enhanced aquifer remediation. Water Resour. Res., 33: 2673-2686.

Rao, P.S.C., Annable, M.D., and Kim, H., 2000. NAPL source zone characterization and remediation technology performance assessment: recent developments and applications of tracer techniques. J. Contam. Hydrol., 45: 63-78.

Rao, P.S.C., Hornsby, A.G., Kilcrease, D.P., and Nkedi-Kizza., 1985. Sorption and

transport of hydrophobic organic chemicals in aqueous and mixed solvent systems: Model development and preliminary evaluation. J. Env. Qual., 14: 376-383.

Rao, P.S.C., H. Kim and M.D. Annable. 2002. Air-water interfacial area, Section 3.3.6, in *Methods of Soil Analysis*, Part 1, J.H. Dane & G. C. Topp (Eds), Second Edition, Soil Science Society of America, Madison, WI (In press).

Rao, P.S.C., Lee, L.S., and Pinal, R., 1990. Cosolvency and sorption of hydrophobic organic chemicals. Environ. Sci. Technol., 24: 647-654.

Rhue, R.D., Rao, P.S.C., and Annable, M.D., 1999. Single-phase microemulsification of a complex light-nonaqueous-phase-liquid: Laboratory evaluation of several mixtures of surfactant/alcohol solutions. J. Env. Qual., 28: 1135-1144.

Rosen, M.J., 1989. Surfactants and interfacial phenomena, second edition. John Wiley & Sons.

Rouse, J.D., Sabatini, D.A., and Harwell J.H., 1993. Minimizing surfactant losses using twin-head anionic surfactants in subsurface remediation. Environ. Sci. Technol., 27: 2072-2078.

Rubino, J.T., and Yalkowsky, S.H., 1987. Cosolvency and cosolvent polarity. Pharm. Res., 4: 220-230.

Saripalli, K.P., 1996. Use of interfacial tracers for characterization of nonaqueous phase liquid (NAPL) distribution in porous media. Ph.D Dissertation. University of Florida.

Saripalli, K.P., Kim, H., Rao, P.S.C., and Annable, M.D., 1997. Measurement of specific fluid-fluid interfacial areas of immiscible fluids in porous media. J. Contam.Hydrol., 30: 375-391.

Saripalli, K.P., Rao, P.S.C., and Annable, M.D., 1998. Determination of specific areas of residual NAPLs in porous media usingthe interfacial tracers technique. Environ. Sci. Tech., 31.

Shiau, B.J., Sabatini, D.A., and Harwell, J.H., 1994. Solubilization and microemulsification of chlorinated solvents using direct food additive (edible) surfactants. Ground Water, 32 :561-569.

Sherwood, T. K., R.L. Pigford , and C.R. Wilke, 1975. Mass transfer, McGrow-Hill, NewYork.

Smith, J.A., and Jeffe, P.R., 1991. Comparision of tetrachloromethane sorption to an alkylammonium-clay and alkyldiammonium-clay. Environ. Sci. Technol., 25:

2054-2058.

Sillan, R. K., Annable, M.D., Rao, P.S., Dai, D., Hatfield, K., Graham, W.D., Wood, A.L., and Enfield, C.G., 1998. Evaluation of in situ cosolvent flushing dynamics using a network of spatially distributed multilevel samplers. Water Resour. Res., 34: 2191-2202

Soerens, T.S., Sabatini, D.A., and Harwell, J.H., 1998. Effects of flow bypassing and nonuniform NAPL distribution on the mass transfer characteristics of NAPL dissolution. Water Resour. Res., 34: 1657-1673.

Sun, S., Inskeep, W.P., and Boyd, S.A.,1995. Sorption of nonionic organic compounds in soil-water systems containing a micelle-forming surfactant. Environ.Sci.Technol., 29: 903-913.

Sun, S., and Jaffe, P.R., 1996. Sorption of Phenanthrene from water onto alumina coated with dianionic surfactants. Environ. Sci.Technol., 30: 2906-2913.

Van Genuchten, M.Th., and Alves, W.J., 1982. Analytical solutions of the one-dimensional convertive-dispersive solute transport equation, U.S. Department of Agriculture, Washington, D.C.

Van Valkenburg, M. E., 1999. Solubilization and mobilization of perchloroethylene by cosolvents in porous media. Ph D dissertation. University of Florida, Gainesville, FL.

Weber, W.J., McGinley, P.M., and Katz, L.E., 1991. Sorption phenomena in subsurface systems: Concepts, models, and effects on contaminant face and transport, Water Res. 25(5), 499-528.

Wilson, J.L., Conrad, S. H., and Mason, W. R., 1990, Laboratory investigation of residual liquid organics. EPA/600/6-90/004, Robert S. Kerr environmental research laboratory, Environmental Protection Agency, Ada.

Wise, W.R., Dai, D., Fitzpatrick, E.A., Evans, L.W., Rao, P.S.C., and Annable, M.D., 1999. Non-aqueous phase liquid characterization via partitioning tracer tests: a modified Langmuir relation to describe partitioning nonlinearities. J. Contam. Hydrol., 36: 153-165.

Wood, A.L., Bouchard, D.C., Brusseau, M.L., and Rao, P.S.C., 1990. Cosolvent effects on sorption and mobility of organic contaminants in soils. Chemosphere, 21:575-587.

Wu B, Sabatini DA, 2000. Using partitioning alcohol tracers to estimate hydrophobicity of high molecular weight LNAPLs. Environ. Sci. Technol., 34 (22): 4701-4707.

Yalkowsky, S.H., and Roseman, T.J., 1986. Solubilization of drugs by cosolvents in techniques of solubilization of drugs, New York.

Zhu, J. and Sykes, J.F., 2000. The influence of NAPL dissolution characteristics on field-scale contaminant transport in subsurface. J. of Contaminant Hydrology, 41: 133-154

Zimmerman, J.B., Kibbey, T.C.G., Cowell, M.A., and Hayes, K.F., 1999. Partitioning of ethoxylated nonionic surfactants into nonaqueous-phase organic liquids: Influence on solubilization behavior. Environ. Sci. Technol., 33: 169-176.

Zou, M., and Rhue, R. D., 1999. Screening commercial surfactants suitable for remediating DNAPL source zones by miscible displacement techniques. Environ. Sci.Technol.

BIOGRAPHICAL SKETCH

Jaehyun Cho was born in Pusan, Korea on January 15, 1963. He graduated from Hae Dong High School in 1982 and attended Pukyeong University in Pusan, Korea. During his study in the University, he served in the Korean Army for two and half years and continued his study. He received a Bachelor of Engineering degree with honors in Environmental Engineering in 1989. He started his graduate study in Seoul National University in 1990 and received a Master of Science degree with honors in February 1992.

After graduation, he worked as a teaching assistant and instructor in Hankuk Foreign University for 2 years, and then as a researcher at the Environmental Research Center in Seoul National University during for a year and a half. He came to the University of Texas, Austin to study English in 1995, and started his graduate study at the University of Colorado, Boulder during spring semester in 1997. In August 1997, he transferred to the Department of Environmental Engineering Sciences of the University of Florida, Gainesville to continue toward a Ph.D.

He was married in 1994 to Yoonjung Hwang. They were blessed with a gifted son, Michael Cho, in March 1997.

I certify that I have read this study and that in my opinion it conforms to acceptable standards of scholarly presentation and is fully adequate, in scope and quality, as a dissertation for the degree of Doctor of Philosophy.

Michael D. Annable, Chair
Associate Professor of
Environmental Engineering
Sciences

I certify that I have read this study and that in my opinion it conforms to acceptable standards of scholarly presentation and is fully adequate, in scope and quality, as a dissertation for the degree of Doctor of Philosophy.

William R. Wise,
Associate Professor of
Environmental Engineering
Sciences

I certify that I have read this study and that in my opinion it conforms to acceptable standards of scholarly presentation and is fully adequate, in scope and quality, as a dissertation for the degree of Doctor of Philosophy.

Kirk Hatfield,
Associate Professor of
Civil and coastal Engineering

I certify that I have read this study and that in my opinion it conforms to acceptable standards of scholarly presentation and is fully adequate, in scope and quality, as a dissertation for the degree of Doctor of Philosophy.

R. Dean Rhue,
Professor of Soil and Water Science

I certify that I have read this study and that in my opinion it conforms to acceptable standards of scholarly presentation and is fully adequate, in scope and quality, as a dissertation for the degree of Doctor of Philosophy.

P. Suresh C. Rao,
Professor of
School of Civil ngineering,
Purdue University

This dissertation was submitted to the Graduate Faculty of the College of Engineering and to the Graduate School and was accepted as partial fulfillment of the requirements for the degree of Doctor of Philosophy.

December, 2001

Pramod P. Khargonekar
Dean, College of Engineering

Winfred M. Phillips
Dean, Graduate School

LD
1780
20 01
.C5435

UNIVERSITY OF FLORIDA
3 1262 08556 6106